AD_____

Award Number: W81XWH-04-1-0466

TITLE: Use of Bifunctional Immunotherapeutic Agents to Target Breast Cancer

PRINCIPAL INVESTIGATOR: Coby B. Carlson, Ph.D.
Laura L. Kiessling, Ph.D.
Paul M. Sondel, M.D. Ph.D.

CONTRACTING ORGANIZATION: University of Wisconsin-Madison
Madison, WI 53706

REPORT DATE: July 2007

TYPE OF REPORT: Annual

PREPARED FOR: U.S. Army Medical Research and Materiel Command
Fort Detrick, Maryland 21702-5012

DISTRIBUTION STATEMENT: Approved for Public Release;
Distribution Unlimited

The views, opinions and/or findings contained in this report are those of the author(s) and should not be construed as an official Department of the Army position, policy or decision unless so designated by other documentation.

REPORT DOCUMENTATION PAGE

Form Approved
OMB No. 0704-0188

Public reporting burden for this collection of information is estimated to average 1 hour per response, including the time for reviewing instructions, searching existing data sources, gathering and maintaining the data needed, and completing and reviewing this collection of information. Send comments regarding this burden estimate or any other aspect of this collection of information, including suggestions for reducing this burden to Department of Defense, Washington Headquarters Services, Directorate for Information Operations and Reports (0704-0188), 1215 Jefferson Davis Highway, Suite 1204, Arlington, VA 22202-4302. Respondents should be aware that notwithstanding any other provision of law, no person shall be subject to any penalty for failing to comply with a collection of information if it does not display a currently valid OMB control number. **PLEASE DO NOT RETURN YOUR FORM TO THE ABOVE ADDRESS.**

1. REPORT DATE *(DD-MM-YYYY)*	**2. REPORT TYPE**	**3. DATES COVERED** *(From - To)*
01-07-2007	Annual	30 MAR 2006 - 29 JUN 2007

4. TITLE AND SUBTITLE

Use of Bifunctional Immunotherapeutic Agents to Target Breast Cancer

5a. CONTRACT NUMBER

5b. GRANT NUMBER
W81XWH-04-1-0466

5c. PROGRAM ELEMENT NUMBER

6. AUTHOR(S)
Coby B. Carlson, Ph.D., Laura L. Kiessling, Ph.D., Paul M. Sondel, M.D. Ph.D.

E-Mail: cobycarlson@yahoo.com

5d. PROJECT NUMBER

5e. TASK NUMBER

5f. WORK UNIT NUMBER

7. PERFORMING ORGANIZATION NAME(S) AND ADDRESS(ES)

University of Wisconsin-Madison
Madison, WI 53706

8. PERFORMING ORGANIZATION REPORT NUMBER

9. SPONSORING / MONITORING AGENCY NAME(S) AND ADDRESS(ES)
U.S. Army Medical Research and Materiel Command
Fort Detrick, Maryland 21702-5012

10. SPONSOR/MONITOR'S ACRONYM(S)

11. SPONSOR/MONITOR'S REPORT NUMBER(S)

12. DISTRIBUTION / AVAILABILITY STATEMENT
Approved for Public Release; Distribution Unlimited

13. SUPPLEMENTARY NOTES

14. ABSTRACT
Strategies to eradicate tumors have long been sought in the medical and scientific research communities. We envisioned that small-molecules could be used to decorate the unwanted cells as "foreign" and evoke a potent immune response to destroy them. We then developed a bifunctional conjugate that contains two binding motifs: one targets a receptor on the surface of cancer cells and the other interacts with naturally occurring human antibody. Through a series of proof-of-principle experiments, we demonstrated that this compound targets cells and can recruit antibodies simultaneously. Moreover, we obtained very promising in vitro cytotoxicity data illustrating that we can selectively target cancer cells over normal ones. These results have led our team to extend the concept into in vivo testing with an animal model (however, this work is at its beginning stages).

15. SUBJECT TERMS
No subject terms provided.

16. SECURITY CLASSIFICATION OF:			**17. LIMITATION OF ABSTRACT**	**18. NUMBER OF PAGES**	**19a. NAME OF RESPONSIBLE PERSON**
a. REPORT	**b. ABSTRACT**	**c. THIS PAGE**			USAMRMC
U	U	U	UU	38	**19b. TELEPHONE NUMBER** *(include area code)*

Standard Form 298 (Rev. 8-98)
Prescribed by ANSI Std. Z39.18

Table of Contents

Page

INTRODUCTION

Over 100 years ago, Paul Ehrlich coined the term "magic bullet" to describe a substance able to seek out and kill disease-causing cells while leaving normal ones unaffected – a concept that continues to guide the design of therapeutics. The targeting strategy that we have pursued has the high selectivity that Paul Ehrlich sought. We have assembled small molecules (termed "bifunctional conjugates") that can (a) target receptors on the cancer cell surface and (b) simultaneously recruit a naturally-occurring human antibody to the tumor cell. The antibody recognition event subsequently results in acute destruction of the unwanted cancer cells. Importantly, multivalent interactions dictate the recruitment of this antibody to the cell surface; the antibody will bind tightly only to a high-density array of the bifunctional conjugate. As such, that display is created on tumor cells expressing high levels of the specific cell-surface receptor but not on normal cells. We have demonstrated that this strategy is effective and affords exquisite sensitivity. Indeed, our synthetic bifunctional ligands selectively kill tumor over normal cells. These results have been presented at 3 venues at scientific meetings, and yielded 2 peer-reviewed publications. Our results to date serve as a basis for implementing and testing our strategy in pre-clinical and translational studies.

BODY

A key initial goal, as outlined in *Task 1*, was to chemically synthesize bifunctional conjugates that could serve as anti-cancer agents. The compounds consist of a high-affinity cancer cell-targeting agent linked to the low-affinity immunogenic carbohydrate epitope known as alpha-Gal. We identified a tight-binding peptidomimetic ligand (an RGD analog) for alpha(v) beta(3) integrin, assembled the carbohydrate with a linker for attachment, and developed a strategy to conjugate these two motifs together (Compound **1**, Figure 1). Our route is modular and therefore can be used to connect any cell-surface targeting agent to the alpha-Gal oligosaccharide (or any other functional epitope). In the course of our studies, we have exploited the modularity of our synthetic approach to generate a fluorescent integrin ligand and a conjugate of the integrin ligand to the anti-cancer agent doxorubicin (vide infra).

With our bifunctional ligand in hand, we examined its ability to interact with the relevant target proteins: the alpha(v) beta(3) integrin and the anti-Gal antibody (*Task 2*). One preliminary objective was to determine whether this bifunctional compound could bind to cancer cells that display alpha(v) beta(3) integrin. We devised a cell-binding assay in which the ability of a compound to inhibit binding of alpha(v) beta(3) integrin-positive cells to fibrinogen and/or vitronectin. We found that our bifunctional ligands serve as potent cell adhesion inhibitors (low nanomolar IC_{50} values), indicating that they are excellent integrin ligands. These results are described in a publication in *ChemBioChem* (see attached). We have also detected binding of the integrin ligand to alpha(v) beta(3)-displaying cells using a fluorescent peptidomimetic derivative (Compound **3**, Figure 1). Using fluorescence microscopy and flow cytometry, we demonstrated that this probe interacts with cells alpha(v) beta(3)-positive but not alpha(v) beta(3)-negative cells (Carlson et al., *ACS Chem. Biol.* **2007**, *2*, 347–355, see attached). These data demonstrate that the bifunctional conjugate binds to the target cell surface receptor.

To determine whether the alpha-Gal epitope within the bifunctional ligand can interact with anti-Gal antibodies, we used flow cytometry. We treated cells displaying alpha(v) beta(3) integrin with the compound and normal human serum (a source of anti-Gal) to test whether the alpha-Gal epitope was effectively displayed on the cell surface and could be bound by the antibodies. Indeed, we could detect the interaction of anti-Gal in the flow cytometer with treated but not

untreated cells (Owen et al., *ChemBiochem* **2007**, *8*, 68–82). These results indicate that both epitopes, the integrin binding and the anti-Gal binding moieties, are functional.

With support that the designed conjugate **1** was indeed bifunctional (i.e., it binds the requisite proteins), we asked whether its ability to recruit anti-Gal to a tumor cell surface would result in cell lysis. To this end, we exposed cells (human melanoma line WM115) that display high levels of alpha(v) beta(3) integrin to the bifunctional ligand and human serum. This mixture contains not only anti-Gal antibodies, but also all the complement proteins necessary to effect cytolysis. Using a fluorescence-based complement-mediated cytotoxicity assay (as proposed in *Task 3*), we assessed the ability of our bifunctional conjugate to promote tumor cell killing. Compound **1** was shown to be highly effective in this assay (Carlson et al., *ACS Chem. Biol.* **2007**, *2*, 347–355, see attached). These results illustrate that the designed bifunctional ligand can recruit endogenous antibodies (anti-Gal) as well as complement to kill tumor cells.

A key feature of our strategy is that it relies on multivalency and therefore was designed to be highly specfic. We envisioned that our approach could discriminate not only between cells with and without the target receptor, but also between cells with the low and high levels of the target. Thus, we sought to investigate how the amount of cell surface integrin influences cells killing. For such a comparison, we needed a panel of various tumor cell lines presenting different levels of the alpha(v) beta(3) integrin. As proposed in *Task 2*, we quantified these levels using fluorescein-labeled integrin ligand **3** as a probe. When these different cell lines were tested in our cytoxocity assay, only tumor cells with high levels of the cell-surface integrin were killed; "normal" cells – those displaying low levels – were unaffected in our assay (Carlson et al., *ACS Chem. Biol.* **2007**, *2*, 347–355, see attached). These results underscore the high selectivity of using multivalent interactions to discriminate between cells.

We wanted to compare the cell type selectivity we achieved with our multivalent targeting to that obtained with a conventional targeted chemotherapeutic. Accordingly, in the past grant period, we synthesized a new conjugate in which the well known chemotherapeutic agent doxorubicin was appended to our tumor-homing agent (Compound **2**, Figure 1). We tested this compound in a cellular cytotoxocity assay to compare the cell-killing selectivities of compounds **1** and **2**. Interestingly, with the traditional targeting agent **2**, all the cells displaying the alpha(v)

beta(3) integrin were susceptible to killing, regardless of the level of cell-surface integrin (Figure 2). In contrast, compound **1** exhibited high selectivity and only triggered a cytotoxic response with cells that had high levels of the integrin. These results highlight the superior specificity of the strategy we have devised.

As stated previously, we postulated that our bifunctional conjugate achieves cell killing through multivalent binding—both anti-Gal binding and complement-mediated cell killing involve multiple interactions. We reasoned that we could test for such a mechanism by examining the percentage of cell killing relative to bifunctional conjugate concentration. Specifically, if cell killing depends on multivalent interactions, cell killing should be highly sensitive to ligand concentration. Indeed, we observed that the concentration of ligand **1** has a dramatic effect on its ability to mediate cell killing (Figure 3). In contrast, there is a much more gradual concentration dependence for doxorubicin conjugate **2**. These data support our mechanistic hypothesis underlying the anti-cancer strategy we have developed.

Given the success of our studies to date, we plan to test our bifunctional conjugates *in vivo*. Our plan was to test conjugate **2** in a mouse xenograft model. One complicating feature of conducting such an *in vivo* test is that mice display the alpha-Gal epitope on their cell surfaces; consequently, unlike humans they do not produce anti-Gal antibodies. An alpha-Gal knockout (KO) mouse has been generated, however, by deleting the glycosyltransferase that generates the alpha-Gal epitope. This strain is available to us (graciously provided by Dr. Galili).

A second requirement for *in vivo* testing is to implant xenografts that are both alpha(v) beta(3) integrin-positive and alpha-Gal negative. To this end, we tested a variety of murine cancer cell lines for the latter attribute. Using an enzyme-linked immunosorbent assay (ELISA, Figure 4), we identified that B16F10 cell line as lacking the alpha-Gal epitope. Moreover, several examples in the literature used this cell line in a xenograft model. We next examined whether this cell line displays alpha(v) beta(3) integrin. We employed both the RGD-fluorescein probe and antibodies directed against the heterodimeric receptor. These experiments indicated that, while alpha(v) beta(3) appears to be present, its cell surface concentration is low (data not shown). Given this result, we are currently investigating methods to increase the number of integrin markers (i.e., transfection of the receptor) and examining other cell types that might have both of the key

characteristics required to test our strategy *in vivo*. It is these experiments we hope to pursue in future studies.

KEY RESEARCH ACCOMPLISHMENTS

- Synthesized a functionalized RGD peptidomimetic ligand (with a linker and a handle for later bioconjugation reactions) that maintains high affinity and excellent selectivity for alpha(v) beta(3) integrin.
- Synthesized of a bifunctional conjugate composed of an immunogenic trisaccharide (alpha-Gal) attached to the RGD mimetic (compound **1**).
- Demonstrated that the bifunctional ligand **1** can bind selectively to cells displaying the alpha(v) beta(3) integrin.
- Found that the bifunctional ligand can bind simultaneously to both alpha(v) beta(3) integrin and the anti-Gal epitope **1**.
- Developed a fluorescence-based assay for complement-dependent cytotoxicity
- Showed that the bifunctional ligand **1** can promote anti-Gal recruitment to tumor cells and subsequent complement-mediated killing of tumor cells.
- Synthesized a traditional anti-cancer agent consisting of the toxin doxorubicin and the integrin ligand (compound **2**).
- Identified a panel of tumor cell lines expressing different levels of the alpha(v) beta(3) integrin using compound **3**.
- Demonstrated that bifunctional ligand **1** promotes selective cell killing and that only those cells with high levels of surface integrin are destroyed. We also showed that this cytotoxicity profile is dramatically different than that of traditional targeted anti-cancer agents, such as conjugate **2**.

REPORTABLE OUTCOMES

Peer-reviewed manuscripts

1. Owen, R.M., Carlson, C.B., Xu, J., Mowery, P., Fasella, E., Kiessling, L.L. "Bifunctional ligands that target cells displaying the alpha(v) beta(3) integrin" *ChemBioChem* **2007** *8* (1), 68−82.

2. Carlson, C.B., Mowery, P., Owen, R.M., Dykhuizen, E.C., Kiessling, L.L. "Selective tumor cell targeting using low-affinity, multivalent interactions" *ACS Chem. Biol*. **2007** 2 (2), 119−127.

News and attention from scientific community

The 2007 paper published in *ACS Chemical Biology* did receive some noteworthy attention from the scientific community and was highlighted in various places around the web.

3. Our research article was featured on the cover of the Feb 2007 issue of the journal.

   http://pubs3.acs.org/acs/journals/toc.page?incoden=acbcct&involume=2&inissue=2

4. News highlight in *Chemical and Engineering News*, "Strength in numbers" written by Celia Henry Arnaud.

   http://pubs.acs.org/cen/news/85/i08/8508notw6.html

Poster / Oral presentations

5. C.B. Carlson, R.M. Owen, P. Mowery, J.A. Hank, P.M. Sondel, L.L. Kiessling. "Bifunctional immunotherapeutic agents for the treatment of cancer." Abstracts of Papers, 228th ACS National Meeting, Philadelphia, PA (2004).

6. C.B. Carlson, R.M. Owen, P. Mowery, E.C. Dyhuizen, L.L. Kiessling. "Bifunctional ligands for selective cell targeting via multivalent interactions". AACR-NCI-EORTC International Conference, Philadelphia, PA (2005).

Funding applied for based on work supported by this award

Based on the progress I achieved with this basic science award, my co-mentors (Laura Kiessling and Paul Sondel) are now pursuing translational science and will be submitting the next phase of this project to the DoD ovarian cancer mechanism for a new grant.

7. Dept. of Defense Ovarian Cancer Research Program Application, Translational Research Partnership "*Ovarian Cancer Immunotherapy Using Redirected Endogenous Anti-Gal Antibody***".**

Patents, licenses, degrees, cell line development, tissue or serum repositories, etc.

N/A

CONCLUSION

This project has allowed us to blend various area of science (e.g., xenotransplantation, synthetic organic chemistry, immunology, and the integrin family of receptors) to tell a complete story that highlights molecular recognition on various levels. Additionally, our basic research has produced a lead compound that we hope to carry through further to pre-clinical and translational studies.

REFERENCES

1. Galili, U., LaTemple, D.C., Radic, M.Z. Transplantation (1998) 65, 1129–1132.

All other relevant references pertaining work that influenced this research project can be found in our *ChemBioChem* and *ACS Chemical Biology* publications.

APPENDICES

Please refer to the *ChemBioChem* and *ACS Chemical Biology* journal articles below.

SUPPORTING DATA

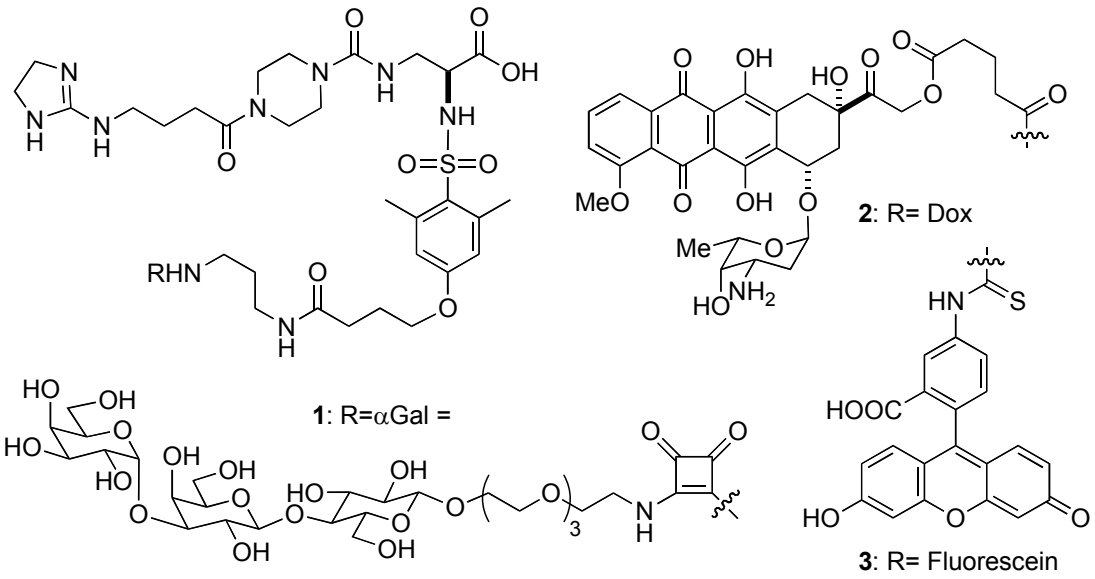

Figure 1. Structures of bifunctional molecules used in the reported anti-cancer studies. Compound **1**, which consists of an alpha(v) beta(3) integrin ligand linked to the alpha-Gal trisaccharide, was designed to test the feasibility of the new anti-cancer strategy that depends upon multivalent binding. Bifunctional conjugate **2** is composed of the integrin ligand linked to doxorubicin (Dox), an anti-cancer agent used in the clinic; its ability to kill tumor cells does not depend on multivalent binding. Attachment of a fluorophore to the integrin ligand generates fluorescent probe **3**, which was employed in microscopy and flow cytometry.

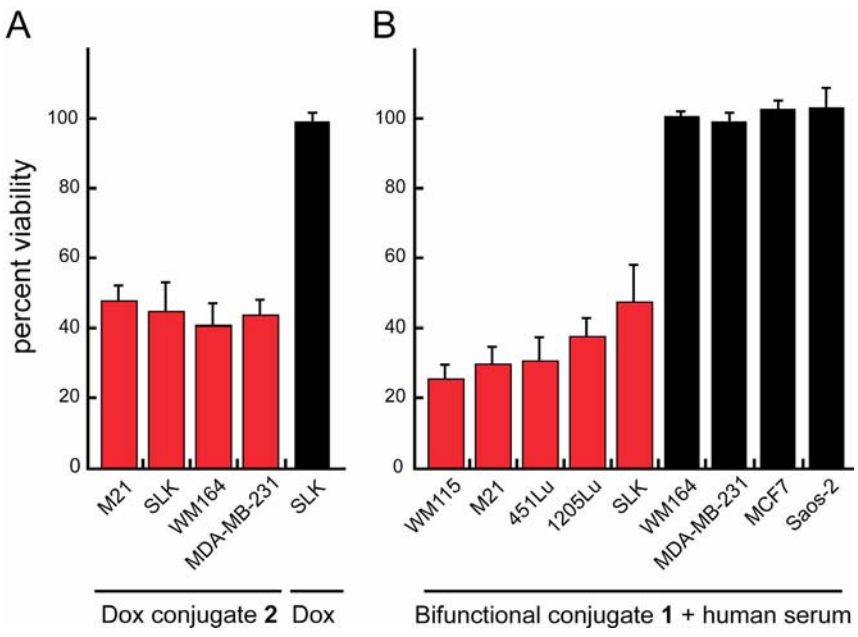

Figure 2. Bifunctional conjugate **1** mediates selective cell killing. a) Four cell lines were treated with compound **1** and their cell viability was assessed using a standard tetrazolium salt-based (MTT) assay. Treatment with the Dox conjugate resulted in >50% cell death, irrespective of the levels of alpha(v) beta(3) integrin (red). Unmodified Dox (25 nM) had no effect on the cells (black); b) Data from all nine cell lines tested in the complement-dependent cytotoxicity assay. The cell lines that were lysed efficiently following treatment with bifunctional ligand **1** (10 nM) and human serum are shown in red; those that were unaffected are depicted in black.

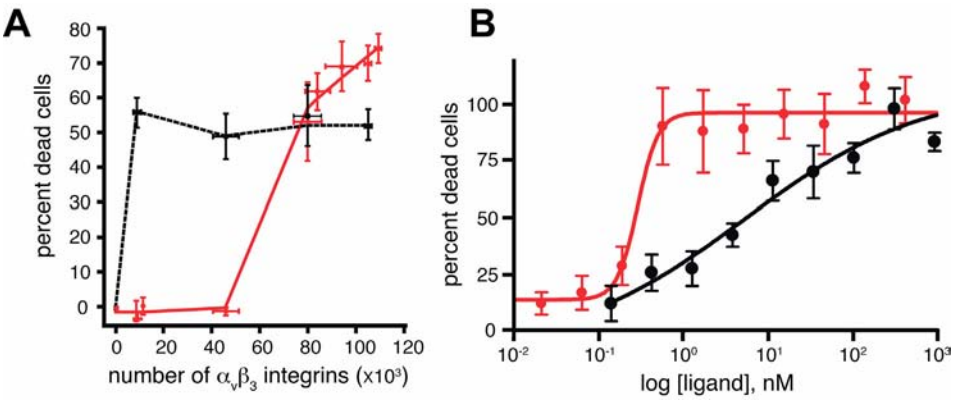

Figure 3. Features of cell recognition by multivalent interactions. A: The number of alpha(v) beta(3) integrin receptors available for binding is plotted against the percentage of dead cells (data from Figure 2). A minimum number of cell-surface target receptors is required to generate a functional multivalent interaction with anti-Gal antibodies following treatment with bifunctional conjugate **1**. The dashed black curve denotes the activity of the Dox conjugate **2**. It kills cells displaying high and low levels of the target receptor. Conversely, cells with a low concentration of integrin receptor are unaffected by alpha-Gal-mediated cytotoxicity, as shown by the solid red curve. B. Dose response curves for compounds **2** (Dox conjugate, black) or **1** (bifuncitional ligand, red). There is marked concentration dependence for the ability of compound **1** to effect cell death, which is indicative of a process involving cooperative multivalent interactions. The gradual dependence on concentration for the doxorubicin conjugate **2** is typical of a process that involves monovalent interactions.

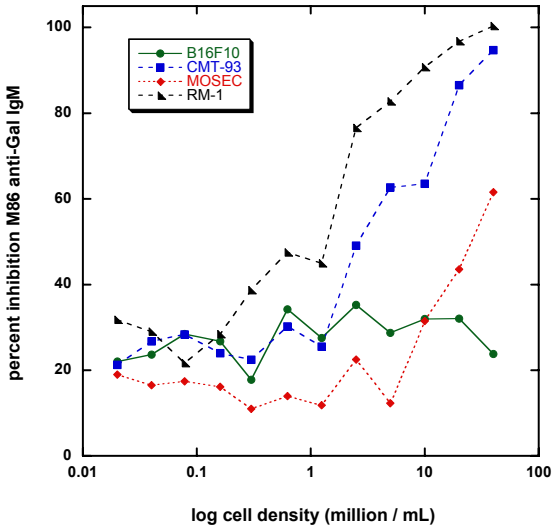

Figure 4. ELISA to test for alpha-Gal epitope on the surface of murine tumor cell lines. This experiment was adapted from a published procedure (see Reference 1). B16F10 cells (green curve) were determined to not have alpha-Gal present on its cell surface, as compared to CMT-93, MOSEC, and RM-1.

FINAL REPORT BIBLIOGRAPHY

All final reports must include a bibliography of all publications and meeting abstracts and a list of personnel (not salaries) receiving pay from the research effort.

Owen, R.M., Carlson, C.B., Xu, J., Mowery, P., Fasella, E., Kiessling, L.L. "Bifunctional ligands that target cells displaying the alpha(v) beta(3) integrin" *ChemBioChem* **2007** *8* (1), 68–82.

Carlson, C.B., Mowery, P., Owen, R.M., Dykhuizen, E.C., Kiessling, L.L. "Selective tumor cell targeting using low-affinity, multivalent interactions" *ACS Chem. Biol*. **2007** 2 (2), 119–127.

C.B. Carlson, R.M. Owen, P. Mowery, J.A. Hank, P.M. Sondel, L.L. Kiessling. "Bifunctional immunotherapeutic agents for the treatment of cancer." Abstracts of Papers, 228th ACS National Meeting, Philadelphia, PA (2004).

C.B. Carlson, R.M. Owen, P. Mowery, E.C. Dykhuizen, L.L. Kiessling. "Bifunctional ligands for selective cell targeting via multivalent interactions". AACR-NCI-EORTC International Conference, Philadelphia, PA (2005).

Personnel supported:

Coby B. Carlson – postdoctoral

April Weir – graduate student

ARTICLE

ACS chemical biology

Selective Tumor Cell Targeting Using Low-Affinity, Multivalent Interactions

Coby B. Carlson[†,‡], Patricia Mowery[‡], Robert M. Owen[†], Emily C. Dykhuizen[†], and Laura L. Kiessling[†,‡,§,*]

[†]Department of Chemistry, 1101 University Avenue, University of Wisconsin–Madison, Madison, Wisconsin 53706, [‡]Department of Biochemistry, 433 Babcock Drive, University of Wisconsin–Madison, Madison, Wisconsin 53706, and [§]University of Wisconsin Comprehensive Cancer Center, Madison, Wisconsin 53706

ABSTRACT This report highlights the advantages of low-affinity, multivalent interactions to recognize one cell type over another. Our goal was to devise a strategy to mediate selective killing of tumor cells, which are often distinguished from normal cells by their higher levels of particular cell surface receptors. To test whether multivalent interactions could lead to highly specific cell targeting, we used a chemically synthesized small-molecule ligand composed of two distinct motifs: (1) an Arg-Gly-Asp (RGD) peptidomimetic that binds tightly ($K_d \approx 10^{-9}$ M) to $\alpha_v\beta_3$ integrins and (2) the galactosyl-α(1–3)galactose (α-Gal epitope), which is recognized by human anti-α-galactosyl antibodies (anti-Gal). Importantly, anti-Gal binding requires a multivalent presentation of carbohydrate residues; anti-Gal antibodies interact weakly with the monovalent oligosaccharide ($K_d \approx 10^{-5}$ M) but bind tightly ($K_d \approx 10^{-11}$ M) to multivalent displays of α-Gal epitopes. Such a display is generated when the bifunctional conjugate decorates a cell possessing a high level of $\alpha_v\beta_3$ integrin; the resulting cell surface, which presents many α-Gal epitopes, can recruit anti-Gal, thereby triggering complement-mediated lysis. Only those cells with high levels of the integrin receptor are killed. In contrast, doxorubicin tethered to the RGD-based ligand affords indiscriminate cell death. These results highlight the advantages of exploiting the type of the multivalent recognition processes used by physiological systems to discriminate between cells. The selectivity of this strategy is superior to traditional, abiotic, high-affinity targeting methods. Our results have implications for the treatment of cancer and other diseases characterized by the presence of deleterious cells.

One hundred years have passed since Paul Ehrlich coined the term "magic bullet" to describe a chemotherapeutic that seeks out and kills disease-causing cells while leaving normal ones unaffected (*1*). This visionary concept remains an inspiration for many targeted drug strategies. Indeed, numerous anticancer drugs rely on the high-affinity monovalent interaction between a cell-binding agent (*e.g.*, monoclonal antibody or fragment thereof) and a tumor-associated antigen to direct a cytotoxic moiety selectively to the tumor (*2*). Despite the potential advantages of this strategy, this mode of cell recognition is abiotic. One critical consequence of such non-natural recognition is that it often lacks the required selectivity. Thus, the toxin can also be delivered to normal cells with low levels of the target receptor.

In physiological systems, multiple low-affinity interactions are used to distinguish one cell type from another (*3, 4*). We have shown previously that a multivalent presentation can improve not only the affinity but also the specificity of ligand–receptor interactions (*5, 6*). On the basis of these results, we sought to compare the selectivity of a traditional cell-targeting approach to an alternative that mimics natural cell recognition processes.

Our multivalent targeting strategy exploits a preexisting immune response that poses a major barrier to xenotransplantation. The immunological differences between humans and most other mammals have prevented the transfer of tissue and organs across species (*7*). The galactosyl-(1–3)galactose (α-Gal) carbohydrate epitope is abundantly expressed on the surface of nearly all mammalian and bacterial cells (*8*). Humans, apes, and Old World monkeys, however, do not display α-Gal on their cell surfaces because they lack the functional glycosyltransferase that catalyzes the assembly of

***Corresponding author,** Kiessling@chem.wisc.edu.

Received for review August 29, 2006 and accepted December 4, 2006.

Published online February 9, 2007

10.1021/cb6003788 CCC: $37.00

© 2007 by American Chemical Society

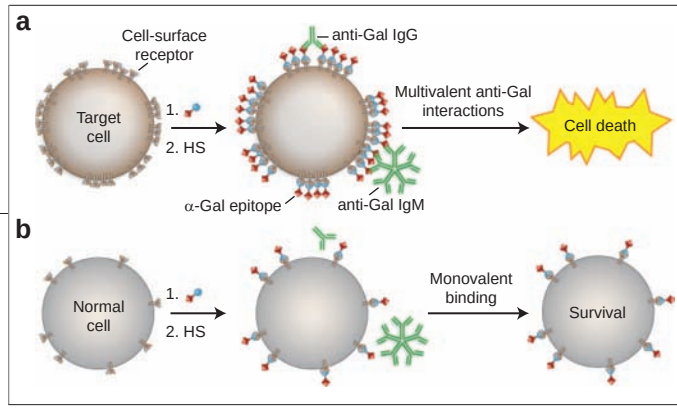

Figure 1. Graphical representation of cell-targeting strategy based on multivalent binding. A bifunctional conjugate ●–◆ (represented by the blue circles attached to red diamonds) binds with high affinity to a cell-surface receptor (*e.g.*, integrin) that is present in high concentration on a target cell. The blue circle represents an integrin ligand. The low-affinity α-Gal epitope (red diamond) recruits bivalent anti-Gal IgG (green) and decavalent anti-Gal IgM (green) when a noncovalent multivalent array is assembled on the cell surface. a) Cells displaying high levels of the target receptor recruit the antibody, which results in complement-mediated cell death. b) Cells with low levels of the target receptor are unaffected, because the monovalent anti-Gal interaction is weak.

this structure (*9*). Consequently, these species generate high concentrations of antibodies to this antigen. In humans, as much as 2% of the total IgG circulating in the bloodstream is anti-Gal (*10*), and the decavalent anti-Gal IgM isotype accounts for 3–8% of the total IgM (*10, 11*). These high antibody titers are maintained in humans throughout their lives, presumably in response to constant exposure to α-Gal found on bacteria within the normal intestinal flora (*12*).

Anti-Gal antibodies are potent activators of the classical complement pathway and are responsible for the hyperacute rejection of xenotransplanted organs (*13, 14*). Like many carbohydrate-binding proteins, anti-Gal antibodies interact only weakly with a single α-Gal epitope ($K_d \approx 10$ μM) but bind with higher functional affinity ($K_d \approx 10^{-11}$ M) to multivalent arrays of the saccharide (*15, 16*). Thus, the apparent binding affinity of anti-Gal is proportional to the valency of α-Gal epitopes presented. We envisioned, therefore, that anti-Gal antibodies could be recruited to selectively target unwanted cells that display high levels of α-Gal.

Bifunctional conjugates that bind to a cell-surface receptor and present α-Gal should render tumor cells susceptible to lysis. It has been shown that circulating antibodies can be redirected to a target cell using small molecules (*17–19*), and synthetic conjugates of α-Gal have been prepared (*20–23*). These studies, however, do not address the importance of multivalent binding, and the selectivity of such agents for cell targeting is unknown. Our objective was to test the utility and specificity of multivalent interactions for targeting cells (Figure 1). A synthetic bifunctional ligand, which uses noncovalent interactions to create a multivalent display on the cell surface, can recruit endogenous human anti-Gal antibodies to achieve highly selective cell killing.

RESULTS AND DISCUSSION

Design and Synthesis of Bifunctional Conjugates. To test our hypothesis, we needed a model system with a cell-surface receptor that is up-regulated on target cells but produced only at low levels by normal cells. We selected the $\alpha_v\beta_3$ integrin. The integrins are a superfamily of heterodimeric proteins that mediate cell–cell attachment and cellular adhesion to the extracellular matrix (*24–26*); many integrins act through recognition of the RGD tripeptide motif (*27, 28*). The $\alpha_v\beta_3$ integrin is displayed in elevated levels on both invasive tumor cells and the endothelium of the tumor vasculature (*29–35*). Because $\alpha_v\beta_3$ is a potential therapeutic target in cancer research, a wide range of small-molecule ligands are known (*36–38*). Several of these compounds have been successfully modified for applications that include molecular imaging, gene therapy, radiotherapy, and targeted drug delivery (*38, 39*).

DeGrado and coworkers previously identified the nonpeptidic RGD mimetic **1** (Figure 2) as a ligand that binds potently and selectively to $\alpha_v\beta_3$ over related integrins (*40*). Guided by the structure of the extracellular segment of $\alpha_v\beta_3$ bound to a cyclic RGD peptide derivative (*41*), we devised compound **2** (Figure 2). This compound possesses a linker terminating in an amino group for subsequent modification. Like the parent ligand **1**, derivatives of **2** bind to $\alpha_v\beta_3$ with high affinity and selectivity (*42*). We used amine **2** to prepare three different bifunctional ligands. First, we treated compound **2** with fluorescein isothiocyanate to generate probe **3** (Figure 2), which provides a means to analyze the levels of $\alpha_v\beta_3$ on various cell lines. Second, we chemically modified doxorubicin (DOX) (*43*) so that it could be appended to compound **2** to yield the cytotoxic agent **4** (Figure 2). This conjugate should exert its deleterious effects subsequent to monovalent binding to the cell surface. Finally, we used conjugate **5**, which was generated *via* dimethyl squarate-mediated coupling (*44*) between compound **2** and the Galα(1–3)Galβ(1–4)Glc trisaccharide possessing an amine-bearing poly(ethylene glycol) linker (Figure 2) (*42*).

Evaluating Cell-Surface Receptor Levels. To investigate the ability of bifunctional conjugate **5** to selectively induce cytotoxicity, we required cells displaying varying amounts of $\alpha_v\beta_3$ integrin. Flow cytometry has been used previously to assess the concentration of both α_v and β_3 integrin subunits, as well as the heterodimer, on different cell lines (*34, 35, 45, 46*). Anti-

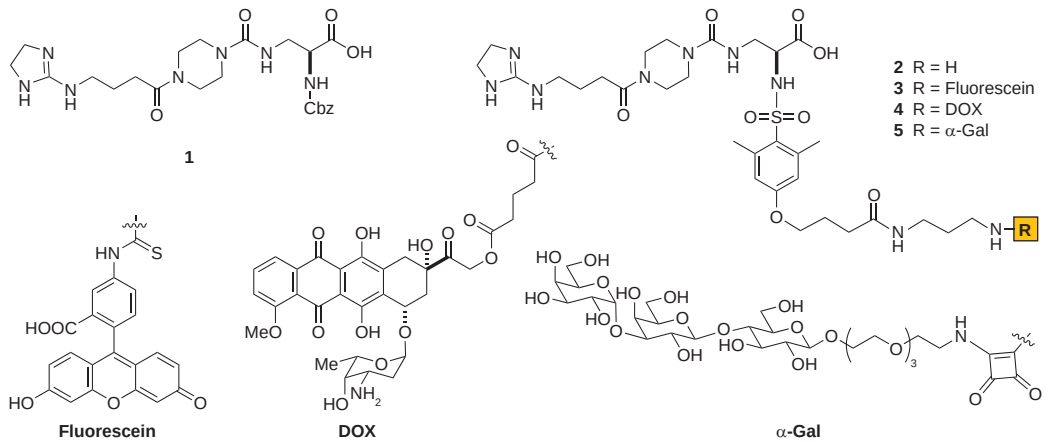

Figure 2. Chemical structures of small-molecule integrin ligands used in this study. The parent compound 1 is a peptidomimetic that selectively binds the $\alpha_v\beta_3$ integrin. It inspired the design of 2, which bears a linker for conjugation to other moieties. Compound 2 can be functionalized to append a fluorophore (3), a cancer chemotherapeutic (4), or the α-Gal carbohydrate epitope (5).

bodies are typically used to measure integrin levels (*e.g.*, anti-human integrin monoclonal antibody followed by a secondary fluorescein-labeled antibody). The number of functionally active $\alpha_v\beta_3$ integrins on the cell surface, however, is the relevant parameter for our targeting strategy. Thus, we took a direct approach to detect those receptors accessible to the integrin ligand.

Using fluorescent integrin ligand **3**, we determined the number of active $\alpha_v\beta_3$ integrins on the cell surface. We conducted titration experiments using nine different human cancer cell lines, including 451Lu, 1205Lu, M21, MCF7, MDA-MB-231, Saos-2, SLK, WM115, and WM164. The modified integrin ligand bound with similar affinity to each cell type (average K_d value of 1.14 ± 1.05 nM; Figure 3, panel a, and Supporting Information). These results are consistent with previously reported binding data (*40*). We used a saturating concentration of probe **3** (10 nM) to measure the mean fluorescence intensity (MFI) for each cell line. In this way, we could compare MFI values (calibrated with fluorescent microspheres) to quantitate the levels of "targetable" $\alpha_v\beta_3$ integrin (Figure 3, panel b). M21 and WM115 cells displayed >100,000 receptors per cell, and we classified these levels as high. MCF7, MDA-MB-231, and Saos-2 cells had much lower levels of this integrin (<10,000 per cell). The amount of detectable cell-surface $\alpha_v\beta_3$ on the remaining cell lines (451Lu, 1205Lu, SLK, and WM164) was intermediate. Thus, with a series of cell lines possessing different amounts of the target receptor, we were poised to assess the importance of multivalent binding.

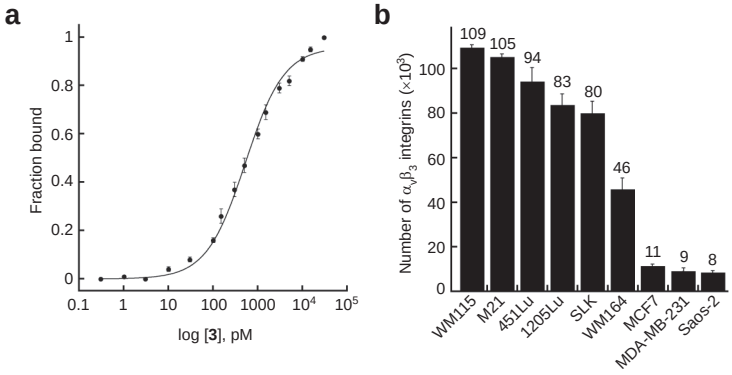

Figure 3. Analysis of $\alpha_v\beta_3$ integrin levels on target cell lines. a) A binding curve generated using flow cytometry for interaction of the fluorescein-labeled derivative 3 with WM115 cells. The apparent dissociation constant (K_d) for this interaction was 0.5 ± 0.04 nM. b) Histogram showing the number of cell-surface integrins measured using flow cytometry with a saturating concentration of derivative 3 (10 nM) and various cell lines.

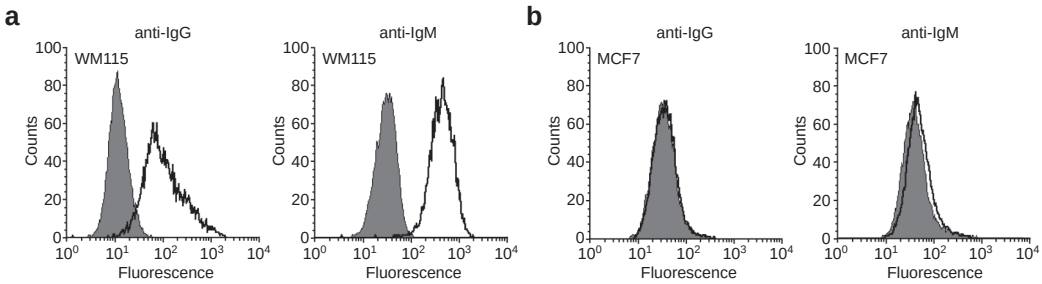

Figure 4. Recruitment of anti-Gal antibodies to the cell surface *via* binding of the bifunctional conjugate 5. Representative flow cytometry plots illustrating the binding of anti-Gal IgG and IgM to a) WM115 cells (high levels of $\alpha_v\beta_3$) and b) MCF7 cells (low levels of $\alpha_v\beta_3$). The MFI was measured after cells were treated with 5, incubated with heat-inactivated HS, and labeled with fluorescein-conjugated goat anti-human IgG or IgM secondary antibodies. WM115 cells showed a positive log shift compared with untreated controls. No antibody binding was detected to MCF7 cells.

Cell and Antibody Binding of Bifunctional α-Gal Conjugate 5. For our synthetic conjugate to function as designed, it must simultaneously bind $\alpha_v\beta_3$ and anti-Gal antibodies. As mentioned above, we recently reported the utility of a series of α-Gal-conjugated RGD mimetics as cell-surface targeting agents and recruiters of anti-Gal antibodies (*38*). In the course of these studies, we developed a fluorescence-based cell adhesion assay to test the binding of these ligands to integrins on cells. The measured IC_{50} values for compound **1** and bifunctional conjugate **5** for $\alpha_v\beta_3$ were 8.1 ± 2 and 1.8 ± 0.2 nM, respectively (*42*). These data are consistent with previously published data for the parent peptidomimetic (IC_{50} value = 1.1 nM) (*40*).

When multiple copies of conjugate **5** bind to $\alpha_v\beta_3$ complexes on the cell surface, a multivalent display of α-Gal is assembled. To evaluate whether anti-Gal IgG and IgM antibodies can bind such a display, we exposed the WM115 and MCF7 cell lines to **5** and then to normal human serum (HS) (a source of anti-Gal). Washed cells were stained with fluorescein-labeled goat anti-human secondary antibodies and subsequently analyzed by flow cytometry. The data indicate that WM115 cells, which display high levels of $\alpha_v\beta_3$, bind anti-Gal IgG and the higher valency IgM (Figure 4, panel a). In contrast, no anti-Gal antibody binding could be detected with MCF7 cells presenting low levels of $\alpha_v\beta_3$ (Figure 4, panel b). These results indicate that upon interaction of the conjugate with cell-surface integrin, anti-Gal can be recruited. Thus, both the anti-Gal-binding epitope and the integrin-binding moiety are accessible to their protein targets (*42*). The finding that anti-Gal is recruited only to the cell displaying a high level of $\alpha_v\beta_3$ integrin highlights the sensitivity of anti-Gal binding to α-Gal epitope valency.

Cytotoxicity of the DOX Conjugate Does Not Depend on $\alpha_v\beta_3$ Levels. RGD-based peptides linked to the cytotoxic agent DOX can induce apoptosis in the tumor vasculature with enhanced efficacy and reduced cytotoxicity (*47–49*). Therefore, we envisioned that compound **4** could serve as an archetype of a traditional targeted chemotherapeutic. Using a standard tetrazolium salt-based method of assessing cell viability (*50*) with a variety of cell lines, we compared the cytotoxicity of **4** to that of free DOX. Upon treatment with compound **4**, we observed significant cytolysis (>50% dead) of each cell line tested (Figure 5, panel a); in contrast, cells were unaffected when exposed to the same concentration of free DOX (25 nM). Indeed, no significant cytotoxicity was observed with free DOX up to 0.5 μM (data not shown). These results emphasize a major problem associated with approaches that rely on monovalent interactions for cell killing: there is little discrimination between cells with low levels of the target receptor and those with high levels.

Conjugate 5 Is Only Cytotoxic to Cells with High $\alpha_v\beta_3$ Levels. To assess the cell-targeting selectivity of the α-Gal conjugate **5**, we employed a complement-dependent cytotoxicity assay. Briefly, cells were internally labeled with a fluorescein diacetate esterase substrate, treated with compound **5**, and exposed to HS; the serum serves as the source of both anti-Gal antibodies and complement. If the bifunctional ligand can bind cell-surface $\alpha_v\beta_3$, recruit anti-Gal antibodies from HS, and activate the complement cascade, cytolysis would occur. Live cells were detected using a fluorescent plate reader. Untreated cells produce the maximum fluorescence emission; a decrease in this signal corresponds to a decrease in the population of live cells, or cytotoxicity. We tested each of the cell lines and observed lysis (>60% dead) of five of the nine cell lines (Figure 5, panel b, red bars). Intriguingly, only those cells express-

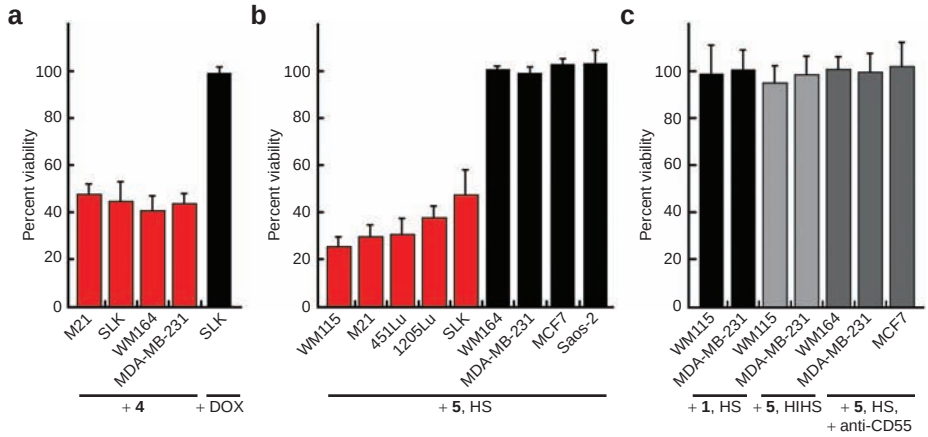

Figure 5. Bifunctional conjugate 5 mediates selective cell killing. a) The viability of four cell lines treated with compound 4 was evaluated using a standard tetrazolium-salt-based assay. Treatment with the DOX conjugate resulted in >50% cell death, irrespective of the levels of $\alpha_v\beta_3$ integrin (red). Unmodified DOX (25 nM) had no effect on the cells tested at this concentration (black). b) Data from all nine cell lines tested in the complement-dependent cytotoxicity assay. The cell lines that were lysed efficiently following treatment with bifunctional ligand 5 (10 nM) and HS are shown in red; those that were unaffected are depicted in black. c) Control experiments for the complement lysis assay are depicted. These include treatment with compound 1 (no α-Gal epitope) and HS (black), the α-Gal conjugate 5 and HIHS (light gray), and 5 with HS in the presence of an anti-CD55 function-blocking antibody (dark gray).

ing high levels of the target receptor were killed. For cell types with low levels of $\alpha_v\beta_3$, complement-mediated destruction was not observed (Figure 5, panel b).

The Cytotoxic Effects of Bifunctional Ligand 5 Depend on Complement-Mediated Lysis. We conducted several experiments to probe the mechanism of the observed cytotoxicity. First, we tested whether the cytotoxic response depends on the display of α-Gal moieties. When the parent compound **1** (which cannot recruit anti-Gal to the cell surface) was employed, no cell killing was observed (Figure 5, panel c). To determine whether the induced response was complement-mediated, we incubated cells with conjugate **5** and heat-inactivated HS (HIHS). This protocol should denature critical complement proteins but does not abolish anti-Gal antibody binding (*10*). Again, no lysis was detected (Figure 5, panel c, light gray bars). Finally, we sought to determine whether nonlysed cell lines were able to evade cellular destruction through the protective effects of one or more complement-regulating proteins (*51*). We used flow cytometry and monoclonal antibodies to known complement regulators (CD46, CD55, and CD59) to analyze three of the four cell lines that were not lysed (WM164, MDA-MB-231, and MCF7) and one that was destroyed (WM115). Only CD55, the receptor previously implicated in complement avoidance in relation to anti-Gal (*52*), was present on the cell surface in significant amounts (see Supporting Information). When we repeated the experiment in the presence of an anti-CD55 antibody, which is known to block the protective function of CD55, no cytolysis was detected (Figure 5, panel c, dark gray bars). Together, these results indicate that the bifunctional ligand **5** is much more selective than traditional cell-targeting agents.

Enhancing Cell-Targeting Selectivity with Multivalency. The exquisite selectivity of α-Gal conjugate **5** contrasts dramatically with that observed for the DOX-linked compound **4**. These differences can be visualized by comparing their relative cell-killing abilities (Figure 6, panel a). Our results with compound **4** are consistent with those of others in which the attachment of a "tumor-homing" agent to DOX results in selectivity for cells that display the target receptor over those that do not (*47–49*). Our data, however, underscore that this selectivity is limited. Thus, conjugates like **4** can kill cells with even low concentrations of targeted cell-surface receptor. Because it can be difficult to identify surface receptors unique to cancer cells, chemotherapeutic agents with such properties are expected to have deleterious side effects.

In contrast to **4**, compound **5** is a highly discriminating cell-targeting agent. It can distinguish between cells

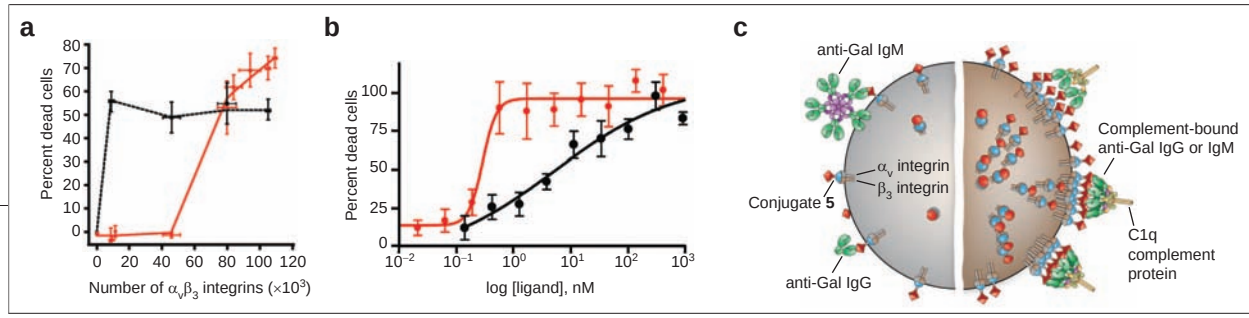

Figure 6. Features of cell recognition by multivalent interactions. a) The number of $\alpha_v\beta_3$ integrin receptors available for binding (data from Figure 3, panel b) is plotted against the percentage of dead cells (data from Figure 5, panel b). The dashed black curve describes the activity of the DOX conjugate 4. It kills cells displaying high and low levels of the target receptor. Conversely, cells with a low concentration of integrin receptor are unaffected by α-Gal-mediated cytotoxicity, as shown by the solid red curve. Bifunctional conjugate 5 results in selective lysis of cell lines with high levels of the target receptor. The cell death response is described by a curve with a much steeper slope and is similar to that displayed in panel b for compound 5. b) Dose response curves for compounds 4 (black) and 5 (red). Cell death by compound 5 displays a marked concentration dependence, an attribute indicative of a process involving cooperative multivalent interactions. The gradual dependence on concentration for the DOX conjugate 4 is typical of a process that involves monovalent interactions. c) A pictorial depiction of complement-mediated cell lysis through interaction with anti-Gal. This process involves several different types of multivalent interactions: anti-Gal binds avidly when it can interact with multiple α-Gal epitopes (as shown on the right), and complement is recruited more effectively when multiple copies of anti-Gal are bound.

with different levels of the target $\alpha_v\beta_3$ integrin receptor (Figure 6, panel a). One explanation for its remarkable selectivity is that cell killing is mediated through low-affinity, multivalent interactions. Because anti-Gal antibodies interact weakly with monovalent epitopes, any interaction with the α-Gal conjugate in solution will be transient. Similarly, anti-Gal is not recruited to cells displaying low levels of α-Gal residues. Only those cells with high levels of α-Gal residues on their surfaces can capture the bivalent (IgG) or decavalent (IgM) antibodies with sufficient avidity.

If cooperative multivalent interactions are critical for the activity of **5**, the concentration curves for cell killing by **5** should be steeper than those for **4**. Using WM115 cells, which possess high levels of $\alpha_v\beta_3$, we generated dose response curves for **4** and **5** (Figure 6, panel b). Compound **4** exhibits cytoxicity over a broad concentration range. In contrast, small changes in the concentration of bifunctional ligand **5** result in large changes in activity. These data provide further support that compound **4** functions *via* monovalent interactions but cell killing by compound **5** depends on multivalency.

Several steps in the cascade of events that culminate in complement-mediated cell lysis involve multivalency. When anti-Gal antibodies of the IgM class engage in multivalent interactions with the target cells, they expose a binding site for the multimeric C1q protein of the complement system. C1q binding initiates a cascade of protease activity, which results in the assembly of a membrane attack complex (MAC). It is this MAC that mediates lysis of the target cell. Thus, the complement system, which is composed of >30 proteins, also depends on multivalent interactions. Accordingly, our strategy exploits multivalent interactions for both cell recognition and cell killing by the immune system (Figure 6, panel c). Intriguingly, the data suggest that there is a threshold response: only cells with sufficient levels of the target $\alpha_v\beta_3$ receptor are destroyed.

Exploiting Multivalency Using Low-Molecular-Weight Ligands. The strategy presented herein has advantages that go beyond its selectivity. Specifically, the mechanism by which the bifunctional ligands trigger cellular destruction does not rely on a non-natural toxin but rather on an endogenous immune response. Because humans are constantly exposed to the α-Gal antigen, a supply of anti-Gal in circulation is ensured. Moreover, unlike the situation with traditional toxins, the agent used for cell killing in our strategy (complement) is tightly controlled and therefore harmless to normal cells. Another major benefit of our strategy is that it employs low-molecular-weight compounds. Many tumor-targeting strategies rely on macromolecular agents, such as antibodies. Although the mode of action of our bifunctional ligands depends on multivalent recognition, the agents we describe are small-molecule ligands. As a consequence, they sidestep problems associated with macromolecular therapeutic agents.

A key feature of the design of our bifunctional conjugate is its modularity. The linkers, cell-surface targeting agent, and low-affinity epitope can be varied, thus affording the means to readily optimize the biological activity of the small molecules. Moreover, this design can be used to target more than one receptor on the cell surface. Another method to achieve selective cell targeting is to engage multiple types of up-regulated receptors. A highly selective cocktail of bifunctional ligands that bind and recruit complement to cancer cells, for example, would be extremely valuable. Finally, though we have presented our strategy in the context of cancer immunotherapy, we predict that this approach will have applications beyond tumor destruction.

Conclusion. As the mechanism of complement-mediated cell lysis indicates, physiological systems

rely on low-affinity, multivalent interactions to distinguish between normal and unwanted target cells. An advantage of such processes is that highly specific recognition can be achieved. Our results indicate that the multivalent recognition mode that we employ can be exploited to selectively direct an endogenous immune response to destroy target cells. We envision that this general strategy and the principles underlying it will lead to new classes of therapeutic agents.

METHODS

Reagents. All chemicals used were purchased from Sigma-Aldrich unless otherwise noted. All cell culture reagents, including minimal essential medium alpha (αMEM), Dulbecco's modified eagle medium (DMEM), Roswell Park Memorial Institute-1640 medium (RPMI), fetal bovine serum (FBS), penicillin–streptomycin (pen–strep), L-glutamine, bovine insulin, and trypsin–EDTA, were purchased from Invitrogen. Accutase cell detachment solution was acquired from Innovative Cell Technologies, Inc. Tissue culture flasks for adherent cells were obtained from Sarstedt. 2′,7′-Bis-(2-carboxyethyl)-5-(and-6)-carboxyfluorescein, acetoxymethyl ester (BCECF-AM) was purchased from Molecular Probes. Bovine serum albumin (BSA) was obtained from Research Organics. V-shaped 96-well plates were obtained from Nalge Nunc, International. Fibrinogen and vitronectin were from CalBiochem. Quantum FITC Premixed MESF Kit was from Bangs Laboratories, Inc. (Fishers, IN). Antibodies mouse anti-human integrin $\alpha_v\beta_3$ (clone LM609), mouse anti-human CD55, FITC-labeled rat anti-mouse IgG, and FITC-labeled goat anti-human IgG and IgM were purchased from Chemicon, International, Lab Vision Corporation, BD Biosciences, and Vector Laboratories, respectively.

Synthesis of Bifunctional Conjugates. Routes to the parent RGD peptidomimetic and its conjugation to the α-Gal trisaccharide epitope (compounds **1**, **2**, and **5**) have been published (*42*). The fluorescent derivative (compound **3**) was generated from the trifluoroacetate salt of amine **2** (1.4 mg, 0.0017 mmol, 1 equiv), which was dissolved in 50 mM borate buffer at pH 9 (100 μL). To this mixture, fluorescein isothiocyanate (0.7 mg, 1.1 equiv) in dimethylformamide (30 μL) was added. The reaction was stirred at RT for 4.5 h and then quenched with 0.2 M AcOH in H_2O (100 μL). The product was purified by HPLC on a Vydac C18 semi-prep column using a 30 min gradient of 0–50% (v/v) CH_3CN in H_2O containing 0.1% TFA (v/v) to yield conjugate **3** in 60% yield. Procedures for the synthesis of the DOX conjugate **4** are detailed in the Supporting Information.

Cell Lines. Human MDA-MB-231 and MCF7 breast carcinoma cells and WM115 melanoma cell lines were purchased from American Type Culture Collection. WM164, 451Lu, and 1205Lu human melanoma cells were obtained from Wistar Institute. M21 human melanoma cells (sorted for high levels of $\alpha_v\beta_3$) and Saos-2 osteosarcoma cells were provided by P.M. Sondel and S. Helfand (UW–Madison). SLK-1 Kaposi's sarcoma cell line was obtained from the National Institutes of Health (NIH) AIDS Research & Reference Reagent Program. All cells were grown either in αMEM, DMEM, or RPMI media with FBS (10%), pen–strep antibiotics (100 U), and glutamine (2 mM). MCF7 cells were grown as above with the addition of 0.01 mg mL^{-1} bovine insulin. Cells were detached from cell culture flasks with trypsin–EDTA for passage. For experiments, Accutase was used to minimize the effects of trypsin on $\alpha_v\beta_3$.

Anti-Gal Antibody Binding. Near confluent cells were harvested, washed, counted, and resuspended at a density of 4×10^5 cells mL^{-1} in integrin binding buffer [IB; 25 mM Tris-HCl, pH = 7.2, NaCl (150 mM), BSA (1.5% w/v), glucose (5 mM), $MgCl_2$ (1.5 mM), and $MnCl_2$ (1.5 mM)] for 60 min at 4 °C. Cells were then diluted to 2×10^5 cells mL^{-1} and incubated with compound **5** (10 nM) on ice for 60 min. Cells were washed with IB and resuspended in a 20% solution of HIHS obtained from a healthy donor. After a 60 min incubation on ice, cells were washed again with IB and incubated again at 4 °C with FITC-conjugated goat anti-human IgG or IgM antibody (5 μg mL^{-1}) for 30 min. Finally, propidium iodide (PI, 5 μg mL^{-1}) was added to washed cells and immediately analyzed for fluorescence using a FACSCalibur flow cytometer (Becton Dickinson). Data were analyzed using CellQuest software (Becton Dickinson). An identical assay omitting the bifunctional conjugate assessed background fluorescence. The relative fluorescence is reported as the ratio above background. Experiments were repeated in triplicate.

Levels of Cell-Surface Integrin $\alpha_v\beta_3$. Near confluent cells were harvested with Accutase and activated in IB as described above. Cells were then diluted to 2×10^5 cells mL^{-1} and incubated with fluorescein-labeled compound **3** (10 nM) on ice for 60 min. Cells were washed twice before being analyzed for fluorescence by flow cytometry. The linearity of the instrument was first validated using the Quantum FITC Premixed MESF Kit, and a standard fluorescence curve was then generated. Taking the signal (MFI) measured from samples stained with **3**, the resulting value for molecules of equivalent soluble fluorescence (MESF) was determined. The MESF unit corresponds to the fluorescence intensity of a given number of pure fluorochrome molecules in solution and, in our case, is equal to the number of $\alpha_v\beta_3$ integrins on the cell surface. Experiments were repeated at least three different times for each cell line.

Complement-Dependent Cytotoxicity Assay. Confluent cultures of cells were detached with Accutase, washed, counted, and resuspended at 1.25×10^6 cells mL^{-1} in PBS. Cells were fluorescently labeled with BCECF-AM (0.2 μg mL^{-1}) for 30 min at 37 °C and then washed and diluted to 4×10^5 cells mL^{-1} for activation in binding buffer. After 60 min on ice, cells were further diluted to 2×10^5 cells mL^{-1}, and conjugate **5** (10 nM) was added. V-shaped 96-well microtiter plates were treated with 200 μL of "blocking buffer" [25 mM Na_2CO_3, pH = 9.6, BSA (1.5% w/v), and Tween-20 (0.5% w/v)] for 2 h at rt. The blocking solution was removed, and the wells washed three times with 200 μL of IB. Ten thousand cells per well were added to the rinsed wells in the presence of 20% normal HS and incubated for a minimum of 2 h at 37 °C. Following this period, cells were spun at 500 rpm for 10 min in an Allegra 6KR centrifuge (Beckman Coulter), and nonlysed cells were quantified as the fluorescent signal was read from the bottom on an EnVision 2100 plate reader (Perkin Elmer). For maximum cell lysis, the cationic detergent cetyltrimethylammonium bromide was added to the wells at a 2% (w/v) final concentration. The spontaneous release of fluorescence (background, BG) was determined without addition of conjugate **5**. Cytotoxicity is calculated by the following equation: $[(\text{sample} - \text{BG})(\text{max} - \text{BG})^{-1}] \times 100$.

Cell Viability Assay for Determining Cytotoxicity of Conjugate 3. Confluent cultures of M21, WM164, MDA-MB-231, and Saos-2 cells were detached and resuspended in media at 100,000 cells mL^{-1} (M21 and WM164) or 250,000 cells mL^{-1} (MDA-MB-231 and Saos-2). One hundred microliters of these

cell suspensions were transferred to each well of a clear, flat-bottom 96-well microtiter plate (Corning) and incubated overnight. Wells were then treated with RGD–DOX conjugate **4** (25 nM) in DMEM for 18–24 h. All wells were then washed with fresh culture medium. Cytotoxicity was assessed using the CellTiter 96 AQueous non-radioactive cell proliferation assay kit from Promega. After addition of the 3-(4,5-dimethylthiazol-2-yl)-5-(3-carboxymethoxyphenyl)-2-(4-sulfophenyl)-2*H*-tetrazolium, inner salt solution, the plate was incubated for an additional 1–2 h. The absorbance at 490 nm was recorded using an ELx800 microplate reader from Bio-Tek Instruments, Inc. Maximum cell death was induced by adding a final concentration of 2% SDS (w/v) to 100 μL of the cell suspension. Untreated cells were considered to be "100% alive" in this assay. Cytotoxicity results are calculated by [sample − max][untreated − max]$^{-1} \times 100$ and are presented as percent viability. No significant cytotoxicity was observed with free DOX up to 0.5 μM.

Acknowledgments: This paper is dedicated to Samuel J. Danishefsky upon his receipt of the 2006 Award in Chemical Sciences from the National Academy of Sciences. We thank P. Sondel and J. Hank for numerous helpful conversations and Y. He for his expertise in carbohydrate chemistry. This research was supported by the Department of Defense (DoD) (Grant DAMD17-01-1-00757) and the National Institutes of Health (Grant AI55258). C.B.C. was supported by the DoD Breast Cancer Research Program (Grant W81XWH-04-1-0466). Views and opinions of and endorsements by the authors do not reflect those of the U.S. Army or the DoD. R.M.O. thanks Pharmacia Corp. for a fellowship. P.M. acknowledges the Molecular Biosciences Training Program (Grant GM07215). The UWCCC Flow Cytometry Facility is supported through Core Grant CA14520.

Supporting Information Available: This material is free of charge *via* the Internet.

Competing Interests Statement: The authors declare that they have no competing financial interests.

REFERENCES

1. Winau, F., Westphal, O., and Winau, R. (2004) Paul Ehrlich—in search of the magic bullet, *Microbes Infect. 6*, 786–789.
2. Wu, A. M., and Senter, P. D. (2005) Arming antibodies: prospects and challenges for immunoconjugates, *Nat. Biotechnol. 23*, 1137–1146.
3. Mammen, M., Chio, S.-K., and Whitesides, G. M. (1998) Polyvalent interactions in biological systems: implications for design and use of multivalent ligands and inhibitors, *Angew. Chem., Int. Ed. 37*, 2755–2794.
4. Kiessling, L. L., Gestwicki, J. E., and Strong, L. E. (2000) Synthetic multivalent ligands in the exploration of cell-surface interactions, *Curr. Opin. Chem. Biol. 4*, 696–703.
5. Kiessling, L. L., Gestwicki, J. E., and Strong, L. E. (2006) Synthetic multivalent ligands as probes of signal transduction, *Angew. Chem., Int. Ed. 45*, 2348–2368.
6. Mortell, K. H., Weatherman, R. V., and Kiessling, L. L. (1996) Recognition specificity of neoglycopolymers prepared by ring-opening metathesis polymerization, *J. Am. Chem. Soc. 118*, 2297–2298.
7. Galili, U. (2001) The α-gal epitope (Galα1–3Galβ1–4GlcNAc-R) in xenotransplantation, *Biochimie 83*, 557–563.
8. Galili, U., Clark, M. R., Shohet, S. B., Buehler, J., and Macher, B. A. (1987) Evolutionary relationship between the natural anti-Gal antibody and the Galα(1→3)Gal epitope in primates, *Proc. Natl. Acad. Sci. U.S.A. 84*, 1369–1373.
9. Galili, U., Shohet, S. B., Kobrin, E., Stults, C. L. M., and Macher, B. A. (1988) Man, apes, and Old World monkeys differ from other mammals in the expression of α-galactosyl epitopes on nucleated cells, *J. Biol. Chem. 263*, 17755–17762.
10. Galili, U., Rachmilewitz, E. A., Peleg, A., and Flechner, I. (1984) A unique natural human IgG antibody with anti-α-galactosyl specificity, *J. Exp. Med. 160*, 1519–1531.
11. Parker, W., Bruno, D., Holzknecht, Z. E., and Platt, J. L. (1994) Characterization and affinity isolation of xenoreactive human natural antibodies, *J. Immunol. 153*, 3791–3803.
12. Galili, U., Mandrell, R. E., Hamadeh, R. M., Shohet, S. B., and Griffiss, J. M. (1988) Interaction between human natural anti-α-galactosyl IgG and bacteria of the human flora, *Infect. Immun. 56*, 1730–1737.
13. Sandrin, M. S., Vaughan, H. A., Dabkowski, P. L., and McKenzie, I. F. C. (1993) Anti-pig IgM antibodies in human serum react predominantly with Gal(α1–3)Gal epitopes, *Proc. Natl. Acad. Sci. U.S.A. 90*, 11391–11395.
14. Mollnes, T. E., and Fiane, A. E. (2003) Perspectives on complement in xenotransplantation, *Mol. Immunol. 40*, 135–143.
15. Wieslander, J., Maansson, O., Kallin, E., Gabrielli, A., Nowack, H., and Timpl, R. (1990) Specificity of human antibodies against Galα(1–3)Gal carbohydrate epitope and distinction from natural antibodies reacting with Galα(1–2)Gal or Galα(1–4)Gal, *Glycoconjugate J. 7*, 85–100.
16. Wang, J.-Q., Chen, X., Zhang, W., Zacharek, S., Chen, Y., and Wang, P. G. (1999) Enhanced inhibition of human anti-Gal antibody binding to mammalian cells by synthetic α-Gal epitope polymers, *J. Am. Chem. Soc. 121*, 8174–8181.
17. Shokat, K. M., and Schultz, P. G. (1991) Redirecting the immune response: ligand-mediated immunogenicity, *J. Am. Chem. Soc. 113*, 1861–1862.
18. Bertozzi, C. R., and Bednarski, M. D. (1992) A receptor-mediated immune response using synthetic glycoconjugates, *J. Am. Chem. Soc. 114*, 5543–5546.
19. Lussow, A. R., Buelow, R., Fanget, L., Peretto, S., Gao, L., and Pouletty, P. (1996) Redirecting circulating antibodies *via* ligand–hapten conjugates eliminates target cells *in vivo*, *J. Immunother. 19*, 257–265.
20. Li, J., Zacharek, S., Chen, X., Wang, J., Zhang, W., Janczuk, A., and Wang, P. G. (1999) Bacteria targeted by human natural antibodies using α-Gal conjugated receptor-specific glycopolymers, *Bioorg. Med. Chem. 7*, 1549–1558.
21. Chen, Y., Zhang, W., Chen, X., Wang, J., and Wang, P. G. (2001) αGal-conjugated anti-rhinovirus agents: chemo-enzymatic syntheses and testing of anti-Gal binding, *J. Chem. Soc., Perkin Trans. 1*, 1716–1722.
22. Holle, L., Song, W., Hicks, L., Holle, E., Holmes, L., Wei, Y. Z., Li, J. H., Wagner, T., and Yu, X. Z. (2004) *In vitro* targeted killing of human endothelial cells by coincubation of human serum and NGR peptide conjugated human albumin protein bearing α(1-3) galactose epitopes, *Oncol. Rep. 11*, 613–616.
23. Naicker, K. P., Li, H., Heredia, A., Song, H., and Wang, L.-X. (2004) Design and synthesis of αGal-conjugated peptide T20 as novel antiviral agent for HIV-immunotargeting, *Org. Biomol. Chem. 2*, 660–664.
24. Hynes, R. O. (1992) Integrins—versatility, modulation, and signaling in cell-adhesion, *Cell 69*, 11–25.
25. Clark, E. A., and Brugge, J. S. (1995) Integrins and signal-transduction pathways—the road taken, *Science 268*, 233–239.
26. Giancotti, F. G., and Ruoslahti, E. (1999) Transduction–integrin signaling, *Science 285*, 1028–1032.
27. Ruoslahti, E., and Pierschbacher, M. D. (1987) New perspectives in cell-adhesion—RGD and integrins, *Science 238*, 491–497.
28. Plow, E. F., Haas, T. A., Zhang, L., Loftus, J., and Smith, J. W. (2000) Ligand binding to integrins, *J. Biol. Chem. 275*, 21785–21788.
29. Brooks, P. C., Montgomery, A. M. P., Rosenfeld, M., Reisfeld, R. A., Hu, T. H., Klier, G., and Cheresh, D. A. (1994) Integrin $\alpha_v\beta_3$ antagonists promote tumor-regression by inducing apoptosis of angiogenic blood-vessels, *Cell 79*, 1157–1164.

30. Hynes, R. O. (2002) A reevaluation of integrins as regulators of angiogenesis, *Nat. Med. 8*, 918–921.
31. Friedlander, M., Brooks, P. C., Shaffer, R. W., Kincaid, C. M., Varner, J. A., and Cheresh, D. A. (1995) Definition of two angiogenic pathways by distinct α_v integrins, *Science 270*, 1500–1502.
32. Pasqualini, R., Koivunen, E., and Ruoslahti, E. (1997) αv integrins as receptors for tumor targeting by circulating ligands, *Nat. Biotechnol. 15*, 542–546.
33. Arap, W., Pasqualini, R., and Ruoslahti, E. (1998) Cancer treatment by targeted drug delivery to tumor vasculature in a mouse model, *Science 279*, 377–380.
34. Wong, N. C., Mueller, B. M., Barbas, C. F., Ruminski, P., Quaranta, V., Lin, E. C., and Smith, J. W. (1998) α_V integrins mediate adhesion and migration of breast carcinoma cell lines, *Clin. Exp. Metastasis 16*, 50–61.
35. Allman, R., Cowburn, P., and Mason, M. (2000) *In vitro* and *in vivo* effects of a cyclic peptide with affinity for the $\alpha_V\beta_3$ integrin in human melanoma cells, *Eur. J. Cancer 36*, 410–422.
36. Miller, W. H., Keenan, R. M., Willette, R. N., and Lark, M. W. (2000) Identification and *in vivo* efficacy of small-molecule antagonists of integrin $\alpha_V\beta_3$ (the vitronectin receptor), *Drug Discovery Today 5*, 397–408.
37. Cacciari, B., and Spalluto, G. (2005) Nonpeptidic $\alpha_v\beta_3$ antagonists: recent developments, *Curr. Med. Chem. 12*, 51–70.
38. Meyer, A., Auemheimer, J., Modlinger, A., and Kessler, H. (2006) Targeting RGD recognizing integrins: drug development, biomaterial research, tumor imaging and targeting, *Curr. Pharm. Des. 12*, 2723–2747.
39. Temming, K., Schiffelers, R. M., Molema, G., and Kok, R. J. (2005) RGD-based strategies for selective delivery of therapeutics and imaging agents to the tumour vasculature, *Drug Resist. Updates 8*, 381–402.
40. Corbett, J. W., Graciani, N. R., Mousa, S. A., and DeGrado, W. F. (1997) Solid-phase synthesis of a selective $\alpha_V\beta_3$ integrin antagonist library, *Bioorg. Med. Chem. Lett. 7*, 1371–1376.
41. Xiong, J.-P., Stehle, T., Zhang, R., Joachimiak, A., Frech, M., Goodman, S. L., and Arnaout, M. A. (2002) Crystal structure of the extracellular segment of integrin $\alpha_V\beta_3$ in complex with an Arg-Gly-Asp ligand, *Science 296*, 151–155.
42. Owen, R. M., Carlson, C. B., Xu, J., Mowery, P., Fasella, E., and Kiessling, L. L. (2006) Bifunctional ligands that target cells displaying the αvβ3 integrin, *ChemBioChem 8*, 68–82.
43. Nagy, A., Schally, A. V., Armatis, P., Szepeshazi, K., Halmos, G., Kovacs, M., Zarandi, M., Groot, K., Miyazaki, M., Jungwirth, A., and Horvath, J. (1996) Cytotoxic analogs of luteinizing hormone-releasing hormone containing doxorubicin or 2-pyrrolinodoxorubicin, a derivative 500–1000 times more potent, *Proc. Natl. Acad. Sci. U.S.A. 93*, 7269–7273.
44. Tietze, L. F., Arlt, M., Beller, M., Gluesenkamp, K. H., Jaehde, E., and Rajewsky, M. F. (1991) Squaric acid diethyl ester: a new coupling reagent for the formation of drug biopolymer conjugates. Synthesis of squaric acid ester amides and diamides, *Chem. Ber. 124*, 1215–1221.
45. Samaniego, F., Young, D., Grimes, C., Prospero, V., Christofidou-Solomidou, M., DeLisser, H. M., Prakash, O., Sahin, A. A., and Wang, S. Z. (2002) Vascular endothelial growth factor and Kaposi's sarcoma cells in human skin grafts, *Cell Growth Differ. 13*, 387–395.
46. Dickerson, E. B., Akhtar, N., Steinberg, H., Wang, Z. Y., Lindstrom, M. J., Padilla, M. L., Auerbach, R., and Helfand, S. C. (2004) Enhancement of the antiangiogenic activity of interleukin-12 by peptide targeted delivery of the cytokine to $\alpha_V\beta_3$ integrin, *Mol. Cancer Res. 2*, 663–673.
47. Arap, W., Pasqualini, R., and Ruoslahti, E. (1998) Cancer treatment by targeted drug delivery to tumor vasculature in a mouse model, *Science 279*, 377–380.
48. de Groot, F. M. H., Broxterman, H. J., Adams, H., van Vliet, A., Tesser, G. I., Elderkamp, Y. W., Schraa, A. J., Kok, R. J., Molema, G., Pinedo, H. M., and Scheeren, H. W. (2002) Design, synthesis, and biological evaluation of a dual tumor-specific motive containing integrin-targeted plasmin-cleavable doxorubicin prodrug, *Mol. Cancer Ther. 1*, 901–911.
49. Burkhart, D. J., Kalet, B. T., Coleman, M. P., Post, G. C., and Koch, T. H. (2004) Doxorubicin-formaldehyde conjugates targeting $\alpha_V\beta_3$ integrin, *Mol. Cancer Ther. 3*, 1593–1604.
50. Mosmann, T. (1983) Rapid colorimetric assay for cellular growth and survival: application to proliferation and cytotoxicity assays, *J. Immunol. Methods 65*, 55–63.
51. Morgan, B. P., and Meri, S. (1994) Membrane-proteins that protect against complement lysis, *Springer Semin. Immunopathol. 15*, 369–396.
52. Jager, U., Takeuchi, Y., and Porter, C. D. (1999) Induction of complement attack on human cells by Gal(alpha1,3)Gal xenoantigen expression as a gene therapy approach to cancer, *Gene Ther. 6*, 1073–1083.

CHEMBIOCHEM

DOI: 10.1002/cbic.200600339

Bifunctional Ligands that Target Cells Displaying the $\alpha_v\beta_3$ Integrin

Robert M. Owen,[a] Coby B. Carlson,[a, b] Jinwang Xu,[a] Patricia Mowery,[b] Elisabetta Fasella,[a] and Laura L. Kiessling*[a, b, c]

*Strategies to eliminate tumor cells have long been sought. We envisioned that a small molecule could be used to decorate the offending cells with immunogenic carbohydrates and evoke an immune response. To this end, we describe the synthesis of bifunctional ligands possessing two functional motifs: one binds a cell-surface protein and the other binds a naturally occurring human antibody. Our conjugates combine an RGD-based peptidomimetic, to target cells displaying the $\alpha_v\beta_3$ integrin, with the carbohydrate antigen galactosyl-α(1–3)galactose [Galα(1–3)Gal or α-Gal]. To generate such bifunctional ligands, we designed and synthesized RGD mimetics **1b** and **2c**, which possess a free amino group for modification. These compounds were used to generate bifunctional derivatives **1c** and **2d**, with dimethyl squarate serving as the linchpin; thus, our synthetic approach is modular. To evaluate the binding of our peptidomimetics to the target $\alpha_v\beta_3$-displaying cells, we implemented a cell-adhesion assay. Results from this assay indicate that the designed, small-molecule ligands inhibit $\alpha_v\beta_3$-dependent cell adhesion. Additionally, our most effective bifunctional ligand exhibits a high degree of selectivity (4000-fold) for $\alpha_v\beta_3$ over the related $\alpha_v\beta_5$ integrin, a result that augurs its utility in specific cell targeting. Finally, we demonstrate that the bifunctional ligands can bind to $\alpha_v\beta_3$-positive cells and recruit human anti-Gal antibodies. These results indicate that both the integrin-binding and the anti-Gal-binding moieties can act simultaneously. Bifunctional conjugates of this type can facilitate the development of new methods for targeting cancer cells by exploiting endogenous antibodies. We anticipate that our modifiable $\alpha_v\beta_3$-binding ligands will be valuable in a variety of applications, including drug delivery and tumor targeting.*

Introduction

Methods to deliver biologically active compounds selectively to unwanted cells are needed. Cell-targeting agents have a wide range of potential therapeutic applications, including diagnostic imaging[1] and the destruction of cellular pathogens.[2,3] One especially attractive use of cell targeting is the selective delivery of cancer chemotherapeutic agents[4,5]—an objective that has prompted studies since Ehrlich described the "magic bullet" concept in 1906.[6] In the typical approach, a targeting moiety that recognizes a cancer-associated epitope is used to direct a cytotoxic drug or protein toxin. A major problem with this strategy is that the toxic agent often causes undesirable side effects.[7] Specifically, protein toxins and small-molecule anticancer agents can destroy not only the target cells but also normal ones. We envisioned an alternative strategy that relies on redirecting endogenous antibodies to cancer cells.

We sought to harness the natural human immune response against the α-Gal epitope to test our hypothesis.[8] This carbohydrate antigen is well known to be immunogenic; indeed, it serves as the major barrier in xenotransplantation.[9] Attempts to transplant porcine donor organs into primates have revealed the importance of hyperacute rejection as a complication. This rejection is mediated by complement, which is recruited when primate anti-Gal antibodies bind to the surface-display of α-Gal on the porcine donor cells.[10] Human cells do not display the α-Gal epitope, unlike most mammalian and bacterial cells.[11] Presumably, it is exposure to these foreign cells that elicits the high level of anti-Gal antibody found in humans. We reasoned that exploiting this known response to reject tumor cells could afford an attractive anticancer strategy. To test our hypothesis, we required bifunctional conjugates that contain, in addition to the α-Gal epitope, a targeting moiety that recognizes an appropriate cell-surface receptor relevant for cancer (Figure 1). Although many biomarkers are upregulated on tumor cells, we sought a receptor that can be targeted with ligands that bind with both high affinity and high specificity. To this end, we examined small-molecule inhibitors of the $\alpha_v\beta_3$ integrin.

Integrins are heterodimeric cell-adhesion receptors that facilitate communication between a cell and its surroundings.[12] Integrins comprise two separate polypeptide chains, and the

[a] *Dr. R. M. Owen, Dr. C. B. Carlson, Dr. J. Xu, Dr. E. Fasella, Prof. Dr. L. L. Kiessling*
Department of Chemistry, University of Wisconsin–Madison
Madison, WI 53706 (USA)

[b] *Dr. C. B. Carlson, Dr. P. Mowery, Prof. Dr. L. L. Kiessling*
Department of Biochemistry, University of Wisconsin–Madison
Madison, WI 53706 (USA)

[c] *Prof. Dr. L. L. Kiessling*
University of Wisconsin Comprehensive Cancer Center
Madison, WI 53706 (USA)
Fax: (+1) 608-265-0764
E-mail: kiessling@chem.wisc.edu

InterScience® DISCOVER SOMETHING GREAT

© 2007 Wiley-VCH Verlag GmbH & Co. KGaA, Weinheim

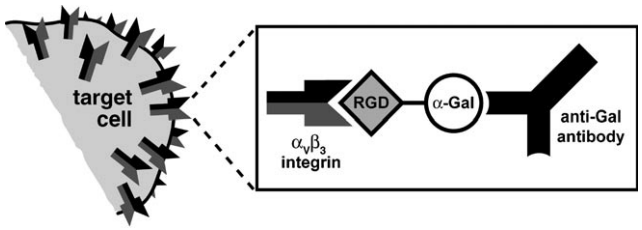

Figure 1. Schematic description of anti-Gal antibody recruitment to the target cell surface by a bifunctional ligand. One portion of the conjugate is designed to selectively bind to cells displaying the $\alpha_v\beta_3$ integrin, while the other displays the α-Gal carbohydrate epitope, which can interact with anti-Gal antibodies.

complex of these α- and β-subunits dictates integrins' binding specificity and ultimate biochemical function. The $\alpha_v\beta_3$ integrin mediates the attachment of cells to the extracellular matrix and has been implicated in tumor-induced angiogenesis, tumor invasion, and metastasis.[13,14] This integrin is upregulated on both cancer cells and tumor-associated blood vessels; however, $\alpha_v\beta_3$ is absent or present only at low levels on most normal tissues.[15] Experiments with arginine-glycine-aspartic acid (RGD) peptide conjugates suggest that integrins can serve as cell-surface receptors for recruiting anti-Gal antibodies.[16] Given its location on the cell surface and its role in cancer, we reasoned that $\alpha_v\beta_3$ would serve as an excellent target receptor.

Because they can be readily generated, the most common integrin ligands used are peptides. Linear peptide sequences containing the RGD motif are known to bind integrins, and these have been employed as cell-targeting agents.[17] Because of the low affinity and promiscuity of such linear peptides, however, their utility for selective cell targeting is limited. Peptide derivatives, such as cyclic Arg-Gly-Asp-D-Phe-Lys [c(-RGDfK-); **3a**, Scheme 1], have been used as tumor-homing agents due to their selectivity for $\alpha_v\beta_3$ over the closely related $\alpha_{IIb}\beta_3$ integrin.[18–20] Although more discriminating than its linear counterparts, this derivative is also a ligand for the $\alpha_v\beta_5$ integrin, a receptor highly expressed on many normal cell types. For our studies, we required integrin ligands that could be used for the construction of bifunctional conjugates and that are selective for the $\alpha_v\beta_3$ integrin. Although there are a few examples,[21–25] nonpeptidic derivatives that satisfy these criteria are rare. Several uses have been described for peptidomimetics that exhibit selectivity in integrin targeting.[26] In one example, an integrin-binding small molecule was modified so that it could be conjugated to a variety of antibodies for tumor targeting.[27–30] This ligand and others equipped with handles for modification, however, bind the closely related integrins $\alpha_v\beta_3$ and $\alpha_v\beta_5$. We set out to expand the toolkit of integrin ligands by generating compounds with the desired attributes that are selective for $\alpha_v\beta_3$.

Here, we report the modular synthesis of novel functionalized $\alpha_v\beta_3$ integrin ligands. We generated several bifunctional conjugates by appending the α-Gal trisaccharide to these ligands, thereby highlighting the benefits of our modular synthetic strategy. We also implement an integrin-dependent cell-adhesion assay to assess the inhibitory potencies of these compounds. Our results indicate that these peptidomimetics maintain their binding affinity and possess high specificity for $\alpha_v\beta_3$. Moreover, the modular assembly method that we employ should facilitate the development of bifunctional conjugates for a variety of cell-targeting applications.

Results and Discussion

Bifunctional conjugate design

The importance of the $\alpha_v\beta_3$ integrin has fueled the discovery of numerous small-molecule ligands.[31,32] As a starting point for our studies, we utilized potent $\alpha_v\beta_3$ antagonists with well-characterized integrin-selectivity profiles. We selected two inhibitors: the cyclic RGD peptide mimetic **1a** and the non-peptidic compound **2a** (Scheme 1). Compound **1a** inhibits binding of purified $\alpha_v\beta_3$ to an immobilized RGD-containing ligand with an IC_{50} value of 20 nM; it preferentially binds $\alpha_v\beta_3$ over the platelet integrin $\alpha_{IIb}\beta_3$ with 1000-fold greater activity.[33,34] Com-

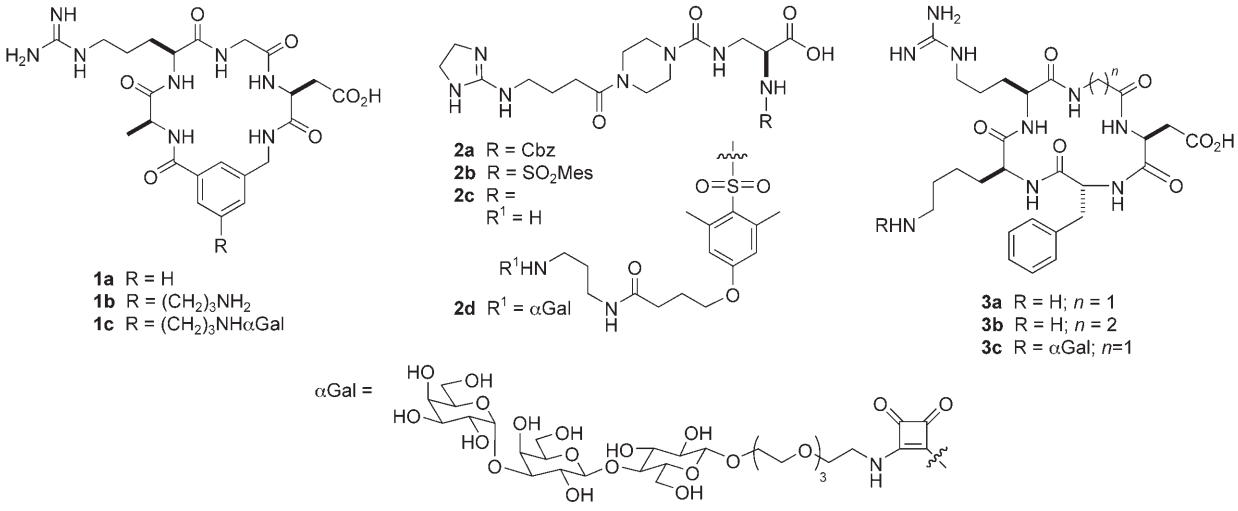

Scheme 1. Target functionalized $\alpha_v\beta_3$ integrin ligands (**1b**, **1c**, **2c**, **2d**, **3c**) and the parent compounds (**1a**, **2b**, **3a**) from which they are derived.

 © 2007 Wiley-VCH Verlag GmbH & Co. KGaA, Weinheim

pound **2a** is a potent inhibitor ($IC_{50} = 1.1$ nM) and is at least 400-fold more selective for $\alpha_v\beta_3$ over even more closely related integrins, including $\alpha_v\beta_5$.[35]

To generate the bifunctional conjugates, we devised a modular synthetic strategy. One facile method for linking two compounds is through the use of squaric acid esters.[36] Because the rate of formation of the squaric acid diamide is slower than formation of the monoamide, dimethyl squarate can be used to form a conjugate from two different amine-containing compounds. Thus, we needed an α-Gal derivative and an integrin-binding ligand—each bearing a free amino group. The former can be synthesized readily, as the amine can be appended through an anomeric substituent. To generate an integrin-binding moiety with the desired features, we analyzed the available structural and functional data.

To install a substituent that would preserve the integrin binding and the selectivity of the prototype ligands, we analyzed the structure of the $\alpha_v\beta_3$ integrin complex with the cyclic peptide ligand c(RGDf-*N*[*Me*]V) (Figure 2A).[37] Determination of this structure by X-ray crystallography revealed that, while the critical RGD motif contacts both subunits of the protein, the remaining two residues (D-Phe and *N*-methyl-Val) are solvent exposed. As long as they do not alter the conformation of the RGD-mimicking moiety, structural modifications of this exposed region should be permitted (Figure 2B). Accordingly, amine-bearing compound **1b** should maintain integrin binding (Scheme 1). Similarly, **2a** analogues that bear an appropriate substituent at the amine group α to the carboxylic acid should be accommodated.[38] Specifically, compound **2a** can be elaborated by introducing a functionalized mesityl sulfonamide to provide compound **2b**; studies optimizing RGD-mimetic activity had revealed that other $\alpha_v\beta_3$ inhibitors with arylsulfonamide groups at corresponding positions have excellent potencies.[39] If derivative **2b** possesses the predicted potency, we envisioned introducing a linker via this aryl sulfonamide substituent, as in compound **2c**. With these blueprints, we set out to build the target integrin ligands.

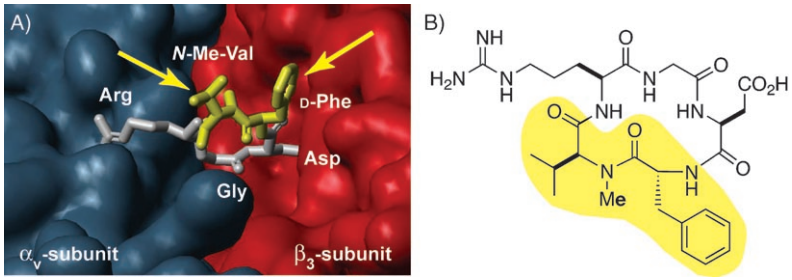

Figure 2. Structural model used to guide the design of integrin-binding compounds. A) Structure of the extracellular domain of $\alpha_v\beta_3$ integrin bound to a cyclic peptide containing the RGD recognition motif as determined by X-ray crystallographic analysis by Xiong et al.[37] The yellow arrows indicate the solvent-exposed regions of the molecule. B) Chemical structure of c(RGDf-*N*[Me]V). The residues highlighted in yellow correspond to parts of the compound that might be modified chemically without perturbing binding to the receptor.

Synthesis of peptidomimetic integrin ligands

Our initial efforts focused on the synthesis of cyclic peptide **1b**, which could be assembled either by solid-phase methods or in solution.[40,41] Guided by a report,[42] we sought to generate the relevant linear peptide using solid-phase synthesis and then cyclize it in solution. Accordingly, a route to non-natural amino acid **6** was required (Scheme 2). We reasoned that the aminopropyl side chain could be introduced by Pd-catalyzed cross coupling. The requisite aryl iodide **4** was synthesized in high yield from the known aniline derivative by using the Sandmeyer reaction.[43] Subsequent introduction of the alkynyl side chain under modified Sonogashira conditions provided the trisubstituted aromatic ring system in excellent yield.[44] Conversion of the benzylic alcohol to the azide group under standard conditions and subsequent hydrolysis of the methyl ester provided intermediate **5**. This compound then was transformed into the desired Fmoc-protected amino acid **6** by dual reduction of the azide and alkynyl functionalities with Pearlman's catalyst. Subsequent protection of the benzylic amine was effected under standard conditions. With amino acid **6** in hand, the desired protected peptide sequence was synthesized and cleaved under standard Fmoc solid-phase peptide synthesis (SPPS) conditions. The crude peptide was then cyclized with benzotriazole-1-yl-oxytrispyrrolidinophosphonium hexafluorophosphate (PyBOP) in dimethylformamide (DMF). The protecting groups were removed with trifluoroacetic acid (TFA), and the product was purified by high performance liquid chromatography (HPLC) to provide ligand **1b** in 11 steps and 22% overall yield.

In addition to preparing cyclic peptide **1b**, we also sought to generate sulfonamide-containing inhibitors **2b** and **2c**. We envisioned that the former would be a valuable comparator in assessing the relative potency of **2c** as an $\alpha_v\beta_3$ integrin ligand (vida infra). In their initial studies, DeGrado and co-workers synthesized ligand **2a** on a solid support as part of a larger

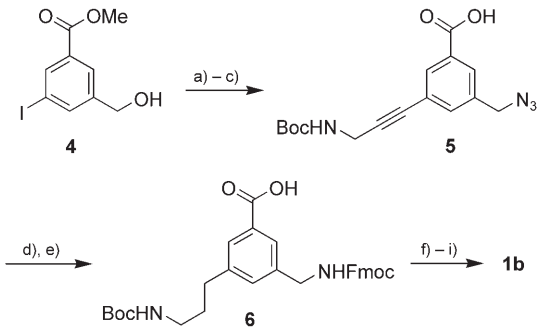

Scheme 2. Synthesis of the non-natural amino acid **6** and its use in generating a cyclic RGD mimetic **1b**: a) $PdCl_2(PPh_3)_2$, CuI, THF, Et_3N, *N*-Boc-propargyl amine, 98%; b) MsCl, Et_3N, toluene, NaN_3, Bu_4NBr, H_2O; c) LiOH, THF, H_2O, 85% over 2 steps; d) $Pd(OH)_2/C$, MeOH; e) Fmoc-OSu, Et_3N, ACN/H_2O, 65% over 2 steps; f) standard Fmoc SPPS; g) 1% TFA, CH_2Cl_2; h) PyBOP, DIPEA, DMF (1.5 mM); i) TFA, TIS, H_2O, 45% over 4 steps.

 © 2007 Wiley-VCH Verlag GmbH & Co. KGaA, Weinheim

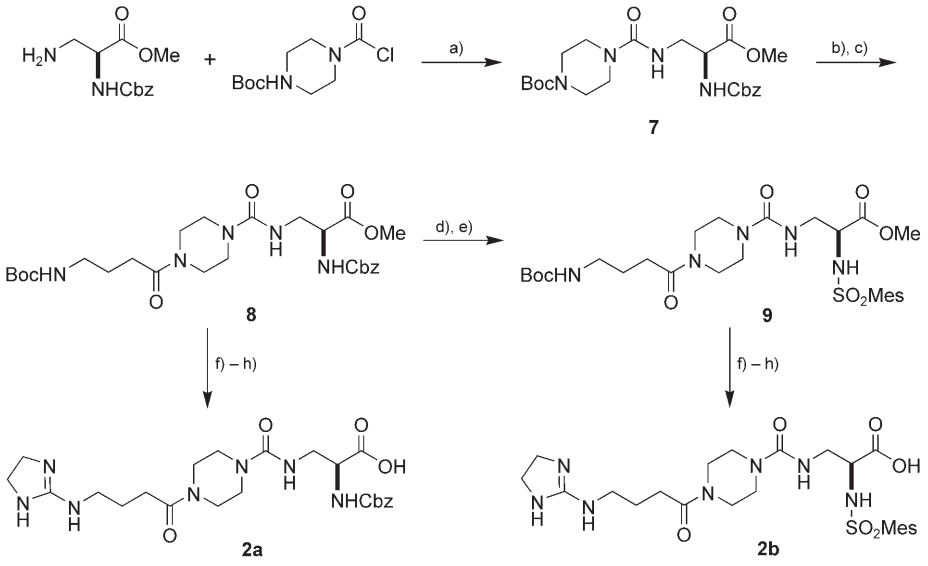

Scheme 3. Synthesis of the nonpeptidic RGD mimetic **2a** and its sulfonamide analogue **2b**: a) Et_3N, CH_2Cl_2, 92%; b) HCl, dioxane, MeOH; c) *N*-Boc-4-aminobutyric acid, EDCI, DMAP, Et_3N, CH_2Cl_2, 89% over 2 steps; d) H_2, $Pd(OH)_2$/C, MeOH, $CHCl_3$; e) $ClSO_2Mes$, Et_3N, CH_2Cl_2, 88% over 2 steps; f) HCl, dioxane, MeOH; g) 2-methylthio-2-imidazoline hydroiodide, MeOH, Et_3N, Δ; h) LiOH, H_2O, 82% for **2a** and 70% for **2b** over 3 steps.

combinatorial library.[35] For our studies, however, we required quantities larger than those conveniently prepared by SPPS. We therefore developed an iterative, solution-phase route (Scheme 3).

Our route began with the commercially available diaminopropionic acid, which we esterified to form the known methyl ester derivative.[38] Initial attempts to introduce the urea linkage by using the coupling agent employed in the solid-phase route, *para*-nitrophenyl chloroformate, proved unsuccessful. Treatment with a known piperazine-derived chloroformamide,[45] however, provided the desired intermediate **7** in high yield. The cyclic secondary amine was liberated by acid-induced cleavage of the Boc protecting group, and this product was subjected to amide bond-forming conditions to afford compound **8** in excellent overall yield. After removal of the Boc group, the arginine mimic was introduced by using 2-methylthio-2-imidazoline hydroiodide; hydrolysis of the methyl ester provided known compound **2a** (Scheme 3).

Compound **8** could readily be elaborated to generate sulfonamide **2b**. To this end, the Cbz protecting group was removed by hydrogenolysis, and the resulting amine was treated with 2-mesitylenesulfonyl chloride to provide **9** in high yield. The desired compound **2b** was generated in three additional steps: removal of the Boc-protecting group, introduction of the guanidine group as above, and cleavage of the methyl ester (Scheme 3).

To embed a linker within the aryl sulfonamide group of **2c**, we assembled aryl sulfonyl chloride **10** (Scheme 4). We subjected the commercially available 3,5-dimethylphenol to alkylation with 4-bromoethyl butyrate, and the resulting ethyl ester was converted to the acid under standard hydrolytic conditions. We explored the direct conversion of this intermediate to the corresponding sulfonyl chloride with chlorosulfonic acid; however, the desired product was not isolated. As a result, we masked the acid group to generate the 2,2,2-trichloroethyl ester; this protecting group was selected because of its stability to acids and compatibility with our synthetic route. Indeed, treatment of the ester with chlorosulfonic acid readily generated protected sulfonyl chloride **10**.

The presence of the linker within the aryl sulfonamide of compound **2c** necessitated some changes to the route used to assemble **2b** (Scheme 4). Compound **10** was modified with *N*-β-Boc-protected diaminopropionic acid derivative to generate the expected sulfonamide. After removal of the Boc group, the free amine could be modified with the aforementioned pi-

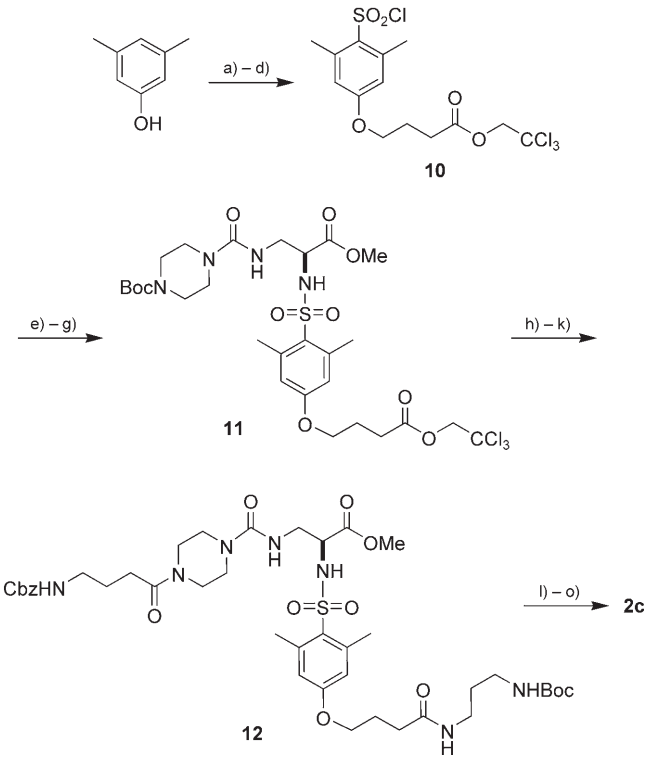

Scheme 4. Synthetic route for the preparation of linker-functionalized compound **2c**: a) ethyl-4-bromobutyrate, K_2CO_3, KI, DMF; b) NaOH, EtOH/H_2O, 77% over 2 steps; c) EDCI, DMAP, $HOCH_2CCl_3$, CH_2Cl_2, 95%; d) $ClSO_2Cl$, CH_2Cl_2, 51%; e) NH_2-Dap(Boc)-OMe, Et_3N, CH_2Cl_2, 81%; f) 4 N HCl, dioxane; g) Boc-protected piperazine-derived chloroformamide,[45] Et_3N, CH_2Cl_2, 84% over 2 steps; h) 4 N HCl, dioxane; i) Cbz-4-aminobutyric acid, EDCI, DMAP, Et_3N, CH_2Cl_2, 94% over 2 steps; j) Zn, THF, 1 M KH_2PO_4; k) Boc-$NH(CH_2)_3NH_2$, EDCI, NHS, Et_3N, CH_2Cl_2, 83% over 2 steps; l) H_2, $Pd(OH)_2$/C, MeOH/$CHCl_3$, 100%; m) 2-methylthio-2-imidazoline hydroiodide, MeOH, Et_3N, Δ; n) LiOH, H_2O; o) TFA, 54% over 3 steps.

 © 2007 Wiley-VCH Verlag GmbH & Co. KGaA, Weinheim

perazine-derived chloroformamide to produce compound **11**. Removal of the Boc protecting group under acidic conditions afforded the free secondary amine. Initially, we synthesized a compound in which the 4-aminobutyric acid moiety was protected with a Boc group (i.e., in analogy to compound **8**). Unfortunately, cleavage of the Boc group en route to introduction of the guanidine derivative led to a complex product mixture. A switch in protecting group from Boc to Cbz solved the problem. Removal of the 2,2,2-trichloroethyl ester was effected by Zn. Initial attempts to directly couple the resulting acid with a mono-Boc-protected diamine[46] under standard, single-step amide bond-forming reaction conditions provided compound **12**—but only in low yield. Converting the acid to the succinimidyl (NHS) ester prior to coupling greatly increased the yields of the desired product. Hydrogenolysis of the Cbz protecting group efficiently provided the resulting primary amine in quantitative yield. This compound was ultimately converted to the substituted guanidine derivative, and the remaining protecting groups were removed under standard conditions to afford target compound **2c** in 15 steps from 3,5-dimethylphenol (Scheme 4).

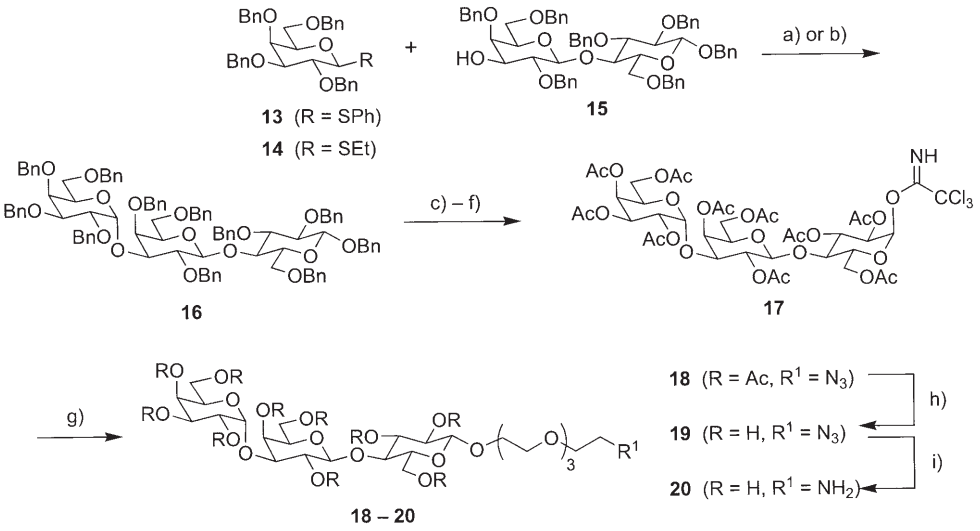

Scheme 5. Synthetic route to the α-Gal trisaccharide possessing an oligo(ethylene glycol)-based linker **20**: a) $PhHgOTf$, CH_2Cl_2, 90%; b) $CuBr_2/Bu_4NBr$, 80%; c) H_2, 10% Pd/C, EtOAc/MeOH/H_2O/AcOH; d) Ac_2O, DMAP, pyridine, 92% over 2 steps; e) NH_2NH_2·HOAc, DMF; f) Cl_3CCN, DBU, CH_2Cl_2, 75% over 2 steps; g) H-$(OCH_2CH_2)_4$-N_3, BF_3·OEt_2, CH_2Cl_2, 4 Å MS, 58%; h) cat. NaOMe, MeOH; i) H_2, $Pd(OH)_2$/C, MeOH/$CHCl_3$, 98% over 2 steps.

Preparation of the α-Gal epitope

To generate the bifunctional conjugates, we planned to tether an $\alpha_v\beta_3$ integrin ligand to the α-Gal epitope through a linker at the carbohydrate anomeric position. The disaccharide Galα(1–3)Gal is the minimal structure suggested to be required for anti-Gal antibody recognition. Still, equilibrium-binding studies indicate that this carbohydrate binds only weakly to the anti-Gal antibody ($IC_{80} = 3.3$ mM).[47] In addition, we found that even multivalent presentations of this epitope are poor ligands for anti-Gal antibodies (unpublished results). In contrast, the interaction of the trisaccharide Galα(1–3)Galβ(1–4)Glc for the anti-Gal antibody is at least threefold stronger. Moreover, it appears that this epitope can recruit naturally occurring anti-Gal antibodies.[48] As a linker, we used an oligo(ethylene glycol)-based moiety terminated with an azide group. This structure was added to provide adequate separation between the two recognition motifs, because both the cell-surface receptor and the anti-Gal antibody must bind simultaneously. Studies with surface-bound displays of $\alpha_v\beta_3$ integrin ligands have indicated that linkers that can span approximately 20 Å (at their full extension) are required for efficient interaction with $\alpha_v\beta_3$-positive cells.[49] Lastly, the azide serves as a masked amino group; it can be converted under mild conditions into a substrate for squarate coupling. Thus, the desired trisaccharide **20** was selected for synthesis (Scheme 5).

Several methods for preparing α-galactosyl trisaccharides have been reported.[50–53] The key challenge is to form the alpha linkage efficiently and with excellent stereoselectivity. To exploit the anomeric effect in forming the axial anomer, conditions that result in an S_N1-like mechanism with a late transition state should favor the desired product. We initially followed a previously published protocol describing the high-yielding reaction (>90%) between a 3′-OH group on a lactosyl acceptor and a benzyl-protected galactosyl donor with an anomeric phenyl sulfoxide group.[54] We repeated this procedure and obtained the fully protected trisaccharide in high yield (90%), but only as an inseparable α/β isomeric mixture. Accordingly, we turned our attention to a metal-catalyzed reaction of a phenyl thiogalactoside **13** galactosyl donor. We reasoned that this process should proceed along the desired mechanistic pathway. Indeed, the glycosylation reaction of **13** and **15**[55] in the presence of phenylmercury triflate[56] gave exclusively the α-glycoside **16** in excellent yield (90%).

To avoid using a toxic catalyst in the assembly of carbohydrate **16**, several other glycosylation conditions were examined. The most efficient procedure tested employed the donor ethyl thiogalactoside **14** and copper(II) bromide–tetrabutylammonium bromide as a promoter,[57] and led to **16** in 80% yield along with some (10%) recovered disaccharide starting material **15**. Although it remains less efficient than the classical mercury-catalyzed glycosylation reaction, we found this latter method effective.

 © 2007 Wiley-VCH Verlag GmbH & Co. KGaA, Weinheim

We appended the anomeric linker after generating the trisaccharide, as this strategy allows for the introduction of different anomeric substituents. We converted compound **16** into an appropriate glycosyl donor, the peracetylated trichloroacetimidate derivative **17**, in four steps. The glycosylation reaction proceeded smoothly to afford compound **18**, which possesses the azide-bearing linker. Removal of the acetate protecting groups had to be carried out at low temperature (4 °C) with a catalytic amount of sodium methoxide (NaOMe) to attain quantitative yields of **19**. At room temperature or under more alkaline reaction conditions, undesired side reactions occurred. The azido sugar **19** was reduced by catalytic hydrogenation to give the desired amine **20** in 8 steps and 35% or 31% overall yield from **13** or **14**, respectively. With access to appropriately functionalized integrin-targeting ligands and the oligosaccharide unit, we turned to assembling bifunctional conjugates.

Bifunctional conjugates

As described, a critical objective of our initial studies was to synthesize bifunctional conjugates that contain a cell-surface-targeting agent and a moiety that could direct the immune response to tumor cells. Because different ligands can serve as the tumor homing agents or the immune system activating components, the modularity of dimethyl squarate-mediated coupling is attractive.[36] This conjugation chemistry is both chemoselective and compatible with unprotected carbohydrate epitopes.[58,59] With regard to integrin ligand coupling, it is known that primary amine groups can be selectively functionalized in the presence of guanidinium groups.[60,61] Still, the utility of dimethyl squarate for assembling this type of complex conjugate was untested; nevertheless, we sought to apply it to the construction of conjugates **1c**, **2d**, and **3c**.

Because amine-bearing unprotected carbohydrates can react selectively with dimethyl squarate, we used trisaccharide **20** as the initial coupling partner. As expected, this compound underwent a chemoselective reaction to provide compound **21** (Scheme 6). To generate the bifunctional ligands, compound **21** was incubated under basic, aqueous conditions with the putative $\alpha_v\beta_3$ integrin ligand **1b** or **2c**. After complete consumption of the integrin ligand, the desired products **1c** and **2d**, respectively, were isolated in high yields. The same synthetic strategy was applied to tether the cyclic RGD peptide, c-(-RGDfK-) **3a**, to the α-Gal moiety, thereby yielding conjugate **3c**. Because the activity of **3a** as an $\alpha_v\beta_3$-targeting ligand has been well characterized, we envisioned that **3c** could be used to calibrate our binding studies.

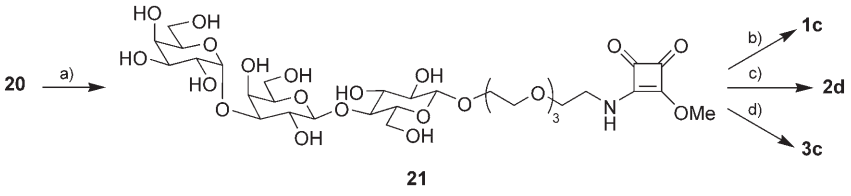

Scheme 6. Strategy for the modular synthesis of bifunctional conjugates **1c**, **2d**, and **3c** by using a squarate-mediated coupling reaction: a) dimethyl squarate, Et_3N, $MeOH/H_2O$, 69%; b) compound **1b**, 50 mM borate buffer (pH 9), 71%; c) compound **2c**, 50 mM borate buffer (pH 9), 66%; d) compound **3a**, 50 mM borate buffer (pH 9), 45%.

Integrin-binding assay

To ascertain whether our compounds would be useful as cell-surface-targeting agents, a method was needed to evaluate their potency and selectivity for $\alpha_v\beta_3$. To this end, we examined their ability to inhibit the binding of WM115 cells, an $\alpha_v\beta_3$-positive human melanoma cell line, to fibrinogen, a known protein ligand for the $\alpha_v\beta_3$ integrin.[62] By adapting a cell-adhesion assay that had been applied to assess inhibitors of VLA-4 binding to VCAM-1,[63] we devised a high-throughput assay for identifying $\alpha_v\beta_3$ ligands. Briefly, individual V-shaped wells of a microtiter plate were coated with fibrinogen and then blocked. WM115 tumor cells, labeled with a membrane-permeable fluorescein [5-carboxyfluorescein diacetoxymethyl ester (BCECF-AM)], were added to the wells in the presence of various concentrations of compound. After incubation, the plate was gently centrifuged to concentrate the nonadherent cells in the bottoms of the wells; the fluorescence emission from the resulting pellets was measured from below. Each of the known inhibitors (**1a**, **2a**, and **3a**) was capable of preventing adhesion of the cells to fibrinogen, and their IC_{50} values were in the expected (10^{-9} M) range (Table 1). The relative potencies determined with this assay are consistent with those from previous studies,[18,33–35] a result that underscores the utility of this assay. The observed inhibition depends on the structure of the peptidomimetic. Compound **3b**,[49] in which the critical glycine residue has been replaced with β-alanine, was unable to inhibit binding (IC_{50} value $\gg$ 5 μM).

The potent IC_{50} values for the bifunctional compounds (Table 1) support the validity of our attachment strategy. For example, the trisaccharide substituent of conjugate **3c** had minimal effect on its inhibitory potency (compare with **3a**). This result is consistent with previous studies involving modification of compound **3a**.[64,65] In contrast, when the α-Gal epitope was introduced in conjugate **1b** to afford **1c**, the latter was more than tenfold less active. Ultimately, the functionalized derivatives based on ligand **2a** proved to be the most potent. As hypothesized, conjugate **2b**, in which the Cbz group is replaced by a mesitylsulfonamide moiety, is 15-fold more active than **2a**. Further modification of the 4-position of the mesityl group led to minimal changes in the observed potency, as can be seen by the IC_{50} value of 1.3 nM for compound **2c**. Interestingly, the bifunctional compound **2d** is slightly more potent than the corresponding integrin ligand **2a**. These data provide clear evidence that each of the designed bifunctional conjugates can bind to the $\alpha_v\beta_3$ integrin.

 © 2007 Wiley-VCH Verlag GmbH & Co. KGaA, Weinheim

Table 1. Inhibition constants (IC_{50} values) of compounds **1a–c**, **2a–d**, and **3a–c** determined in an assay assessing the binding of $\alpha_v\beta_3$-positive WM115 cells to immobilized fibrinogen.

Compound	IC_{50} [nM]	Compound	IC_{50} [nM]
1a	61 ± 30	**1b**	68 ± 100
1c	930 ± 600	**2a**	8.1 ± 2
2b	0.55 ± 0.2	**2c**	1.3 ± 0.4
2d	1.8 ± 0.7	**3a**	24 ± 6
3b	> 5000	**3c**	47 ± 50

In addition to high affinity, our targeting strategy requires that the bifunctional ligands possess high selectivity for the target $\alpha_v\beta_3$ integrin. To assay for specificity over a key related integrin, $\alpha_v\beta_5$, we utilized MCF7 human breast carcinoma cells, which are known to display $\alpha_v\beta_5$. Vitronectin, the natural protein ligand for this receptor,[62] was substituted for fibrinogen in our fluorescence-based cell-binding assay. Under these conditions, we measured a significantly higher IC_{50} value of 7.8 ± 5.7 μM for conjugate **2d**, which represents more than a 4000-fold decrease in potency. This value suggests that compound **2d** is even more selective for $\alpha_v\beta_3$ integrin than the compound (**2a**) upon which it is based. These data suggest that conjugates based on our the potent inhibitor **2d** will exhibit excellent cell-targeting selectivity.

Antibody-binding assay

For our synthetic conjugates to function as designed, they must bind to $\alpha_v\beta_3$-displaying cells and interact simultaneously with anti-Gal antibodies. To evaluate whether they can act in this capacity, we incubated an $\alpha_v\beta_3$-positive cell line, M21 human melanoma cells, with 10 nM of compound **2d** and human serum; the latter serves as a source of anti-Gal IgG. To test for binding of anti-Gal, washed cells were treated with a fluorescein-labeled anti-human IgG secondary antibody and subsequently analyzed by flow cytometry. In the absence of **2d**, the cells displayed no anti-Gal binding; however, cells treated with **2d** exhibited a significant increase in the fluorescence signal (Figure 3). These results indicate that bifunctional ligand **2d** maintains its ability to interact with anti-Gal antibodies when bound to the surface of $\alpha_v\beta_3$-positive cells. Because both the integrin binding domain and the anti-Gal epitope can function simultaneously, our results bode well for using these or related bifunctional ligands as novel tumor-targeting agents.

Conclusions

In summary, we have successfully developed a modular route to bifunctional conjugates that target cells displaying the $\alpha_v\beta_3$ integrin. In devising integrin ligands with the appropriate attributes, we designed and synthesized two $\alpha_v\beta_3$-binding small molecules with excellent potencies. In addition, the selectivity of compound **2d** for $\alpha_v\beta_3$ over related integrins indicates that it is a valuable new addition to the limited set of functionalized non-peptidic ligands that bind this receptor.

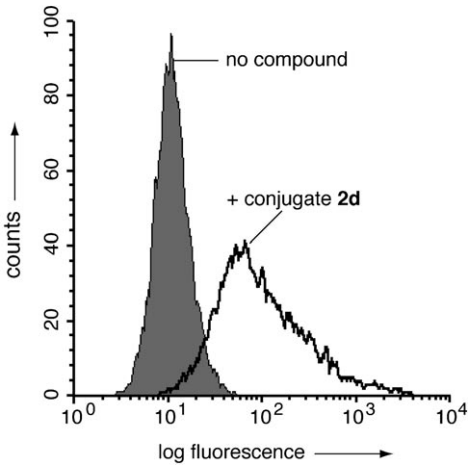

Figure 3. Representative flow cytometry histogram illustrating anti-Gal antibody binding to M21 cells. M21 tumor cells were treated with bifunctional conjugate **2d** and human serum, a source of anti-Gal IgG. Antibody binding was detected by flow cytometry and a fluorophore-labeled secondary anti-human antibody.

The sites for modification integrated into our $\alpha_v\beta_3$ integrin ligands and the dimethyl squarate coupling chemistry that we have employed can be exploited for a variety of purposes. For instance, the handles we have installed can be used to immobilize the integrin ligands, thereby creating surfaces for $\alpha_v\beta_3$-positive cell adhesion or growth.[26,66] Alternatively, these handles can serve as points of attachment to tumor imaging agents. Finally, our functionalized integrin ligands can be used to append protein or small-molecule toxins to create novel antitumor agents.

Experimental Section

General: All materials were obtained from commercial suppliers and used as provided unless otherwise noted. Reaction solvents were purified by distillation by using standard protocols. Tetrahydrofuran (THF), diethyl ether, toluene, and benzene were distilled from sodium metal and benzophenone under an argon atmosphere. Triethylamine and dichloromethane were distilled from calcium hydride. Methanol was distilled from magnesium. Dimethylformamide (DMF) was rendered amine-free by treatment with Dowex 50WX8–200 cation-exchange resin (H^+ form, 1 g L^{-1}). Dimethylsulfoxide (DMSO) was stored over 3 Å molecular sieves. All moisture- and air-sensitive reactions were carried out in flame-dried glassware under an atmosphere of nitrogen. Liquid reagents were introduced by oven-dried glass syringes. To monitor the progress of reactions, thin-layer chromatography (TLC) was performed with Merck (Darmstadt) silica gel 60 F_{254} precoated plates by eluting with the solvents indicated. Analyte visualization was accomplished by busing a multiband UV lamp and charring with one of the following stains: *p*-anisaldehyde, ninhydrin, potassium permanganate, or phosphomolybdic acid. Flash chromatography (FC) was performed on Scientific Adsorbents Incorporated silica gel (32–63 μM, 60 Å pore size) by using distilled reagent-grade hexanes and ACS-grade ethyl acetate or methanol and chloroform. ^1H and ^{13}C NMR spectra were recorded on Bruker AC-300 or Varian Inova-500 spectrometers, and chemical shifts are reported relative to tetramethylsilane (TMS) or residual solvent peaks in parts per

 © 2007 Wiley-VCH Verlag GmbH & Co. KGaA, Weinheim

million. Yields were calculated for materials that appeared as a single spot by TLC and homogeneous by ^{1}H NMR. HPLC was performed on a Spectra-Physics UV2000 instrument, with UV absorption at 220 nm and/or 254 nm for analyte detection. Samples were eluted on reversed-phase C18 columns from Vydac (Protein & Peptide $l=220$ mm, i.d. $=5$ or 10 mm, 10 or 22 μm particle size). Liquid chromatography/mass spectroscopy (LCMS) measurements were performed on a Shimadzu LCMS 2010.

Biological studies: All chemicals were from Sigma–Aldrich unless otherwise noted. All cell-culture reagents, including minimal essential medium alpha (αMEM), RPMI-1640, fetal bovine serum (FBS), penicillin-streptomycin (pen-strep), L-glutamine (Gln), insulin, and trypsin-EDTA, were from Invitrogen. Tissue culture flasks for adherent cells were obtained from Sarstedt (Newton, NC). The dye 2′,7′-bis-(2-carboxyethyl)-5-(and-6)-carboxyfluorescein, acetoxymethyl ester (BCECF-AM) was from Molecular Probes (Eugene, OR). Bovine serum albumin (BSA) was from Research Organics (Cleveland, OH). V-shaped 96-well plates were obtained from Nalge Nunc, International (Rochester, NY). Fibrinogen and vitronectin were from Cal-Biochem (San Diego, CA). FITC-labeled goat anti-human IgG was from Vector Laboratories (Burlingame, CA).

Tumor cells: Human MCF7 breast carcinoma cells and WM115 melanoma cell lines were from American Type Culture Collection (Manassas, VA). M21 cells (sorted for high levels of $\alpha_v\beta_3$ integrin) were kindly provided by Drs. P. M. Sondel and S. C. Helfand (University of Wisconsin–Madison). WM115 cells were grown in αMEM supplemented with 10% FBS, Gln (2 mM), and 100 U antibiotics pen-strep. MCF7 cells were grown as above, but the medium was further supplemented with insulin (0.01 mg mL^{-1}). M21 cells were cultured in RPMI-1640 supplemented with 10% FBS, Gln (2 mM), and 100 U pen-strep. All cells were detached from flasks with 0.05% trypsin-EDTA.

Synthesis of compound 4: The known aniline derivative[43] (1.0 g, 5.7 mmol) was dissolved in a 1:1 (*v*/*v*) mixture of acetone and aqueous H_2SO_4 (3 N, 260 mL), and the solution was cooled to −20 °C. A solution of $NaNO_2$ (9.0 g, 0.13 mol) in H_2O (70 mL) was added dropwise, during which time the mixture became gummy. To this suspension, a solution of urea (1.4 g, 23 mmol) and KI (33.0 g, 200 mmol) in H_2O (50 mL) was added dropwise. Nitrogen gas evolved from the reaction during the course of the addition. The mixture was removed from the ice bath and stirred for 3 h at RT. Saturated aqueous $NaHCO_3$ (200 mL) was added to the mixture, and the acetone was removed under reduced pressure. The resulting solution was extracted with EtOAc (3×100 mL), and the combined organic extracts were washed with saturated aqueous $NaHCO_3$ (2×80 mL) and brine (2×80 mL) and then dried (Na_2SO_4). The solvents were removed under reduced pressure, and the residue was purified by FC (hexane/EtOAc 1:1) to yield **4** as a white solid (1.53 g, 92%). ^{1}H NMR (300 MHz, $CDCl_3$): $\delta=8.23$ (m, 1H), 7.92 (m, 1H), 7.88 (m, 1H), 4.66 (s, 2H), 3.89 (s, 3H); ^{13}C NMR (75 MHz, $CDCl_3$): $\delta=165.49$, 143.23, 139.64, 137.01, 131.40, 126.66, 126.47, 93.77, 77.40, 76.97, 76.55, 63.23, 52.34; LRMS (EI): calcd for $C_9H_9IO_3$ $[M]^+$ 292.0; found 292.0.

Synthesis of compound 5: Aryl iodide **4** (490 mg, 1.7 mmol), *N*-Boc-propargyl amine (520 mg, 3.4 mmol), and $PdCl_2(PPh_3)_2$ (36 mg, 0.050 mmol) were dissolved in THF (7 mL); Et_3N (490 μL, 3.4 mmol) was added, and the reaction mixture was stirred for 10 min at RT. CuI (9.5 mg, 0.050 mmol) was then added, and the reaction mixture was stirred for 1.5 h at RT. After this time, the THF was removed under reduced pressure, and the residue was suspended in EtOAc (15 mL). The resulting suspension was washed with 5% aqueous citric acid (2×5 mL), saturated aqueous $NaHCO_3$ (2×5 mL), 1% aqueous sodium diethyldithiocarbamate (2×5 mL), and brine (2×5 mL) and dried (Na_2SO_4). The solvents were removed under reduced pressure, and the residue was purified by FC (hexane/EtOAc 3:1 to 2:1) to yield the alkyne product (534 mg, 98%). ^{1}H NMR (300 MHz, $CDCl_3$): $\delta=7.89$ (s, 2H), 7.53 (s, 1H), 5.09 (br s, 1H), 4.63 (s, 2H), 4.09 (d, $J=5.1$ Hz, 1H), 3.86 (s, 3H), 3.25 (br s, 1H), 1.43 (s, 9H); ^{13}C NMR (75 MHz, $CDCl_3$): $\delta=166.39$, 155.49, 141.88, 134.01, 131.64, 130.32, 127.50, 123.23, 86.42, 81.93, 79.94, 63.90, 52.29, 31.04, 28.34; LRMS (ESI): calcd for $C_{34}H_{42}N_2NaO_{10}$-$[2M+Na]^{2+}$ 661.2; found 661.2.

The above alkyne (530 mg, 1.7 mmol) was dissolved in THF (8 mL), Et_3N (960 μL, 6.6 mmol) was added, and the mixture was cooled to 0 °C. Methanesulfonyl chloride (200 μL, 2.50 mmol) was added dropwise, and the reaction mixture was stirred at RT for 1.5 h. A solution of NaN_3 (860 mg, 13 mmol) and Bu_4NBr (54 mg, 0.17 mmol) in water (2 mL) was then added, and the mixture was heated at reflux for 20 min. After cooling, the reaction mixture was diluted with EtOAc (15 mL), washed with 5% aqueous citric acid (2×5 mL), saturated aqueous $NaHCO_3$ (2×5 mL), and brine (2×5 mL) and dried (Na_2SO_4). Removal of the solvents under reduced pressure followed by purification by FC (hexane/EtOAc 7:1) provided the azide as an oil (508 mg, 89%). ^{1}H NMR (300 MHz, $CDCl_3$): $\delta=8.01$ (t, $J=1.6$ Hz, 1H), 7.89 (t, $J=1.7$ Hz, 1H), 7.52 (t, $J=1.7$ Hz, 1H), 4.92 (br s, 1H), 4.35 (s, 2H), 4.13 (d, $J=5.8$ Hz, 1H), 3.90 (s, 3H), 1.45 (s, 9H); ^{13}C NMR (75 MHz, $CDCl_3$): $\delta=165.79$, 155.28, 136.17, 135.06, 132.45, 130.87, 128.67, 123.79, 110.06, 87.12, 81.43, 53.78, 52.32, 30.99, 28.27; LRMS (ESI): calcd for $C_{17}H_{20}N_4NaO_4$ $[M+Na]^+$ 367.1; found 367.1.

This azide intermediate (500 mg, 1.45 mmol) was dissolved in THF/MeOH (10 mL, 10:1), and a solution of LiOH (120 mg, 2.9 mmol) in H_2O (3 mL) was added. The mixture was stirred for 3 h, then THF and MeOH were removed under reduced pressure. HCl (1 N) was added to the remaining liquid, and the mixture was extracted with EtOAc (3×10 mL). The combined organic layers were washed with brine (3×10 mL) and dried (Na_2SO_4). The solvent was removed under reduced pressure to yield **5** (461 mg, 96%) as a white solid. ^{1}H NMR (300 MHz, CD_3OD): $\delta=7.95$ (t, $J=1.4$ Hz, 1H), 7.91 (t, $J=1.4$ Hz, 1H), 7.56 (t, $J=1.4$ Hz, 1H), 4.42 (s, 2H), 4.07 (s, 2H), 1.45 (s, 9H); ^{13}C NMR (75 MHz, CD_3OD): $\delta=168.88$, 158.38, 138.69, 136.58, 133.68, 133.29, 130.36, 125.61, 88.94, 82.16, 81.10, 55.02, 31.79, 29.14; LRMS (ESI): calcd for $C_{16}H_{17}N_4O_4$ $[M-H]$ 329.1; found 329.1.

Synthesis of amino acid 6: Azide **5** (460 mg, 1.39 mmol) was dissolved in MeOH/$CHCl_3$ (30 mL, 30:1) and solid $Pd(OH)_2/C$ (120 mg) was added. The reaction mixture was placed under 1 atm of H_2 for 3 h and then filtered through Celite. Removal of solvent under reduced pressure provided the crude amine which was used directly in the next reaction. ^{1}H NMR (300 MHz, CD_3OD): $\delta=7.97$ (br s, 1H), 7.89 (br s, 1H), 7.26 (br s, 1H), 4.19 (s, 2H), 3.06 (t, $J=6.8$ Hz, 2H), 2.72 (t, $J=6.8$ Hz, 2H), 1.81 (p, $J=7.5$, 2H), 1.43 (s, 9H); LRMS (ESI): calcd for $C_{16}H_{25}N_2O_4$ $[M+H]^+$ 309.2; found 309.2.

The crude amine was dissolved in water (2 mL), and Et_3N was added to adjust the solution to pH 8. The mixture was cooled to 0 °C, a solution of 9-fluorenylmethyloxycarbonyl-*N*-hydroxysuccinimide (Fmoc-OSu; 520 mg, 1.5 mmol) dissolved in acetonitrile (6 mL) was then added, and the pH of the solution was readjusted to 8. After 1.3 h at RT, the pH was adjusted to 5 with 1 N HCl; the acetonitrile was removed under reduced pressure. The remaining solution was acidified to pH 2, washed with EtOAc and CH_2Cl_2 (3× 10 mL each), and the organic layers were dried (Na_2SO_4). The solvents were removed under reduced pressure, the resulting residue

 © 2007 Wiley-VCH Verlag GmbH & Co. KGaA, Weinheim

was dissolved in MeOH, the mixture was adsorbed onto silica gel, and the resulting mixture was placed atop a silica gel column with CH_2Cl_2. Elution with hexane/EtOAc (2:1) with 1% acetic acid provided **6** (480 mg, 65% over two steps) as a white solid, which contained a trace of fluorenyl by-products. ^{1}H NMR (300 MHz, $CDCl_3$/CD_3OD): δ = 7.72 (m, 4H), 7.57 (d, J = 7.7 Hz, 2H), 7.27 (m, 5H), 4.31 (m, 3H), 4.15 (t, J = 6.5 Hz, 1H), 3.03 (t, J = 7.1 Hz, 2H), 2.62 (t, J = 7.4 Hz, 2H), 1.75 (t, J = 7.4 Hz, 2H), 1.39 (s, 9H); ^{13}C NMR (75 MHz, $CDCl_3$/CD_3OD): δ = 168.33, 156.98, 156.45, 143.34, 141.88, 140.69, 138.97, 131.49, 130.42, 128.02, 127.06, 126.45, 125.74, 127.46, 19.26, 78.52, 66.25, 43.79, 43.67, 39.25, 32.13, 30.77, 27.52; LRMS (ESI): calcd for $C_{31}H_{33}N_2O_6$ $[M+H]^+$ 529.2; found 529.3.

Solid-phase synthesis of peptide 1b: Synthesis was performed manually in a 10 mL polyethylene syringe containing a polypropylene frit. Fmoc-Gly-Sasrin resin (0.69 mmol g^{-1} loading, 114 mg, 0.0786 mol; Bachem) was swelled in and washed with CH_2Cl_2 and DMF prior to use. To effect cleavage of the Fmoc group, a solution of piperidine in DMF (20%, 4 mL) was drawn up into the syringe, and the vessel was agitated for 5 min. The resin was washed with DMF (2×), and the process was repeated. The resin was washed with DMF (3×), CH_2Cl_2 (3×), MeOH (1×), and DMF (3×), and the success of the cleavage was assessed by Kaiser test. Next, the desired amino acid (4 equiv), PyBOP (4 equiv) and HOBt (4 equiv) were dissolved in a minimal amount of DMF. *N*,*N*-diisopropylethylamine (DIPEA; 4 equiv) was added, and the solution was drawn into the syringe. The reaction vessel was agitated for 2 h, the resin was washed with DMF (3×), CH_2Cl_2 (3×), MeOH (1×), and DMF (3×), and the success of the coupling was assessed again by the Kaiser test. This process was repeated for each amino acid residue. After final Fmoc cleavage, the resin was first washed with CH_2Cl_2 (3×). A 1% TFA solution (5 mL) was drawn into the syringe and agitated for 15 min and then expelled into a mixture of CH_2Cl_2 and Et_3N. This process was repeated (5×), and the resin was washed with CH_2Cl_2 (2×). Concentration of the cleavage solutions under reduced pressure provided the crude, side-chain-protected linear peptide (58 mg). Identity of the product was confirmed by LCMS (ESI): calcd for $C_{48}H_{74}N_9O_{13}S$ $[M+H]^+$ 1016.5; found 1016.4.

To effect cyclization in solution, a portion of the crude peptide (43 mg, 0.042 mmol) was dissolved in distilled DMF (30 mL, 0.0015 mM), and PyBOP (26 mg, 0.050 mmol) and DIPEA (23 μL, 0.13 mmol) were added. The reaction mixture was stirred for 12 h at RT, a second portion of PyBOP (26 mg, 0.050 mmol) and DIPEA (23 μL, 0.13 mmol) was added, and the reaction mixture was stirred for an additional 12 h. Water was added, and the solvents were removed under high vacuum. The identity of the product was confirmed by LCMS (ESI): calcd for $C_{48}H_{74}N_9O_{13}S$ $[M+H]^+$ 998.5; found 998.4.

The crude cyclized product was dissolved in a TFA deprotection cocktail (TFA/triisopropylsilane (TIS)/H_2O, 95:2.5:2.5, 5 mL), and the solution was stirred for 2 h. The majority of the TFA was removed under a stream of N_2 gas, and the remainder was precipitated into cold diethyl ether with filtration through a plug of glass wool. The resulting solid was collected and purified by HPLC to yield **16** (13 mg, 45%) as the mono TFA salt. ^{1}H NMR (500 MHz, CD_3OD): δ = 7.59 (s, 1H), 7.54 (s, 1H), 7.31 (s, 1H), 4.63 (d, J = 16.3 Hz, 1H), 4.49 (m, 2H), 4.32 (q, J = 7.3 Hz, 1H), 4.23 (d, J = 16.5 Hz, 1H), 4.21 (d, J = 18 Hz, 1H), 3.73 (d, J = 17.1 Hz, 1H), 3.13 (m, 2H), 3.00 (dd, J = 17.1, 6.5 Hz, 1H), 2.94 (t, J = 7.9 Hz, 2H), 2.76 (t, J = 8.8 Hz, 2H), 2.67 (dd, J = 17.1, 7.4 Hz, 1H), 2.05 (m, 1H), 1.99 (p, J = 7.9 Hz, 2H), 1.72–1.55 (m, 3H), 4.54 (d, J = 7.4 Hz, 3H), 1.36 (m, 2H); ^{13}C NMR (125 MHz, CD_3OD): δ = 176.46, 174.59, 174.21, 172.97, 172.00, 171.41, 158.77, 142.23, 141.43, 135.68, 137.71, 126.65, 125.58, 53.88, 53.41, 52.47, 43.10, 43.02, 42.02, 40.36, 35.84, 33.34, 30.26, 229.49, 26.52, 17.52; HRMS (ESI): calcd for $C_{26}H_{40}N_9O_{17}$ $[M+H]^+$ 590.3051; found 590.3069.

Synthesis of compound 7: Methyl *N*-α-benzyloxycarbonyl-L-2,3-diaminopropionate (200 mg, 0.7 mmol) was dissolved in CH_2Cl_2 (3.5 mL), Et_3N (300 μL, 2.10 mmol) was added, and the suspension was cooled to 0 °C. The known chloroformamide[45] (250 mg, 0.90 mmol) was then added, and the solution was stirred overnight at RT. The reaction mixture was then diluted with EtOAc (20 mL), washed with 5% aqueous citric acid (2×10 mL), saturated aqueous $NaHCO_3$ (2×10 mL), and brine (2×10 mL), and dried (Na_2SO_4). The solvents were removed under reduced pressure, and the resulting residue was purified by FC (hexane/EtOAc 2:3 to 0:1) to yield **7** (294 mg, 92%) as an oil. ^{1}H NMR (300 MHz, $CDCl_3$): δ = 7.32 (m, 5H), 6.42 (d, J = 7.3 Hz, 1H), 5.59 (t, J = 5.6 Hz, 1H), 5.07 (m, 2H), 4.37 (m, 1H), 3.71 (s, 3H), 3.61 (m, 2H), 3.32 (m, 8H), 1.46 (s, 9H); ^{13}C NMR (75 MHz, $CDCl_3$): δ = 170.84, 157.56, 156.41, 154.42, 135.99, 128.37, 128.07, 127.93, 80.03, 66.95, 54.85, 52.57, 43.36, 43.09, 28.23; LRMS (ESI): calcd for $C_{22}H_{32}N_4NaO_7$ $[M+Na]^+$ 487.2; found 487.2.

Synthesis of compound 8: Compound **7** (715 mg, 1.54 mmol) was dissolved in 4 N HCl/dioxane (8 mL), and the resulting solution was stirred for 15 min at RT during which time an oil precipitated. The solution was sparged with nitrogen to remove HCl, and the solvent was removed under reduced pressure to yield the crude amine. This compound, *N*-Boc-4-aminobutyric acid (370 mg, 1.8 mmol) and 4-dimethylamino pyridine (DMAP; 12 mg, 0.18 mmol) were dissolved in CH_2Cl_2 (7.5 mL). The solution was cooled to 0 °C, and 1-ethyl-3-(3-dimethylaminopropyl)carbodiimide (EDCI; 345 mg, 1.80 mmol) was added. The reaction mixture was stirred for 5 min at 0 °C, and Et_3N (780 μL, 5.4 mmol) was then added. After 6 h at RT, the reaction mixture was diluted with EtOAc (50 mL), washed with 5% aqueous citric acid (2×20 mL), saturated aqueous $NaHCO_3$ (2×20 mL), and brine (2×20 mL) and dried (Na_2SO_4). The solvents were removed under reduced pressure, and the resulting residue was purified by FC (MeOH/CH_2Cl_2 5:95 to 10:90) to yield **8** (732 mg, 89%) as a white, foamy solid. ^{1}H NMR (300 MHz, $CDCl_3$): δ = 7.30 (m, 5H), 6.34 (d, J = 7.2 Hz, 1H), 5.57 (t, J = 5.0 Hz, 1H), 5.05 (m, 2H), 4.9 (t, J = 5.6 Hz, 1H), 4.35 (m, 1H), 3.70 (s, 3H), 3.67–3.49 (m, 4H), 3.35 (s, 4H), 3.24 (m, 2H), 3.12 (q, J = 6.2 Hz, 2H), 6.2 (t, J = 7.2 Hz, 2H), 1.77 (p, J = 6.9 Hz, 2H), 1.39 (s, 9H); ^{13}C NMR (75 MHz, $CDCl_3$): δ = 171.09, 170.94, 157.63, 156.38, 156.02, 136.04, 128.33, 128.02, 127.86, 78.97, 66.81, 55.04, 52.46, 44.87, 43.49, 43.23, 42.70, 40.83, 39.97, 30.26, 28.23, 25.16; LRMS (ESI): calcd for $C_{26}H_{39}NaO_8$ $[M+Na]^+$ 572.3; found 572.1.

Synthesis of compound 9: Compound **8** (186 mg, 0.338 mmol) was dissolved in MeOH/$CHCl_3$ (40:1, 7 mL). $Pd(OH)_2$/C (50 mg) was added, and the reaction mixture was placed under 1 atm of H_2 for 7 h. The solution was filtered through Celite, and the solvents were removed under reduced pressure. The crude amine was dissolved in CH_2Cl_2 (3.5 mL), Et_3N (150 μL, 1.0 mmol) was then added followed by 2-mesitylenesulfonyl chloride (89 mg, 0.41 mmol). The reaction mixture was stirred at RT for 3.5 h, diluted with EtOAc (20 mL), washed with 5% aqueous citric acid (2×10 mL), saturated aqueous $NaHCO_3$ (2×10 mL), and brine (2×10 mL), and dried (Na_2SO_4). The solvents were removed under reduced pressure, and the resulting material was purified by FC (5:95 MeOH/CH_2Cl_2) to yield **9** (17.8 mg, 88%) as a white solid. ^{1}H NMR (300 MHz, $CDCl_3$): δ = 6.92 (s, 2H), 6.13 (d, J = 7.8 Hz, 1H), 5.44 (t, J = 5.5 Hz, 1H), 5.5 (t, J = 5.5 Hz, 1H), 3.90 (td, J = 7.7, 3.7 Hz, 1H), 3.69 (ABX_2, J_{AB} = 13.4 Hz, J_{AX_1} = 6.3 Hz, J_{AX_2} = 3.4 Hz, 1H), 3.61 (m, 2H), 3.54 (s, 3H), 3.49–3.31 (m, 8H), 3.16 (q, J = 6.2 Hz, 2H), 2.60 (s, 6H), 2.36 (t, J =

 © 2007 Wiley-VCH Verlag GmbH & Co. KGaA, Weinheim

6.9, 2H), 2.27 (s, 3H), 1.82 (p, $J=6.5$ Hz, 2H), 1.42 (s, 9H); ^{13}C NMR (75 MHz, $CDCl_3$): $\delta=171.32$, 170.50, 157.60, 156.24, 142.72, 139.29, 133.09, 132.11, 79.19, 55.73, 53.90, 45.16, 43.68, 43.60, 43.52, 41.16, 40.27, 30.57, 28.51, 25.44, 22.65, 21.03; LRMS (ESI): calcd for $C_{22}H_{32}N_4NaO_7$ $[M+Na]^+$ 620.3; found 620.3.

Synthesis of compound 2a: Intermediate **8** (72 mg, 0.13 mmol) was dissolved in MeOH (2 mL). A solution of 4 N HCl/dioxane (1 mL) was then added, the reaction mixture was stirred at RT for 1.5 h, and the solvents were removed under reduced pressure. The residue and 2-methylthio-2-imidazoline hydroiodide (48 mg, 0.20 mmol) were dissolved in MeOH/Et_3N (1:1, 1.4 mL). The resulting solution was heated to reflux for 2.25 h, and the progress of the reaction was monitored by LCMS (1 μL reaction diluted into 100 μL 0.4% aqueous formic acid). The solvents were removed under reduced pressure, and the residue was subsequently dissolved in MeOH/H_2O (3.3:1, 2.6 mL) containing LiOH (27 mg, 0.65 mmol). The reaction mixture was stirred for 1.5 h and neutralized with 1 N HCl, and the solvents were removed under reduced pressure. The resulting reside was purified by HPLC to provide **2b** (54 mg, 82%) as a white solid. ^{1}H NMR (300 MHz, CD_3OD): $\delta=7.32$ (m, 5H), 5.11 (AB, $J_{AB}=12.3$ Hz, 1H), 5.05 (AB, $J_{AB}=12.3$ Hz, 1H), 4.35 (dd, $J=8.1$, 4.5 Hz, 1H), 3.68 (m, 5H), 3.55 (m, 2H), 3.45 (m, 5H), 3.33 (m, 2H), 3.20 (t, $J=7.0$ Hz, 2H), 2.46 (t, $J=6.5$ Hz, 2H), 1.86 (p, $J=7.2$ Hz, 2H); ^{13}C NMR (75 MHz, CD_3OD): $\delta=174.10$, 173.43, 161.78, 160.36, 158.81, 138.45, 129.76, 129.32, 129.14, 67.95, 56.42, 46.42, 44.91, 44.34, 43.47, 42.71, 30.72, 25.76; HRMS (ESI): calcd for $C_{23}H_{33}N_7NaO_6$ $[M+Na]^+$ 504.2571; found 504.2588.

Synthesis of compound 2b: Intermediate **9** (51 mg, 0.085 mmol) was dissolved in MeOH (2 mL). A solution of 4 N HCl/dioxane (1 mL) was then added, the reaction mixture was stirred at RT for 2 h, and the solvents were removed under reduced pressure. The resulting residue and 2-methylthio-2-imidazoline hydroiodide (31 mg, 0.13 mmol) were dissolved in MeOH/Et_3N (1:1 0.9 mL). The resulting solution was heated to reflux for 4 h, a further portion of 2-methylthio-2-imidazoline hydroiodide (20 mg, 0.082 mmol) was added, and the reaction mixture was heated for an addition 2 h, the progress of the reaction was monitored by LCMS (1 μL reaction diluted into 100 μL 0.4% aqueous formic acid). The solvents were removed under reduced pressure, and the residue was subsequently dissolved in MeOH/H_2O (3.3:1, 1.9 mL) containing LiOH (17 mg, 0.41 mmol). The reaction mixture was stirred for 1.5 h and neutralized with 1 N HCl, and the solvents were removed under reduced pressure. The resulting reside was purified by HPLC to provide **2b** (33 mg, 70%) as a white solid. ^{1}H NMR (500 MHz, CD_3OD): $\delta=6.89$ (s, 2H), 3.98 (dd, $J=9.0$, 4.6 Hz, 1H), 3.70 (s, 4H), 3.57 (m, 5H), 3.44 (m, 2H), 3.35 (t, $J=4.7$ Hz, 2H), 3.21 (m, 3H), 2.61 (s, 6H), 2.48 (t, $J=6.9$ Hz, 2H), 2.27 (s, 3H), 1.87 (t, $J=7.2$ Hz, 2H); ^{13}C NMR (125 MHz, CD_3OD): $\delta=173.47$, 161.78, 160.06, 143.83, 140.77, 135.76, 133.14, 57.05, 46.41, 44.89, 44.79, 44.34, 43.48, 42.69, 30.73, 25.76, 23.50, 21.22; HRMS (ESI): calcd for $C_{24}H_{38}N_7O_6S$ $[M+H]^+$ 552.2604; found 552.2626.

Synthesis of compound 10: 3,5-Dimethylphenol (2.0 g, 16 mmol) and ethyl 4-bromobutyrate (3.1 mL, 21 mmol) were dissolved in distilled DMF (55 mL). Potassium carbonate (2.5 g, 18 mmol) and potassium iodide (270 mg, 1.63 mmol) were added, and the resulting suspension was heated to 65 °C for 20 h. The reaction mixture was then cooled to RT and poured into ice, and the resulting solution was extracted with Et_2O (3×50 mL). The combined organic layers were washed with 5% aqueous citric acid (2×40 mL), saturated aqueous $NaHCO_3$ (2×40 mL), and brine (2×40 mL) and dried (Na_2SO_4). The solvent was removed under reduced pressure to yield the alkylated product as a viscous oil (3.4 g). ^{1}H NMR (300 MHz, $CDCl_3$): $\delta=6.60$ (br s, 1H), 6.53 (br s, 2H), 4.15 (q, $J=7.2$ Hz, 2H), 3.98 (t, $J=6.2$ Hz, 2H), 2.51 (t, $J=7.4$ Hz, 2H), 2.29 (d, $J=0.6$ Hz, 6H), 2.09 (p, $J=7.1$ Hz, 2H), 1.28 (t, $J=4.4$ Hz, 3H).

The crude material isolated above (3.4 g, 14 mmol) was dissolved in EtOH/H_2O (1:2, 71 mL) containing NaOH (1.7 g, 43 mmol), and the reaction mixture was stirred for 3 h at RT. The EtOH was removed under reduced pressure, and the remaining liquid was washed with Et_2O (2×40 mL). The aqueous layer was then acidified to pH 3 with concentrated HCl and extracted with EtOAc (3×50 mL). The combined organic layers were washed with brine (2×40 mL) and dried (Na_2SO_4), and the solvent was removed under reduced pressure. The resulting solid was recrystallized from hexane/EtOAc to yield the acid intermediate as a colorless solid (2.6 g, 77% two steps). ^{1}H NMR (300 MHz, $CDCl_3$): $\delta=6.60$ (m, 1H), 6.53 (br s, 2H), 4.00 (t, $J=6$ Hz, 2H), 2.59 (t, $J=7.2$ Hz, 2H), 2.29 (s, 6H), 2.11 (p, $J=6.2$ Hz, 2H); ^{13}C NMR (75 MHz, $CDCl_3$): $\delta=179.76$, 158.56, 138.96, 122.35, 122.02, 66.04, 30.43, 24.19, 21.20; LRMS (ESI): calcd for $C_{12}H_{15}O_3$ $[M-H]$ 207.1; found 207.1.

This acid (5.2 g, 25 mmol) and 2,2,2-trichloroethanol (2.6 mL, 27 mmol) were dissolved in CH_2Cl_2 (125 mL), and the solution was cooled to 0 °C. EDCI (5.3 g, 27 mmol) and DMAP (300 mg, 2.74 mmol) were added, and the reaction was stirred at 0 °C for 10 min and at RT overnight. The solution was diluted with EtOAc (200 mL), and the organic layer was washed with 5% aqueous citric acid (2×60 mL), saturated aqueous $NaHCO_3$ (2×60 mL), and brine (2×60 mL) and then dried (Na_2SO_4). The solvents were removed under reduced pressure, and the product was purified by FC (hexane/EtOAc 5:1) to yield the protected intermediate as a clear oil (8.0 g, 95%). ^{1}H NMR (300 MHz, $CDCl_3$): $\delta=6.60$ (br s, 1H), 6.52 (br s, 2H), 4.76 (s, 2H), 4.01 (t, $J=5.9$ Hz, 2H), 2.69 (t, $J=7.4$ Hz, 2H), 2.28 (d, $J=0.5$ Hz, 6H), 2.16 (p, $J=7.1$ Hz, 2H); ^{13}C NMR (75 MHz, $CDCl_3$): $\delta=171.64$, 158.76, 139.19, 122.61, 112.24, 94.95, 73.95, 66.19, 30.56, 24.55, 21.43; LRMS (ESI): calcd for $C_{14}H_{17}Cl_3NaO_3$ $[M+Na]^+$ 361.0; found 361.0.

The above masked intermediate (1.2 g, 0.55 mmol) was dissolved in CH_2Cl_2 (5.5 mL), and the solution was cooled to 0 °C. Chlorosulfonic acid (720 μL, 11 mmol) was added over 5 min, and the mixture was allowed to stir at 0 °C for 5 min and then at RT for an 15 min. An additional portion of chlorosulfonic acid (400 μL) was then added over 15 min, and the reaction mixture was stirred for an additional 10 min. The solution was then poured into ice and extracted with ethyl acetate (3×50 mL), then the combined organic layers were dried (Na_2SO_4). The solvents were removed under reduced pressure, and the resulting residue was purified through a plug of silica gel (CH_2Cl_2) to yield sulfonyl chloride **10** as an oil (800 mg, 51%). ^{1}H NMR (300 MHz, $CDCl_3$): $\delta=6.68$ (s, 2H), 4.75 (s, 2H), 4.11 (t, $J=6$ Hz, 2H), 2.90 (s, 6H), 2.68 (t, $J=7.5$ Hz, 2H), 2.19 (p, $J=6.2$ Hz, 2H). This material was used without further purification in the next step.

Synthesis of compound 11: Compound **10** (260 mg, 0.595 mmol) was dissolved in CH_2Cl_2 (2.3 mL), and methyl *N*-β-*tert*-butyloxycarbonyl-L-2,3-diaminopropionate (117 mg, 0.459 mmol) and Et_3N (270 μL, 1.87 mmol) were then added. After 4.5 h at RT, the reaction mixture was diluted with ethyl acetate (10 mL), and the organic layer was washed with 5% aqueous citric acid (2×10 mL), saturated aqueous $NaHCO_3$ (2×10 mL), and brine (2×10 mL) and dried (Na_2SO_4). The solvents were removed under reduced pressure, and the resulting residue was purified by flash FC (hexane/EtOAc 3:1 to 1:1) to yield the desired sulfonamide as a foamy solid (230 mg, 81%). ^{1}H NMR (300 MHz, $CDCl_3$): $\delta=6.59$ (s, 2H), 5.88 (d, $J=8.2$ Hz, 1H), 5.11 (t, $J=6.0$ Hz, 1H), 4.73 (s, 2H), 4.02 (t, $J=6.1$ Hz, 2H), 3.86

 © 2007 Wiley-VCH Verlag GmbH & Co. KGaA, Weinheim

(m, 1H), 3.54 (s, 3H), 3.42 (t, J=6.5 Hz, 2H), 2.64 (t, J=7.2 Hz, 2H), 2.50 (s, 6H), 2.13 (p, J=6.5 Hz, 2H), 1.37 (s, 9H); ^{13}C NMR (75 MHz, $CDCl_3$): δ=171.28, 170.40, 160.35, 155.92, 141.78, 128.21, 116.44, 94.74, 73.85, 66.31, 55.40, 52.74, 43.02, 30.21, 28.15, 24.15, 23.24; LRMS (ESI): calcd for $C_{23}H_{33}Cl_3NaO_9S$ [M+Na]$^+$ 641.1; found 641.0.

The sulfonamide isolated above (312 mg, 0.504 mmol) was dissolved in 4 N HCl/dioxane (2.5 mL), and the reaction mixture was stirred at RT for 1 h. After this time, the mixture was sparged with a stream of N_2 gas to remove excess HCl; the dioxane was then removed under reduced pressure to yield the crude deprotected amine as an oil. ^{1}H NMR (300 MHz, $CDCl_3$): δ=6.68 (s, 2H), 4.79 (s, 2H), 4.46 (brs, 4H), 4.21 (m, 1H), 4.10 (t, J=6.1 Hz, 2H), 3.50 (s, 3H), 3.33 (ABX, J_{AB}=13.3 Hz, J_{AX}=8.5 Hz, J_{BX}=4.7, 2H), 2.70 (t, J=7.2 Hz, 2H), 2.65 (s, 6H), 2.19 (p, J=6.5 Hz, 2H).

The crude amine was dissolved in CH_2Cl_2 (2.5 mL), Et_3N (220 μL, 1.52 mmol) was added, and the solution was cooled to 0 °C. The known chloroformamide[45] (160 mg, 0.645 mmol) was then added, and the solution was stirred overnight at RT. The reaction mixture was diluted with EtOAc (10 mL), washed with 5% aqueous citric acid (2×10 mL), saturated aqueous $NaHCO_3$ (2×10 mL), and brine (2×10 mL), and dried (Na_2SO_4). Removal of the solvent under reduced pressure followed by purification by FC (hexane/EtOAc 3:2 to 0:1) provided compound **11** as a foam (308 mg, 84% two steps). ^{1}H NMR (300 MHz, $CDCl_3$): δ=6.56 (s, 2H), 6.23 (d, J=7.9 Hz, 1H), 5.48 (t, J=5.6 Hz, 1H), 4.71 (s, 2H), 4.0 (t, J=6.0 Hz, 2H), 3.86 (td, J=7.6, 4.6 Hz, 1H), 3.62 (ddd, J=13.7, 6.2, 3.7 Hz, 1H), 3.51 (s, 3H), 3.33 (m, 10H), 2.63 (t, J=7.4 Hz, 2H), 2.56 (s, 6H), 2.12 (p, J=7.0 Hz, 2H), 1.41 (s, 9H); ^{13}C NMR (75 MHz, $CDCl_3$): δ=171.36, 170.53, 160.52, 157.69, 154.61, 141.92, 128.07, 116.57, 94.92, 80.09, 73.97, 66.45, 55.72, 52.79, 43.53, 43.33, 30.31, 28.40, 24.27, 23.34; LRMS (ESI): calcd for $C_{28}H_{41}Cl_3N_4NaO_{10}S$ [M+Na]$^+$ 730.2; found 730.1.

Synthesis of compound 12: Intermediate **11** (825 mg, 1.12 mmol) was dissolved in 4 N HCl/dioxane (7 mL), and the solution was stirred at RT for 1 h. After this time, it was sparged with a stream of N_2 gas to remove excess HCl, and the dioxane was removed under reduced pressure to yield the deprotected amine. CbzNH-$(CH_2)_3$-COOH (330 mg, 1.39 mmol) was added to the crude amine, and the mixture was dissolved in CH_2Cl_2 (6 mL), then cooled to 0 °C. EDCI (270 mg, 1.41 mmol) and DMAP (12 mg, 0.10 mmol) were added, and the reaction mixture was stirred at 0 °C for 10 min and at RT for 5 h. The mixture was then diluted with EtOAc (15 mL), washed with 5% aqueous citric acid (2×15 mL), saturated aqueous $NaHCO_3$ (2×15 mL), and brine (2×15 mL) and dried (Na_2SO_4). The solvents were removed under reduced pressure and purification by FC (EtOAc to MeOH/CH_2Cl_2 5:95) yielded the product (897 mg, 94%). ^{1}H NMR (300 MHz, $CDCl_3$): δ=7.33 (m, 5H), 6.61 (s, 2H), 6.00 (brt, J=7.9 Hz, 1H), 5.37 (brs, 1H), 5.21 (brs, 1H), 5.07 (s, 2H), 4.75 (s, 2H), 4.04 (t, J=6.0 Hz, 2H), 3.88 (td, J=7.6, 3.7 Hz, 1H), 3.73 (m, 1H), 3.59 (m, 2H), 2.59 (s, 3H), 3.39 (m, 8H), 3.24 (q, J=6.3, 2H), 2.67 (t, J=7.3 Hz, 2H), 2.61 (s, 6H), 2.36 (t, J=7.1 Hz, 2H), 2.16 (p, J=7.0 Hz, 2H), 1.85 (p, J=6.8 Hz, 2H); ^{13}C NMR (75 MHz, $CDCl_3$): δ=171.26, 171.08, 170.38, 160.48, 157.45, 156.50, 141.83, 136.59, 128.41, 127.97, 116.54, 94.81, 73.91, 66.39, 55.48, 52.77, 46.57, 44.94, 43.47, 43.36, 40.99, 40.64, 30.34, 30.23, 25.00, 24.18, 23.25; LRMS (ESI): calcd for $C_{28}H_{41}Cl_3N_4NaO_{10}S$ [M+Na]$^+$ 753.2; found 753.2.

The above intermediate (592 mg, 0.695 mmol) was dissolved in THF (40.5 mL), and KH_2PO_4 was added (1 M, 7.5 mL). Zn dust (13 g) was added, and the reaction mixture was stirred for 2 h at RT. It was then acidified with 1 N HCl and filtered through Celite, and the combined washings were extracted with ethyl acetate (3×50 mL). The extractions were combined, washed with brine (2×50 mL), and dried (Na_2SO_4). Removal of the solvents under reduced pressure yielded crude acid (587 mg). ^{1}H NMR (300 MHz, $CDCl_3$/CD_3OD): δ=7.22 (m, 5H), 6.51 (s, 2H), 4.96 (m, 2H), 3.91 (t, J=6.0 Hz, 2H), 3.81 (dd, J=8.2, 4.3 Hz, 1H), 3.45 (m, 3H), 3.27 (m, 8H), 3.09 (t, J=6.6, 2H), 2.49 (s, 6H), 2.37 (t, J=7.4 Hz, 2H), 2.27 (t, H=7.2 Hz, 2H), 1.96 (p, J=6.6 Hz, 2H), 1.70 (p, J=7.0 Hz, 2H); ^{13}C NMR (75 MHz, $CDCl_3$/CD_3OD): δ=175.17, 171.65, 170.40, 160.35, 157.63, 156.78, 141.55, 136.27, 128.14, 127.96, 127.72, 127.55, 116.21, 76.53, 66.50, 66.23, 55.26, 52.25, 44.78, 42.50, 40.87, 40.01, 29.96, 24.78, 24.05, 22.81; LRMS (ESI): calcd for $C_{33}H_{45}N_5O_{11}S$ [M−H] 718.3; found 718.3.

A portion of the acid isolated above (153 mg, 0.212 mmol), EDCI (48 mg, 0.25 mmol), and NHS (29 mg, 0.25 mmol) were dissolved in CH_2Cl_2 (2 mL), and the solution was stirred for 4 h. BocNH-$(CH_2)_3NH_2$[46] (53 mg, 0.25 mmol) and Et_3N (36 μL, 0.63 mmol) were then added, and the mixture was stirred overnight. After dilution with EtOAc (8 mL), the organic layer was washed with 5% aqueous citric acid (2×5 mL), saturated aqueous $NaHCO_3$ (2×5 mL), and brine (2×5 mL) and dried (Na_2SO_4). The solvent was removed under reduced pressure, and FC purification (MeOH/CH_2Cl_2 5:95 to 10:90) yielded **12** (152 mg, 83%); ^{1}H NMR (300 MHz, $CDCl_3$): δ=7.31 (m, 5H), 6.59 (s, 2H), 6.56 (brt, J=5.1 Hz, 1H), 6.15 (d, J=7.3 Hz, 1H), 5.45 (t, J=5.1 Hz, 1H), 5.36 (brt, J=5.3 Hz, 1H), 5.06 (m, 2H), 5.02 (t, J=6.3 Hz, 1H), 3.98 (t, J=5.9 Hz, 2H), 3.89 (td, J=7.7, 3.6 Hz, 1H), 3.66 (ddd, J=13.3, 5.4, 2.9 Hz, 1H), 3.57 (m, 5H), 3.40 (m, 3.43–3.18 (m, 12H), 3.11 (q, J=5.8 Hz, 2H), 2.58 (s, 6H), 2.35 (t, J=7.8 Hz, 4H), 2.08 (p, J=6.6 Hz, 2H), 1.83 (p, J=6.8 Hz, 2H), 1.57 (p, J=6.4 Hz, 2H), 1.41 (s, 9H); ^{13}C NMR (75 MHz, $CDCl_3$): δ=172.58, 171.33, 170.70, 160.79, 157.58, 156.73, 141.88, 136.68, 136.68, 128.54, 128.12, 128.05, 127.94, 116.68, 79.40, 67.16, 66.58, 55.81, 52.89, 45.06, 43.43, 43.25, 41.12, 40.71, 37.17, 36.02, 32.65, 30.39, 30.16, 28.44, 25.15, 25.04, 23.37; LRMS (ESI): calcd for $C_{41}H_{61}N_7NaO_{12}S$ [M+Na]$^+$ 898.4; found 898.3.

Synthesis of ligand 2c: Compound **12** (58 mg, 0.066 mmol) was dissolved in MeOH/$CHCl_3$ (3 mL, 40:1), and solid $Pd(OH)_2$/C (14 mg) was added. The suspension was placed under 1 atm of H_2 for 11 h. The reaction mixture was then filtered through Celite, and the solvent was removed under reduced pressure to afford the monoprotected amine derivative (52 mg, quantitative). ^{1}H NMR (300 MHz, CD_3OD): δ=7.84 (brt, J=4.4 Hz, 1H), 6.55 (s, 2H), 3.86 (m, 3H), 3.46–3.29 (m, 8H), 3.27 (m, 2H), 3.17 (m, 3H), 3.05 (m, 2H), 2.88 (m, 4H), 2.45 (s, 8H), 2.12 (t, J=7.6 Hz, 2H), 1.90 (p, J=5.5 Hz, 2H), 1.81 (p, J=6.6 Hz, 2H), 1.48 (p, J=6.5 Hz, 2H), 1.27 (s, 9H); ^{13}C NMR (75 MHz, CD_3OD): δ=175.56, 172.86, 172.38, 162.18, 159.71, 158.59, 143.28, 130.24, 117.70, 80.10, 68.51, 46.26, 56.98, 52.98, 44.50, 44.59, 43.80, 42.56, 40.66, 38.90, 38.06, 37.94, 33.66; LRMS (ESI): calcd for $C_{33}H_{56}N_7O_{10}S$ [M+H]$^+$ 742.4; found 742.3.

This amine (26 mg, 0.033 mmol) and 2-methylthio-2-imidazoline hydroiodide (12 mg, 0.049 mmol) were dissolved in MeOH and Et_3N (400 μL, 1:1). The reaction mixture was heated at reflux, and the progress of the reaction was monitored by LCMS (1 μL of reaction mixture diluted into 100 μL 0.4% aqueous formic acid). After approximately 4 h, the solvents were removed under reduced pressure. The resulting residue was dissolved in a mixture of MeOH and H_2O (600 μL, 1:2) that contained LiOH (4 mg, 0.1 mmol). The solution was stirred for 5 h, and progress was again monitored by LCMS. The reaction was then neutralized with 1 N HCl, and the solvents were removed under high vacuum. TFA (1.5 mL) was then added, and the reaction mixture was stirred for 1.25 h. Most of the TFA was removed under a stream of N_2 gas, and the product was

 © 2007 Wiley-VCH Verlag GmbH & Co. KGaA, Weinheim

triturated with cold Et_2O. The crude mixture was purified by HPLC to yield **2c** as a white solid (14 mg, 54%). ^{1}H NMR (500 MHz, CD_3OD): δ = 6.69 (s, 2H), 4.03, (t, J = 5.9 Hz, 2H), 3.93 (dd, J = 8.8, 4.6 Hz, 1H), 3.70 (s, 4H), 3.63–3.52 (m, 5H), 3.45 (t, J = 4.9 Hz, 2H), 3.37 (t, J = 5.1 Hz, 2H), 3.27, (t, J = 6.3 Hz, 2H), 3.23 (t, J = 4.7 Hz, 1H), 3.21 (t, J = 6.9 Hz, 2H), 2.92 (t, J = 7.1 Hz, 2H), 2.62 (s, 6H), 2.49 (t, J = 6.8 Hz, 2H), 2.39 (t, J = 7.4 Hz 2H), 2.06 (p, J = 6.4 Hz, 2H), 1.87 (p, J = 6.8 Hz, 2H), 1.82 (p, J = 7.5 Hz, 2H); ^{13}C NMR (125 MHz, CD_3OD): δ = 176.51, 173.49, 162.30, 161.80, 160.07, 143.44, 130.54, 117.82, 68.50, 57.14, 46.44, 44.94, 44.80, 44.48, 44.37, 43.51, 42.74, 38.51, 37.22, 33.54, 30.76, 29.10, 26.66, 25.79, 23.92; HRMS (ESI): calcd for $C_{30}H_{50}N_9O_8S$ $[M+H]^+$ 696.3503; found 696.3510.

Synthesis of trisaccharide 16: A suspension of **15** (14.58 g, 15 mmol), phenyl 2,3,4,6-tetra-*O*-benzyl-1-thio-β-D-galactopyranoside **13** (14.22 g, 22.5 mmol) and molecular sieves (4 Å, 15 g) in CH_2Cl_2 (200 mL) was stirred at RT for 1 h under Ar. A suspension of phenyl mercury triflate (10 g, 23.4 mmol) and 4 Å molecular sieves (5 g) in CH_2Cl_2 (150 mL) was stirred for 15 min, transferred to the previous suspension of sugars and kept at RT for 1 h. Filtration through Celite followed by purification by flash chromatography (hexane/EtOAc 100:10→100:15) gave **16** as an oil (20.3 g, 90%). ^{1}H NMR (500 MHz, $CDCl_3$): 7.45–7.05 (m, 55H), 5.20 (d, J = 3.3 Hz, H-C(1″)), 5.09 (d, J = 11.6 Hz, PhCH), 5.02 (d, J = 10.7 Hz, PhCH), 4.92 (d, J = 12.2 Hz, PhCH), 4.89 (d, J = 11.4 Hz, PhCH), 4.88 (d, J = 11.0 Hz, PhCH), 4.85 (d, J = 12.2 Hz, PhCH), 4.83 (d, J = 10.8 Hz, PhCH), 4.75 (d, J = 10.8 Hz, PhCH), 4.73 (d, J = 11.1 Hz, PhCH), 4.68 (d, J = 11.5 Hz, PhCH), 4.67 (d, J = 11.0 Hz, PhCH), 4.64 (d, J = 11.8 Hz, PhCH), 4.62 (d, J = 11.9 Hz, PhCH), 4.58 (d, J = 12.0 Hz, PhCH), 4.49 (d, J = 11.4 Hz, PhCH), 4.44 (brd, J = 8.0 Hz, 2H; H-C(1), H-C(1′)), 4.43 (d, J = 11.5 Hz, PhCH), 4.34 (d, J = 11.4 Hz, PhCH), 4.33 (d, J = 12.0 Hz, PhCH), 4.32 (d, J = 12.0 Hz, PhCH), 4.28 (d, J = 12.0 Hz, PhCH), 4.27 (t, J = 5.0 Hz, H-C(5″)), 4.24 (d, J = 12.0 Hz, PhCH), 4.20 (d, J = 11.9 Hz, PhCH), 4.11 (dd, J = 3.3, 10.0 Hz, H-C(2″)), 3.96 (brt, J = 9.0 Hz, H-C(4)), 3.92 (dd, J = 2.8, 10.0 Hz, H-C(3″)), 3.91 (d, J = 2.5 Hz, H-C(4″)), 3.78 (dd, J = 7.8, 9.0 Hz, H-C(2′)), 3.67 (d, J = 3.0 Hz, H-C(4′)); 3.77–3.65 (m, 3H; H-C(3′), 2H-C(6)); 3.56–3.30 (m, 7H; H-C(3), H-C(2), 2H-C(6″), 2H-C(6′), H-C(5′)), 3.26 (ddd, J = 2.0, 4.0, 10.0 Hz, H-C(5)); ^{13}C NMR (75 MHz, $CDCl_3$): 139.22 (s), 138.99 (s), 138.72 (s), 138.56 (s), 138.55 (s), 138.53 (s), 138.27 (s, 2C), 138.14 (s, 2C), 137.46 (s), 128.17–127.00 (several d), 102.83 (d) and 102.36 (d, C(1), C(1′)), 95.72 (d, C(1″)), 82.91 (d, C(3)), 81.62 (d, C(2)), 79.09 (d, C(3′)), 78.89 (d, C(3″)), 78.02 (d, C(2′)), 76.46 (d, C(4)), 76.36 (d, C-(2″)), 75.38 (t, $PhCH_2$), 75.09 (d, C(5)), 74.98 (t, $PhCH_2$), 74.83 (d, C(4′)), 74.68 (t, $PhCH_2$), 74.53 (t, $2PhCH_2$), 74.20 (t, $2PhCH_2$), 73.20 (t, $PhCH_2$), 72.96 (t, $PhCH_2$), 72.91 (d, C(4″), C(5′)), 72.32 (t, $PhCH_2$), 70.83 (t, $PhCH_2$), 69.12 (d, C(5″)), 68.86 (t, C(6″)), 68.20 (t, C(6)), 68.02 (t, C(6′)). FAB-MS: calcd for $C_{95}H_{98}O_{16}$ $[M+H+Na]^{2+}$ 1519.7; found 1519.

Synthesis of compound 17: A suspension of **16** (16.8 g) and solid 10% Pd/C (6.0 g) in EtOAc/MeOH/H_2O/AcOH (5:5:2:1, 130 mL) was shaken under H_2 (345 kPa) for 36 h. The mixture was filtered through Celite, and the solid was washed with H_2O and pyridine. The combined filtrate was concentrated. The residue was dried and dissolved in pyridine (100 mL) and treated with Ac_2O (50 mL) and 4-dimethylaminopyridine (200 mg) for 12 h. The sample was subjected to evaporation, then coevaporation with toluene and finally FC (hexane/EtOAc 4:6) to afford the peracetylated acceptor (10.0 g, 92%). ^{1}H NMR (300 MHz, $CDCl_3$): 6.27 (d, J = 3.6 Hz, 0.4H; H-C(1α)); 5.68 (d, J = 8.2 Hz, 0.6H; C(1β)); FAB-MS: *m/z* (%): 989 (100) $[M+Na]^+$, 947 (45), 619 (10), 331 (35).

Hydrazine acetate (350 mg) was added to a solution of the above intermediate (2.0 g, 2.07 mmol) in DMF (15 mL) at 55 °C, and the mixture was stirred for 5 min before water (20 mL) was added. The resulting solution was extracted with EtOAc (10×). The organic phase was concentrated and purified by FC (hexane/EtOAc 3:7 eluent) to give saccharide intermediate with a free reducing end (1.72 g, 89%). FAB-MS: *m/z* (%): 947.2 (100) $[M+Na]^+$, 176 (30).

1,8-Diazabicyclo[5.4.0]undec-7-ene (DBU; 0.300 mL, 1.97 mmol) was added to a solution of this compound (1.70 g, 1.83 mmol) and trichloroacetonitrile (2 mL, 20.0 mmol) in CH_2Cl_2 (10 mL) at −5 °C. The reaction mixture was kept at 0 °C for 2 h, then the resulting trichloracetimidate product was isolated and purified by FC (hexane/EtOAc 3:2) to yield **17** (1.48 g, 75%) as a foam. ^{1}H NMR (300 MHz, $CDCl_3$): 8.67 (s, NH), 6.49 (d, J = 3.9 Hz, H-C(1)), 5.58 (t, J = 9.6 Hz, H-C(3)), 5.47 (brd, J = 3.0 Hz, H-C(4′)), 5.35 (brd, J = 3.0 Hz, H-C(4″)), 5.28 (dd, J = 3.0, 10.0 Hz, H-C(3″)), 5.26 (brs, H-C(1″)), 5.20 (dd, J = 7.9, 10.3 Hz, H-C(2′)), 5.14–5.08 (m, H-C(2″)), 5.07 (dd, J = 3.8, 10.1 Hz, H-C(2)), 4.47 (d, J = 8.0 Hz, H-C(1)), 4.46 (dd, J = 2.0, 12.0 Hz, 1H; H-C(6)), 4.24–4.05 (m, 7H), 3.92–3.79 (m, 3H), 2.17 (s, 3H), 2.15 (s, 3H), 2.14 (s, 3H), 2.10 (s, 3H), 2.08 (s, 6H), 2.07 (s, 3H), 2.06 (s, 3H), 2.02 (s, 3H), 1.96 (s, 3H); FAB-MS: *m/z* (%): 1092.1 (100) $[M+Na]^+$, 989 (55).

Synthesis of compound 18: A suspension of **17** (1.45 g, 1.357 mmol), H-$(OCH_2CH_2)_4$-N_3 (220 μL) and molecular sieves (4 Å, 1.93 g) in CH_2Cl_2 (30 mL) was stirred at room temperature for 1 h, cooled in an ice–acetone bath, and treated with BF_3·OEt_2 (0.8 mL, 6.5 mmol). The reaction mixture was stirred at RT for 2 h, treated with Et_3N for 10 min, and purified directly by FC (hexane/EtOAc 3:7) to give **18** (790 mg, 58%) as an oil. ^{1}H NMR (300 MHz, $CDCl_3$): 5.45 (brd, J = 2.9 Hz, H-C(4″)), 5.32 (brd, J = 3.0 Hz, H-C(4′)), 5.26 (dd, J = 3.3, 10.5 Hz, H-C(2″)), 5.24 (d, J = 3.0 Hz, H-C(1″)), 5.21 (t, J = 9.4 Hz, H-C(3)), 5.16 (dd, J = 8.0, 10.1 Hz, H-C(2′)), 5.09 (dd, J = 3.1, 10.0 Hz, H-C(3″)), 4.92 (dd, J = 7.9, 9.4 Hz, H-C(2)), 4.56 (d, J = 7.7 Hz, H-C(1)), 4.50 (dd, J = 2.0, 12.1 Hz, H-C(6)), 4.42 (d, J = 7.9 Hz, H-C(1′)), 4.23–4.00 (m, 6H), 4.00 (ddd, J = 3.3, 4.8, 13.3 Hz, 1H; $OCH_2CH_2N_3$), 3.83 (dd, J = 3.0, 9.0 Hz, H-C(3′)), 3.80 (brt, J = 5.0 Hz, H-C(5′)), 3.81 (t, J = 9.4 Hz, H-C(4)), 3.68 (ddd, J = 3.3, 8.1, 13.5 Hz, 1H; $OCH_2CH_2N_3$), 3.63 (ddd, J = 2.0, 5.0, 10.0 Hz, H-C(5)), 3.46 (ddd, J = 3.5, 8.5, 13.4 Hz, 1H; CH_2N_3), 3.26 (ddd, J = 3.3, 4.7, 13.2 Hz, 1H; CH_2N_3), 2.12 (s, 3H), 2.11 (s, 6H), 2.08 (s, 3H), 2.04 (s, 3H), 2.03 (s, 6H), 2.02 (s, 6H), 1.92 (s, 3H); ^{13}C NMR (75 MHz, $CDCl_3$): 170.2 (s), 170.1 (s), 170.0 (s), 169.94 (s), 169.91 (s), 169.7 (s), 169.5 (s), 169.5 (s), 168.6 (s), 100.8 (d, C(1′)), 100.1 (d, C(1)), 93.1 (d, C(1″)), 75.7 (d, C(3′)), 72.64 (d, C(3)), 72.61 (d, C(5)), 72.5 (d, C(4)), 71.3 (d, C(2)), 70.5 (d, C(5′)), 69.5 (d, C(2′)), 68.4 (t, OCH_2), 67.4 (d, C(4″)), 66.9 (d, C(3″)), 66.6 (d, C(5″)), 66.2 (d, C(2″)), 64.4 (d, C(4′)), 61.5 (t, C(6)), 61.0 (t, C(6′)), 60.8 (t, C(6″)), 50.23 (t, CH_2N_3), 20.57(q), 20.56 (q), 20.52 (q), 20.47 (q, 2C), 20.44 (q), 20.39 (q), 20.37 (q), 20.34 (q), 20.36 (q); FAB-MAS: *m/z* (%): 1016 (100) $[M+Na]^+$, 619 (15), 331 (25), 169 (25).

Synthesis of azido sugar 19: A solution of **18** (897 mg, 0.83 mmol) in MeOH (30 mL) was treated with a solution of NaOMe (0.8 M, 1 mL) at RT for 12 h. The mixture was neutralized with Amberlite IR-120 and filtered. The filtrate was concentrated to give **19** as a solid (580 mg, 99%). ^{1}H NMR (300 MHz, D_2O + ca. 0.1% MeOH): 4.95 (d, J = 3.8 Hz, H-C(1″)), 4.33 (d, J = 7.7 Hz, 2H; H-C(1), H-C(1′)), 4.05–3.35 (m, 32H), 3.32 (brt, J = 4.4 Hz, 2H; CH_2N_3); ^{13}C NMR (75 MHz, D_2O + ca. 0.1% MeOH): 103.03 (d) and 102.27 (d, C(1), C(1′)), 95.60 (d, C(1″)), 78.77 (d), 77.37 (d), 75.21 (d), 74.90 (d), 74.54 (d), 72.96 (d), 70.98 (d), 69.85 (t), 69.84 (t), 69.78 (t), 69.74 (t), 69.64 (t), 69.47 (d), 69.39 (t), 69.30 (d), 68.89 (t), 68.38 (d), 64.98 (d), 61.16 (t) and 61.14 (t) and 60.31 (t, C(6), C(6′), C(6″)), 50.31 (t, CH_2N_3); MALDI-MS: calcd for $C_{26}H_{47}N_3O_{19}Na$: 728.3 $[M+Na]^+$; found 728.

 © 2007 Wiley-VCH Verlag GmbH & Co. KGaA, Weinheim

Synthesis of amino sugar 20: A suspension of **19** (580 mg, 0.82 mmol) and 20% $Pd(OH)_2/C$ (200 mg) in MeOH (15 mL) and AcOH (0.2 mL) was kept under H_2 (354 kPa) for 8 h. The suspension was filtered, and the filtrate was evaporated to give **20** (520 mg, 98%) as an oil. ^{1}H NMR (300 MHz, D_2O + ca. 0.1% MeOH): 4.93 (d, J=3.6 Hz, H-C(1″)), 4.32 (d, J=7.9 Hz) and 4.31 (d, J=7.5 Hz, H-C(1), H-C(1′)), 4.05–3.35 (m, 32H), 3.01 (t, J=4.8 Hz, 2H; CH_2N); ^{13}C NMR (75 MHz, D_2O + ca. 0.1% MeOH): 103.00 (d) and 102.20 (d, C(1), C(1′)), 95.56 (d, C(1″)), 78.70 (d), 77.31 (d), 75.18 (d), 74.88 (d), 74.54 (d), 72.92 (d), 70.96 (d), 69.77 (t, 3C), 69.66 (d), 69.59 (t), 69.53 (t), 69.43 (d), 69.27 (d), 68.88 (t), 68.35 (d), 66.49 (t), 64.94 (d), 61.15 (t), 61.06 (t) and 60.23 (t, C(6), C(6′), C(6″)), 39.25 (t, CH_2NH_2); MALDI-MS: calcd for $C_{26}H_{49}NO_{19}$: 680.3 $[M+H]^+$; found 680.

Synthesis of carbohydrate 21: Trisaccharide **20** (27 mg, 0.034 mmol) was dissolved in a mixture of MeOH and H_2O (2:1, 1 mL). Dimethylsquarate (7 mg, 0.05 mmol) and Et_3N (6 μL, 0.4 mmol) were added to this solution, and the mixture was stirred for 24 h. Removal of the solvents under reduced pressure and purification of the residue by FC ($MeOH/CH_2Cl_2/H_2O$ 1.5:3:0.2) provided **21** (19 mg, 69%) as a white solid. ^{1}H NMR (300 MHz, CD_3OD/D_2O, ca. 1:2 mixture of rotamers about vinylogous amide): δ=4.98 (d, J=3.7 Hz, 1H), 4.34 (dd, J=7.5, 2.7 Hz, 2H), 4.22 and 4.21 (s, 3H total, rotamers), 4.02 (m, 2H), 2.85–2.26 (m, 30H), 3.19 (m, 2H); ^{13}C NMR (75 MHz, CD_3OD/D_2O, ca. 1:2 mixture of isomers about vinylogous amide bond): δ=189.98, 184.70, 184.63, 178.85, 178.57, 174.59, 174.52, 104.12, 103.34, 96.70, 79.95, 78.53, 76.22, 75.94, 75.60, 73.99, 72.00, 70.81, 70.55, 70.36, 69.84, 69.44, 66.05, 62.13, 61.99, 61.37, 45.23, 44.99; LRMS (MALDI): calcd for $C_{31}H_{51}NNaO_{22}S$: 812.3 $[M+Na]^+$; found 812.2.

Synthesis of conjugate 1c: Peptide **1b** (1.8 mg, 2.6 μmol) and saccharide **21** (2.5 mg, 3.1 μmol) were dissolved in borate buffer (160 μL, 50 mM, pH 9), and the mixture was stirred at RT for 30 h. A solution of HOAc in H_2O (0.2 M, 50 μL) was added, and the reaction mixture was purified by HPLC to yield **1c** (2.5 mg, 71%). ^{1}H NMR (500 MHz, D_2O): δ=7.47 (s, 1H), 7.37 (s, 1H), 7.30 (s, 1H), 5.12 (s, J=4 Hz, 1H), 4.64 (t, J=6.7 Hz, 1H), 4.54 (m, 2H), 4.48 (d, J=7.4 Hz, 1H), 4.44 (d, J=7.2 Hz, 1H), 4.34–4.14 (m, 5H), 4.03–3.91 (m, 4H), 3.88–3.82 (m, 2H), 3.81–3.51 (m, 28H), 3.30 (m, 1H), 3.17 (m, 2H), 2.98 (ABX, J_{AB}=17 Hz, J_{AX}=6.3 Hz, 1H), 2.81 (m, 2H), 2.76 (ABX, J_{AB}=17 Hz, J_{BX}=7.4 Hz, 1H), 2.04 (m, 2H), 1.97 (m,1H), 1.70–1.51 (m, 3H), 1.54 (d, J=7.2 Hz, 3H); LRMS (MALDI): m/z calcd for $C_{56}H_{87}N_{10}O_{28}$: 1347.6 $[M+H]$; found 1347.3; HRMS (ESI): calcd for $C_{56}H_{87}N_{10}NaO_{28}$: 685.2795 $[M+H+Na]^{2+}$; found 685.2875.

Synthesis of conjugate 2d. Inhibitor **2c** (2.1 mg, 2.6 μmol) and saccharide **21** (2.7 mg, 3.4 μmol) were dissolved in borate buffer (160 μL, 50 mM, pH 9) and mixed at RT for 29 h. A solution of AcOH in H_2O (0.2 M, 50 μL) was added, and the mixture was purified by HPLC to yield **2d** (2.5 mg, 66%). ^{1}H NMR (500 MHz, D_2O): δ=6.76 (s, 2H), 5.14 (d, J=3.5 Hz, 1H), 4.50 (dd, J=9.7, 8.2 Hz, 1H), 4.18 (m, 2H), 4.08–3.92 (m, 7H), 3.88–3.47 (m, 36H), 3.39–3.13 (m, 12H), 2.54 (s, 6H), 2.51 (t, J=8.2 Hz, 2H), 2.42 (t, J=6.7 Hz, 2H), 2.08 (m, 2H), 1.86 (p, J=7.2 Hz, 2H), 1.72 (p, J=6.7 Hz, 2H); LRMS (MALDI): calcd for $C_{60}H_{97}N_{10}O_{29}S$ 1453.6 $[M+H]^+$; found 1453.6; HRMS (ESI): calcd for $C_{60}H_{97}N_{10}NaO_{29}S$ 738.3021 $[M+H+Na]^{2+}$; found 738.3005.

Synthesis of conjugate 3c: Peptide **3a** (3.5 mg, 5.8 μmol) and saccharide **21** (4.8 mg, 6.0 μmol) were dissolved in borate buffer (350 μL, 50 mM, pH 9), and the mixture was stirred at RT for 3 days. A solution of HOAc in H_2O (0.2 M, 200 μL) was added, and the product was purified by HPLC to yield **3c** (3.5 mg, 44%). ^{1}H NMR (500 MHz, D_2O): δ=7.34 (t, J=6.8 Hz, 2H), 7.28 (t, J=6.8 Hz, 1H), 7.23 (d, J=6.8 Hz, 2H), 5.14 (d, J=3.9 Hz, 1H), 4.76 (dd, J=7.8, 6.4 Hz, 1H), 4.61 (dd, J=10, 6.5 Hz, 1H), 4.5 (dd, J=7.4, 3.9 Hz, 2H), 4.35 (dd, J=8.7, 5.7 Hz, 1H), 4.19 (m, 3H), 4.08–3.47 (m, 34H), 3.33 (m, 1H), 3.18 (m, 2H), 3.06 (ABX, J_{AB}=13.1 Hz, J_{AX}=6.2 Hz, 1H), 2.96 (ABX, J_{AB}=13.1 Hz, J_{BX}=6.2 Hz, 1H), 2.91 (ABX, J_{AB}=16.9 Hz, J_{AX}=7.7 Hz, 1H), 2.72 (ABX, J_{AB}=17.0 Hz, J_{BX}=6.2 Hz, 1H) 1.86 (m, 1H), 1.66 (m, 2H), 1.51 (m, 5H), 1.02 (m, 1H); LRMS (MALDI): m/z calcd for $C_{57}H_{89}N_{10}O_{28}$: 1361.6 $[M+H]$; found: 1361.3; HRMS (ESI): m/z calcd for $C_{57}H_{89}N_{10}NaO_{28}$: 692.2864 $[M+H+Na]^{2+}$; found: 692.2873.

Integrin-binding assay: WM115 cells were trypsinized and resuspended at 1.25×10^6 cells per mL in PBS, and BCECF-AM (2.5 μg mL^{-1}) was added for 30 min at 37 °C. Cells were washed and diluted to 4×10^5 cells per mL in "binding buffer", which consisted of BSA (1.5%), glucose (5 mM), $MgCl_2$ (1.5 mM), and $MnCl_2$ (1.5 mM) in Tris-buffered saline (TBS), pH 7.2, for 60 min at 4 °C. Cells were then diluted to 5×10^3 cells per mL. Previously, V-bottom 96-well microtiter plates had been coated with fibrinogen (100 μL, 1 μg mL^{-1}) overnight at 4 °C. The solution was aspirated, and the plates were blocked with a "blocking buffer", which consisted of BSA (1.5%) and Tween-20 (0.5%) in Na_2CO_3 (25 mM, pH 9.6), for 2 h at RT. This solution was removed, and the wells were washed with binding buffer (3×). BCECF-AM-labeled cells (5000 cells per well) in binding buffer were added to washed wells with or without compound. The plates were incubated for 15 min at 37 °C and then centrifuged at 1830 g for 10 min in an Allegra 6KR centrifuge (Beckman Coulter, Fullerton, CA). Nonadherent cells were quantified on an EnVision 2100 plate reader (Perkin–Elmer, Boston, MA) set in bottom reading mode.

Each experiment was performed in triplicate and contained a minimum of eight concentrations of compounds in addition to wells coated with fibrinogen that contained no compound and untreated wells blocked with BSA. The percent inhibition was defined as:

$$\frac{FI_{inhibitor}-FI_{fibrinogen}}{FI_{no\ fibrinogen}-FI_{fibrinogen}}$$

where $FI_{inhibitor}$ is the fluorescent signal in the presence of fibrinogen and inhibitor, $FI_{fibrinogen}$ is the signal with no inhibitor present (minimum signal) and $FI_{no\ fibrinogen}$ is the signal in the absence of fibrinogen (maximum signal). For each experiment, the maximal percent inhibition was normalized to 100 percent. IC_{50} values were determined by averaging the percent inhibitions for at least three separate experiments and fitting the resulting curve with the following equation:

$$y = \frac{FI_{max}-FI_{min}}{1+(x/IC_{50})^{slope}+FI_{max}}$$

Fits were performed in ProFit by using individual y errors (standard deviation) and assuming a 5% error in the x values. Initial fits were obtained by using a Monte Carlo fitting routine for a minimum of 80000 iterations. Final fits, including errors, were obtained by using a Levenberg–Marguardt fitting routine.

Anti-Gal antibody binding: Near confluent M21 cells were harvested, washed, counted, and resuspended at a density of 4×10^5 cells per mL for activation in binding buffer for 60 min at 4 °C. Cells were then diluted to 2×10^5 cells per mL and incubated with compound **2d** (10 nM) on ice for 60 min. Cells were washed with binding buffer and resuspended in a 20% solution of heat-inactivated human serum (HIHS) obtained from a healthy donor with signed consent. After a 30–60 min incubation on ice, cells were washed and incubated again at 4 °C with fluorescein-conjugated goat anti-

 © 2007 Wiley-VCH Verlag GmbH & Co. KGaA, Weinheim

human IgG antibody (5 μg mL^{-1}) for 30 min. Finally, propidium iodide (5 μg mL^{-1}) was added to identify dead cells, and the population was immediately analyzed for fluorescence by using a FACSCalibur flow cytometer (Becton Dickinson, San Jose, CA). Data were analyzed by using CellQuest software (Becton Dickinson, San Jose, CA). Omitting the bifunctional conjugate allowed the background fluorescence intensity to be assessed. Binding experiments were repeated in triplicate.

Acknowledgements

This work was supported in part by the Department of Defense (DoD) (DAMD17-01-1-0757) and the NIH (AI055258). C.B.C. was supported by the DoD Breast Cancer Research Program Postdoctoral Award (W81XWH-04-1-0466). The UW–Madison Chemistry NMR facility is supported in part by the NSF (CHE9629688 and CHE9208463) and the NIH (RR08389). The authors thank the UWCCC Flow Cytometry Facility for support through grant CA14520. R.M.O. thanks the Pharmacia Corporation and Eastman Chemical Company for fellowships, and P.M. acknowledges the Molecular Biosciences Training Program (GM07215). We also thank the W. M. Keck Foundation for support for the Center for Chemical Genomics.

Keywords: cancer · carbohydrates · integrins · ligand design · peptidomimetics

[1] M. Rudin, R. Weissleder, *Nat. Rev. Drug Discovery* **2003**, *2*, 123 – 131.
[2] M. A. Lindorfer, C. S. Hahn, P. L. Foley, R. P. Taylor, *Immunol. Rev.* **2001**, *183*, 10 – 24.
[3] J. E. Gestwicki, L. E. Strong, C. W. Cairo, F. J. Boehm, L. L. Kiessling, *Chem. Biol.* **2002**, *9*, 163 – 169.
[4] P. A. Trail, H. D. King, G. M. Dubowchik, *Cancer Immunol. Immunother.* **2003**, *52*, 328 – 337.
[5] V. Guillemard, H. U. Saragovi, *Curr. Cancer Drug Targets* **2004**, *4*, 313 – 326.
[6] A. M. Silverstein, *Nat. Immunol.* **2004**, *5*, 1211 – 1217.
[7] G. P. Adams, L. M. Weiner, *Nat. Biotechnol.* **2005**, *23*, 1147 – 1157.
[8] U. Galili, *Alpha-Gal and Anti-Gal: Alpha-1,3-Galactosyltransferase, Alpha-Gal Epitopes, and the Natural Anti-Gal Antibody, Vol. 32*, Kluwer/Plenum, New York, **1999**.
[9] U. Galili, L. Wang, D. C. LaTemple, M. Z. Radic, *Subcell. Biochem.* **1999**, *32*, 79 – 106.
[10] T. E. Mollnes, A. E. Fiane, *Mol. Immunol.* **2003**, *40*, 135 – 143.
[11] U. Galili, S. B. Shohet, E. Kobrin, C. L. M. Stults, B. A. Macher, *J. Biol. Chem.* **1988**, *263*, 9858 – 9866.
[12] R. O. Hynes, *Cell* **2002**, *110*, 673 – 687.
[13] B. P. Eliceiri, D. A. Cheresh, *Curr. Opin. Cell Biol.* **2001**, *13*, 563 – 568.
[14] B. Felding-Habermann, *Clin. Exp. Med.* **2003**, *20*, 203 – 213.
[15] P. C. Brooks, R. A. F. Clark, D. A. Cheresh, *Science* **1994**, *264*, 569 – 571.
[16] A. Janczuk, J. Li, W. Zhang, X. Chen, Y. Chen, J. Fang, J. Wang, P. G. Wang, *Curr. Med. Chem.* **1999**, *6*, 155 – 164.
[17] L. D. D'Andrea, A. Del Gatto, C. Pedone, E. Benedetti, *Chem. Biol. Drug Des.* **2006**, *67*, 115 – 126.
[18] R. Haubner, R. Gratias, B. Diefenbach, S. L. Goodman, A. Jonczyk, H. Kessler, *J. Am. Chem. Soc.* **1996**, *118*, 7461 – 7472.
[19] M. Pfaff, K. Tangemann, B. Muller, M. Gurrath, G. Muller, H. Kessler, R. Timpl, J. Engel, *J. Biol. Chem.* **1994**, *269*, 20 233 – 20 238.
[20] K. Temming, R. M. Schiffelers, G. Molema, R. J. Kok, *Drug Resist. Updates* **2005**, *8*, 381 – 402.
[21] M. E. Duggan, L. T. Duong, J. E. Fisher, T. G. Hamill, W. F. Hoffman, J. R. Huff, N. C. Ihle, C. T. Leu, R. M. Nagy, J. J. Perkins, S. B. Rodan, G. Wesolowski, D. B. Whitman, A. E. Zartman, G. A. Rodan, G. D. Hartman, *J. Med. Chem.* **2000**, *43*, 3736 – 3745.
[22] J. D. Hood, M. Bednarski, R. Frausto, S. Guccione, R. A. Reisfeld, R. Xiang, D. A. Cheresh, *Science* **2002**, *296*, 2404 – 2407.
[23] T. D. Harris, S. Kalogeropoulos, T. Nguyen, S. Liu, J. Bartis, C. Ellars, S. Edwards, D. Onthank, P. Silva, P. Yalamanchili, S. Robinson, J. Lazewatsky, J. Barrett, J. Bozarth, *Cancer Biother. Radiopharm.* **2003**, *18*, 627 – 641.
[24] C. A. Burnett, J. Xie, J. Quijano, Z. Shen, F. Hunter, M. Bur, K. C. P. Li, S. N. Danthi, *Bioorg. Med. Chem.* **2005**, *13*, 3763 – 3771.
[25] S. Biltresse, M. Attolini, J. Marchand-Brynaert, *Biomaterials* **2005**, *26*, 4576 – 4587.
[26] A. Meyer, J. Auemheimer, A. Modlinger, H. Kessler, *Curr. Pharm. Des.* **2006**, *12*, 2723 – 2747.
[27] C. Rader, S. C. Sinha, M. Popkov, R. A. Lerner, C. F. Barbas III, *Proc. Natl. Acad. Sci. USA* **2003**, *100*, 5396 – 5400.
[28] M. Popkov, C. Rader, B. Gonzalez, S. C. Sinha, C. F. Barbas III, *Int. J. Cancer* **2004**, *119*, 1194 – 1207.
[29] L. S. Li, C. Rader, M. Matsushita, S. K. Das, C. F. Barbas III, R. A. Lerner, S. C. Sinha, *J. Med. Chem.* **2004**, *47*, 5630 – 5640.
[30] F. Guo, S. K. Das, B. M. Mueller, C. F. Barbas III, R. A. Lerner, S. C. Sinha, *Proc. Natl. Acad. Sci. USA* **2006**, *103*, 11 009 – 11 014.
[31] W. H. Miller, R. M. Keenan, R. N. Willette, M. W. Lark, *Drug Discovery Today* **2000**, *5*, 397 – 408.
[32] B. Cacciari, G. Spalluto, *Curr. Med. Chem.* **2005**, *12*, 51 – 70.
[33] A. C. Bach II, J. R. Espina, S. A. Jackson, P. F. W. Stouten, J. L. Duke, S. A. Mousa, W. F. DeGrado, *J. Am. Chem. Soc.* **1996**, *118*, 293 – 294.
[34] J. Luna, T. Tobe, S. A. Mousa, T. M. Reilly, P. A. Campochiaro, *Lab Instrum.* **1996**, *75*, 563 – 573.
[35] J. W. Corbett, N. R. Graciani, S. A. Mousa, W. F. DeGrado, *Bioorg. Med. Chem. Lett.* **1997**, *7*, 1371 – 1376.
[36] L. F. Tietze, M. Arlt, M. Beller, K. H. Gluesenkamp, E. Jaehde, M. F. Rajewsky, *Chem. Ber.* **1991**, *124*, 1215 – 1221.
[37] J.-P. Xiong, T. Stehle, R. Zhang, A. Joachimiak, M. Frech, S. L. Goodman, M. A. Arnaout, *Science* **2002**, *296*, 151 – 155.
[38] M. S. Egbertson, B. Bednar, R. A. Bednar, G. D. Hartman, R. J. Gould, R. J. Lynch, L. M. Vassallo, S. D. Young, *Bioorg. Med. Chem. Lett.* **1996**, *6*, 1415 – 1420.
[39] D. G. Batt, J. J. Petraitis, G. C. Houghton, D. P. Modi, G. A. Cain, M. H. Corjay, S. A. Mousa, P. J. Bouchard, M. S. Forsythe, P. P. Harlow, F. A. Barbera, S. M. Spitz, R. R. Wexler, P. K. Jadhav, *J. Med. Chem.* **2000**, *43*, 41 – 58.
[40] J. N. Lambert, J. P. Mitchell, K. D. Roberts, *J. Chem. Soc. Perkin Trans. 1* **2001**, 471 – 484.
[41] J. S. Davies, *J. Pept. Sci.* **2003**, *9*, 471 – 501.
[42] D. Boturyn, P. Dumy, *Tetrahedron Lett.* **2001**, *42*, 2787 – 2790.
[43] P. Chand, Y. S. Babu, S. Bantia, N. M. Chu, L. B. Cole, P. L. Kotian, W. G. Laver, J. A. Montgomery, V. P. Pathak, S. L. Petty, D. P. Shrout, D. A. Walsh, G. W. Walsh, *J. Med. Chem.* **1997**, *40*, 4030 – 4052.
[44] S. Thorand, N. Krause, *J. Org. Chem.* **1998**, *63*, 8551 – 8553.
[45] K. D. Rice, A. R. Gangloff, E. Y. L. Kuo, J. M. Dener, V. R. Wang, R. Lum, W. S. Newcomb, C. Havel, D. Putnam, L. Cregar, M. Wong, R. L. Warne, *Bioorg. Med. Chem. Lett.* **2000**, *10*, 2357 – 2360.
[46] P. G. Mattingly, *Synthesis* **1990**, 366 – 368.
[47] U. Galili, L. M. Khushi, *Transplantation* **1996**, *62*, 256.
[48] K. P. Naicker, H. Li, A. Heredia, H. Song, L.-X. Wang, *Org. Biomol. Chem.* **2004**, *2*, 660 – 664.
[49] M. Kantlehner, D. Finsinger, J. Meyer, P. Schaffner, A. Jonczyk, B. Diefenbach, B. Nies, H. Kessler, *Angew. Chem.* **1999**, *111*, 587 – 590; *Angew. Chem. Int. Ed.* **1999**, *38*, 560 – 562.
[50] J. W. Fang, J. Li, X. Chen, Y. N. Zhang, J. Q. Wang, Z. M. Guo, W. Zhang, L. B. Yu, K. Brew, P. G. Wang, *J. Am. Chem. Soc.* **1998**, *120*, 6635 – 6638.
[51] C. Gege, W. Kinzy, R. R. Schmidt, *Carbohydr. Res.* **2000**, *328*, 459 – 466.
[52] R. J. Hinklin, L. L. Kiessling, *J. Am. Chem. Soc.* **2001**, *123*, 3379 – 3380.
[53] Y. H. Wang, Q. Y. Yan, J. P. Wu, L. H. Zhang, X. S. Ye, *Tetrahedron* **2005**, *61*, 4313.
[54] A. K. Sarkar, K. L. Matta, *Carbohydr. Res.* **1992**, *233*, 245.
[55] K. H. Jung, M. Hoch, R. R. Schmidt, *Liebigs Ann. Chem.* **1989**, 1099.
[56] P. J. Garegg, C. Henrichson, T. Norberg, *Carbohydr. Res.* **1983**, *116*, 161 – 165.
[57] S. Sato, M. Mori, Y. Ito, T. Ogawa, *Carbohydr. Res.* **1986**, *155*, C6 – C10.
[58] V. P. Kamath, P. Diedrich, O. Hindsgaul, *Glycoconjugate J.* **1996**, *13*, 315 – 319.
[59] P. I. Kitov, D. R. Bundle, *J. Chem. Soc. Perkin Trans. 1* **2001**, 838 – 853.

 © 2007 Wiley-VCH Verlag GmbH & Co. KGaA, Weinheim

[60] H. G. Lerchen, J. Baumgarten, K. von dem Bruch, T. E. Lehmann, M. Sperzel, G. Kempka, H. H. Fiebig, *J. Med. Chem.* **2001**, *44*, 4186 – 4195.
[61] N. Zanatta, A. M. C. Squizani, L. Fantinel, F. M. Nachtigall, H. G. Bonacorso, M. A. P. Martins, *Synthesis* **2002**, 2409 – 2415.
[62] E. F. Plow, T. A. Haas, L. Zhang, J. Loftus, J. W. Smith, *J. Biol. Chem.* **2000**, *275*, 21 785 – 21 788.
[63] M. Weetall, R. Hugo, C. Friedman, S. Maida, S. West, S. Wattanasin, R. Bouhel, G. Weitz-Schmidt, P. Lake, *Anal. Biochem.* **2001**, *293*, 277 – 287.
[64] S. Liu, D. S. Edwards, M. C. Ziegler, A. R. Harris, S. J. Hemingway, J. A. Barrett, *Bioconjugate Chem.* **2001**, *12*, 624 – 629.
[65] N. Nasongkla, X. Shuai, H. Ai, B. D. Weinberg, J. Pink, D. A. Boothman, J. M. Gao, *Angew. Chem.* **2004**, *116*, 6483 – 6487; *Angew. Chem. Int. Ed.* **2004**, *43*, 6323 – 6327.
[66] B. P. Orner, R. Derda, R. L. Lewis, J. A. Thomson, L. L. Kiessling, *J. Am. Chem. Soc.* **2004**, *126*, 10 808.

Received: August 12, 2006
Published online on December 8, 2006

 © 2007 Wiley-VCH Verlag GmbH & Co. KGaA, Weinheim